Aus dem Forschungslabor der Urologischen Klinik
des Universitätsklinikum Düsseldorf
Direktor: Prof. Dr. med. P. Albers

DNA Hypomethylation and Gene Expression in Bladder Cancer

Inaugural-Dissertation

zur Erlangung des Doktorgrades
der Mathematisch-Naturwissenschaftlichen Fakultät
der Heinrich-Heine-Universität Düsseldorf

vorgelegt von

Olusola Yakub Dokun
aus Osun state, Nigeria

Düsseldorf, Juni 2009

TABLE OF CONTENTS

INTRODUCTION

1.1 DNA methylation: an overview

DNA methylation is a reversible modification of DNA, characterized in mammalian cells by the addition of a methyl group from S-adenosylmethionine to the carbon 5 position of selected cytosine residues that precede a guanine residue. This reaction is catalysed by DNA methyltransferases, which include DNMT1, DNMT3A and DNMT3B. DNMT1 is a maintenance methyltransferase that preferentially transfers methyl groups to hemimethylated DNA subsequent to replication. DNMT3A and DNMT3B are de novo methyltransferases capable of transferring methyl groups to CpG dinucleotides of unmethylated DNA [Goll et al, 2005]. DNMT1 and DNMT3B act cooperatively in many instances during development [Kim et al, 2002; Reik 2007], but also to repress genes in human cancer [Rhee et al, 2002]. The DNMT3A plays an active role in paternal and maternal imprinting [Kaneda et al, 2004]. In male germ cell development, it forms heterotetramers with a further member of the DNMT family, DNMT3L, which lacks important catalytic amino acids and acts as a regulatory subunit [Cheng and Blumenthal, 2008].

Because methylated cytosines tend to mutate towards thymines in the course of evolution, there are fewer than expected CpG dinucleotides in the mammalian genome. The majority of these are nearly always methylated. However, CpG dinucleotides clustered in stretches of DNA known as CpG islands are nearly always unmethylated (>95%). CpG islands are now defined as having minimum G:C content of 55% and a CpG to GpC ratio of at least 0.65 [Laird et al, 2003]. They vary in size from 0.5 to 5 kb and are associated with about 50% of mammalian genes. These CpG islands are predominantly located around the transcriptional start site including the basal promoter region of human genes. Methylation within these islands is associated with repression of the corresponding gene [Esteller 2008; Jone and Baylin 2007]. The fraction of CpG-islands at the 5'-end of genes that are methylated in various normal somatic cells is estimated as around 5% [Weber et al, 2007], but the fraction increases in certain pathological states (see below).

DNA methylation plays vital roles in the regulation of gene expression, cellular differentiation and development, genomic imprinting, X-chromosome inactivation, repression of retrotransposons, maintenance of chromosome integrity, brain function and development of the immune system [Miranda and Jones, 2007; Schulz and Dokun, 2009]. DNA methylation is part of the complex epigenetic network that regulates gene expression and genomic structure. DNA methylation and DNA methyltransferases interact mutually with

proteins that function in the modification of histones and remodelling of chromatin. This interaction regulates the DNA methylation patterns throughout the genome and at specific genes under normal states as well as in disease state.

Histones in transcriptionally active chromatin regions and in particular at CpG-islands and other active regulatory regions are acetylated at various sites. Sequences methylated at CpG sites by DNA methyltransferases (DNMT1, DNMT3A or DNMT3B) are targeted by methyl-binding domain (MBD) proteins like MBD2 and MeCP2. The presence of MBDs attracts histone deacetylases (HDAC1 and HDAC2) and chromatin remodeling activities resulting in the stable transformation of the chromatin structure from an open to a closed conformation that prevents transcriptional activation. This inactive epigenetic state is characterized by deacetylated histones.

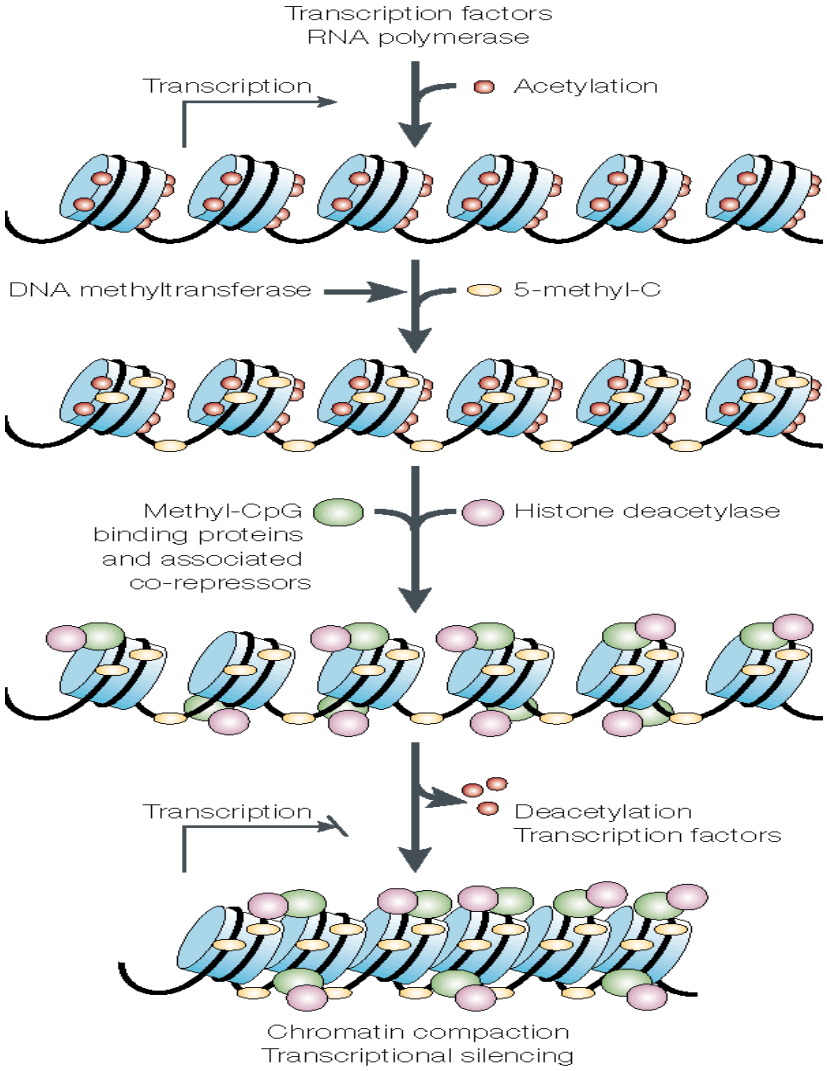

Figure 1.1 The effect of DNA methylation on chromatin structure as depicted by Robertson and Wolffe, 2000

Figure 1.1 summarizes the interaction between DNA methylation and histone acetylation as it was understood about a decade ago. Over the last years, important additional insights have been gained.

First, a much larger number of enzymes and other factors have been identified that are involved in the maintenance of epigenetic states. These include various histone acetylases vs deacetylases, methylases vs demethylases, kinases vs phosphatase, ubiquitinases vs deubiquitinases which oppose each other in a way that eventually leads to a stable epigenetic state [Vaissiere et al, 2008]. This means that histone modifications are now regarded as highly dynamic and principally reversible, even the methylation of lysines and arginines in histones. Examples of enzymes involved in these processes and relevant in the context of the present thesis are the histone acetylases MYST4, which acetylates lysine K16 of histone H4 (H4K16), among others [Fraga et al, 2005], the protein acetylase PCAF, which acetylates various lysines in H3 [Schiltz et al, 1999], and the NAD^+-dependent "Sirtuin" protein deacetylases SIRT1 and SIRT7 [Saunders and Verdin, 2007]. Notably, these enzymes also acetylate or deacetylate a number of transcription factors in addition to histones. As an example of histone demethylases, the Jumonji domain protein JMJD1A removes methyl groups from mono- or dimethylated H3K9 by an oxidative process [Tsukuda et al. 2006; Lan et al, 2008].

Another mechanism for establishment of epigenetic states, in addition to posttranslational modifications of the standard histones, is provided by the insertion of variant histones in nucleosomes [Tagami et al, 2004]. These can promote or prohibit DNA methylation. For instance, the histone variant MacroH2A, encoded by the *H2AFY* gene, is associated with facultative heterochromatin like the inactive X-chromosome of females [Nusinow et al, 2007; Chow and Brown, 2003]. In contrast, the H3.3 variant is associated with active genes and prevents DNA methylation [Loppin et al, 2005].

Secondly, as first shown in Neurospora [Dobosy and Selker, 2001], chromatin modification and factors that associate with them can direct DNA methylation. Although it is still unknown how the specificity of DNA de-novo-methylation is achieved in mammalian cells and especially during the various stages of development and in pathological states such as cancer, some factors potentially involved have been discovered. Thus, at certain genes, polycomb group proteins, such as the histone H3K27 trimethylase EZH2, serve as a recruitment platform for DNA methyltransferases [Vire et al, 2006]. Similarly DNA methylation at some repeat sequences requires the Lymphoid-specific helicase (LSH)

[Muegge 2005] and at others the ATRX protein [Nan et al, 2007]. Mutations in the latter gene cause the eponymous human hereditary disease [Gibbons et al, 2000].

Most patterns of DNA methylation are set up during fetal development. Cells start in a pluripotent state, from which they can differentiate into many cell types. As they develop, their gene-expression programmes become more defined and restricted. Genes that are required later in development are transiently held by histone modifications in a repressed state, which is easily reversed when expression of these genes is needed. However, long term epigenetic silencing of transposons, imprinted genes and pluripotency associated genes in somatic cells are conferred by DNA methylation [Reik 2007].

Similarly, early in development one of the pair of X chromosomes in females is inactivated and this inactivation is stably inherited through subsequent somatic cell divisions [Chow et al, 2005]. The process is initiated by transcription of the non-coding XIST RNA, which subsequently recruits many of the epigenetic features generally associated with heterochromatin such as histone modifications, macroH2A and ultimately DNA methylation [Chang et al, 2006; Ogawa et al, 2008].

In adult somatic cells, a limited degree of DNA de novo methylation and demethylation occurs during cell division, while most methylation patterns are perpetuated by the action of DNMT1 after replication. Notably, shorter term cyclic methylation and demethylation have been reported recently to occur in quiescent cells during transcription [Kangaspeska et al, 2008].

Another recent insight is that the contribution of DNA methylation to the regulation of gene expression may dramatically depend on the CpG content of a gene. Methylation of CpG islands is rather strictly correlated with transcriptional silencing. Conversely, DNA methylation of genes that contain few CpG sites in their regulatory regions may have only effects in rare cases, especially if their transcription depends on a transcription factor that is sensitive to methylation in its recognition site. This constitutes a second mechanism by which DNA methylation can inhibit gene expression, independent of or in addition to the binding of MBD proteins. The relationship of methylation to gene expression has turned out to be particularly complex in genes with intermediate CpG content [Weber et al, 2007], as illustrated by data gained during the course of this thesis [Dokun et al, 2008]. In brief, genes with intermediate CpG content are often characterised by variable methylation patterns and significant transcription of such genes may occur despite the presence of methylation in their promoters.

1.2 The multiple roles of DNA methylation in cancer

The DNA methylation patterns observed in cancers are frequently quite different from those of the normal counterpart tissues [Widschwendter and Jones, 2002]. Although cancers often exhibit decreased methylcytosine content throughout the bulk of the genome, this "hypomethylation" often co-exists with the occurrence of heavy abnormal methylation within a number of CpG islands. "Hypermethylation" changes are functionally implicated in the development and progression of many tumors, because, in particular, repression of many tumor suppressor genes is linked to hypermethylation of their promoter CpG islands [Strathdee and Brown 2002].

1.3 DNA hypermethylation

1.3.1 Causes of DNA hypermethylation

A number of mechanisms have been suggested for the etiology of cancer-specific methylation changes observed in tumorigenesis. Initially, it was proposed that increased DNMT1 activity led to methylation of CpG islands and associated loss of gene expression [Baylin et al, 1991]. However, follow-up studies revealed that when the levels of DNMT1 are adjusted for proliferation markers the increase in expression largely disappears [Laird 1997; Kanai et al, 2001, Kimura et al. 2001]. DNMT1 and DNMT3B in particular are regulated with the cell cycle and their increased expression is probably a consequence of increased proliferation of tumor cells. Another proposed mechanism was that both DNMT1 and p21 compete for the same binding site on proliferating cell nuclear antigen (PCNA). Binding of DNMT1 to PCNA is critical for directing it to the replication complex during S-phase. Therefore induction of p21 at the onset of tumorigenesis might inhibit the formation of the DNMT1-PCNA complex, resulting in depletion of genome-wide methylation and subsequently targeting of the free DNMT1 to CpG islands [Chuang et al, 1997]. This ingenious hypothesis was refuted by observations in various cancer types that global hypomethylation and hypermethylation at individual genes occur at different stages of tumor development and quite independent of each other (see below).

There is also convincing evidence that infectious agents are capable of influencing the methylation pattern. *H. pylori* infection has been implicated in eliciting hypermethylation of CpG islands at the onset of gastric tumor development [Nardone et al, 2007]. Hepatitis B virus infection has been linked to increased CDKN2A/p16 methylation and progression of

hepatocellular carcinoma [Jicai et al, 2006]. Likewise, a role has also been proposed for human papilloma virus (HPV) in the hypermethylation of *APC, DAPK,* and *MGMT* in cervical carcinoma [Lafon-Hughes et al 2008]. The mechanisms involved have however not been clarified.

The most current hypothesis proposes that hypermethylation could be due to active repression by chromatin modifying factors that additionally recruit DNA methyltransferases. For some genes, this mechanism has been outlined in detail. As an example the PRC1 polycomb complex represses the p16 promoter in the CDKN2A gene in stem cells [Park et al, 2003], but in some cancers this repression leads to abnormal DNA methylation. For instance, the knockdown of SUZ12, a key component of Polycomb Repressive Complex 2 (PRC2) reverts not only histone modification but also initiates DNA demethylation of PML-RARα target genes. The polycomb group proteins might therefore be critical in the establishment and maintenance of the aberrant silencing of tumor suppressor genes during transformation induced by the leukemia-associated PML-RARα fusion protein [Villa et al, 2007].

The mechanism implicated in hypermethylation in adult cancers may thus resemble that leading to de-novo-methylation in normal and malignant (i.e. embryonal carcinoma) embryonic cells. In embryonic stem cells, genes that become later DNA-methylated exist in a 'transcription-ready' state characterized by a 'bivalent' promoter chromatin pattern containing the repressive mark, trimethylated H3K27, conferred by Polycomb group proteins, as well as the active mark, methylated H3K4. Interestingly, embryonic carcinoma cells add two key repressive marks, dimethylated H3K9 and trimethylated H3K9, both associated with DNA hypermethylation in adult cancers. It is therefore possible that the genes hypermethylated in cancer cells carry chromatin marking patterns that leave them vulnerable to aberrant DNA hypermethylation and gene silencing during tumor initiation and progression. In particular, it has been suggested that in the development of cancers in somatic cells hypermethylation may occur in stem or progenitor cells with bivalent marking and transient silencing of such genes [Ohm et al, 2007].

Furthermore, genes methylated in cancer cells are often specifically packaged with nucleosomes containing histone H3 trimethylated on Lys27. This chromatin mark is present on the unmethylated CpG islands of these genes early in development and then maintained in differentiated cell types by the activities of an EZH2-containing Polycomb complex. In cancer cells, as opposed to normal cells, the presence of this complex initiates the recruitment of DNA methyltransferases, leading to de novo methylation [Schlesinger et al, 2007]. This idea is supported by the overexpression of certain Polycomb components, such as EZH2, in

many cancers, including those of the breast, prostate and bladder [Pietersen et al, 2008, Hoffmann et al, 2007]. On the other hand, not all genes hypermethylated in cancer are polycomb targets and not all polycomb targets do become hypermethylated. Thus, many details of this mechanism remain to be elucidated.

1.3.2 Consequences of DNA hypermethylation

DNA hypermethylation is involved in the repression of many tumor suppressor genes, such as *RB1, VHL, p16, BRCA1 and APC,* in many familial and sporadic tumors [Gronsbaek et al, 2007]. Hence DNA hypermethylation is another inactivation mechanism alternative to genetic mechanisms like point mutations or deletion and is selected for during cancer development [Esteller 2007; Jones and Baylin 2007].

Another group of genes silenced by DNA hypermethylation in tumors are involved in DNA repair. For instance, the transcriptional inactivation of the mismatch repair gene *MLH1* due to DNA hypermethylation of its promoter is a critical step in the development of a subgroup of colorectal cancers [Cunningham et al, 1998]. There are also reports of hypermethylation-mediated silencing of the related *MSH2* gene in heritable colorectal and other cancers [Suter et al, 2004; Chan et al, 2006]. In the same manner, hypermethylation mediated-silencing of *MGMT* increases the risk of cancer development by exposure to certain carcinogens, but conversely sensitises cancer cells to the effect of alkylating compounds used in chemotherapy [Esteller et al, 2002]. Assays for MGMT methylation are therefore becoming used in the clinic to optimize the choice of chemotherapeutic drugs. Also *FANCF*, a gene encoding a component of the Fanconi protein complex involved in DNA repair, undergoes hypermethylation-mediated transcriptional inactivation in ovarian cancer, which is only found in rare cases of bladder cancer [Neveling et al, 2007].

Furthermore, some genes such as *RASSFIA* and *CDKN2A* are methylated in many different cancers whereas others are methylated in specific cancers only. As an example, methylation of *GSTP1* is found in a restricted range of cancers, including prominently prostate carcinoma, whereas the gene is actually overexpressed in other cancer types and contributes to chemotherapy resistance [Hayes et al. 2005]. Genes frequently methylated in breast cancer include estrogen receptor alpha (*ESR1*), *TIMP3* and E-cadherin (*CDH1*) as well as *BRCA1* whereas genes predominantly methylated in haematological cancers include *CDKN2B, CDKN1A, SDC4* and *MDR* [Yang et al, 2001; Das and Singal, 2004].

1.4 DNA hypomethylation

DNA hypomethylation occurs in many cancers, such as prostate cancer, bladder cancer, hepatocellular carcinoma and cervical cancer in comparison to their normal counterparts [Ehrlich, 2002]. The overall decrease in methylcytosine results quantitatively from decreased methylation of those sequences most densely methylated in the normal cell genome, namely retroelements and certain tandem repeats like satellites. To a smaller degree, demethylation of genes contributes. DNA hypomethylation is linked to genetic instability characterized by chromosomal aberration and elevated mutation rates [Wilson et al, 2007]. It could lead to the activation of some oncogenes and retrotransposons. DNA hypomethylation correlates with tumor progression and prognosis in many cancers [Sato et al, 2003] including bladder carcinoma [Neuhausen et al, 2006]. The extent of DNA hypomethylation varies both within and among different cancer types; some types of cancer do not exhibit a major reduction in the amount of methylated cytosines, e.g. renal cell carcinomas [Florl et al 1999] and some leukemias. DNA hypomethylation occurs at the onset of breast and colon cancers [Kondo and Issa, 2004; Suter et al, 2004], but for other types such as hepatocellular carcinoma the extent of hypomethylation increases with stage and grade [Lin et al, 2001]. In bladder cancer hypomethylation appears to set in early [Florl et al 1999], whereas in prostate cancer it is associated with progression [Florl et al, 2004; Yegnasubramanian et al, 2008].

1.4.1 Causes of DNA hypomethylation

The methyl group availability is influenced by different types of food components, and the absence or low intake of these components could lead to deficiencies in the amount of methyl groups available. In cancer cells with an enhanced requirement for such compounds including Vitamins such as folic acid, B6 and B12 required to support resynthesis of dietary methionine used in methylation reactions, this could result in hypomethylation.. Some of the genes critical to the recycling and availability of methionine harbor polymorphisms, and some such polymorphisms are related to increased risk of cancer development [Hoffman and Schulz, 2005].

In animal models, knockdown or deficiencies in the activities of one or several of the DNA methyltransferases lead to genome-wide hypomethylation and subsequently chromosomal instabilities [Gaudet et al, 2003; Eden et al, 2003]. In humans inherited deficiencies in DNMT3B cause hypomethylation of sequences such as satellites, but not of LINE retrotransposons. However, alterations in the expression of the DNMT3 enzymes do not seem

to constitute a critical factor in the hypomethylation observed in cancers [Hoffman and Schulz, 2005; Wilson et al, 2007]. Despite its increased expression in many cancers, DNMT1 may not be sufficient for maintaining DNA methylation levels, because the coordination between the enzyme activity and DNA replication is disturbed as a consequence of defects in RB1 [Pradhan et al, 2002]. There are also reports suggesting that the splice variant DNMT3B4 serves as an inhibitor of DNA methylation in human hepatocellular carcinoma by actively competing with DNMT3B3 for the same binding site on pericentromeric satellite regions on hepatocellular carcinoma cells [Saito et al, 2002; Kanai et al 2004].

Environmental factors such as UV radiation, chemicals and infections causing cancer could also contribute to hypomethylation of the genomic DNA. DNA damage caused by carcinogens leads to activation of DNA repair. During DNA repair by nucleotide excision or strand-break repair, methylated cytosine is replaced by cytosine, leading to hypomethylation around the site of damage [Koturbash et al, 2005; Susuki et al, 2006]. In keeping with this idea, the GADD45A protein often induced as a consequence of DNA damage by p53 or BRCA1 has been proposed to induce hypomethylation through interaction with nucleotide excision repair proteins [Barreto et al. 2007].

1.4.2 Consequences of DNA hypomethylation

DNA methylation serves as a defence mechanism against genomic parasites. In humans, endogenous retroelements constitute about 45% of the genome and are epigenetically repressed by DNA methylation [Schulz et al, 2006]. Repression of transcription of LINE-1 retrotransposons is mediated by MeCP2 and MBD2 binding to methylated DNA [Steinhoff et al, 2003]. DNA hypomethylation leads to induction of expression from these elements in cancers. Once expressed, retrotransposons are capable of relocating and integrating into other sites within the genome, leading to insertional mutagenesis [Bera et al, 1998]. This may represent one mechanism by which global demethylation could compromise genomic stability and promote cancer formation and progression. For example, hypomethylation increases the frequency of spontaneous tumor formation in mouse models [Gaudet et al, 2003; Eden et al, 2003].

DNA methylation is involved in the regulation of expression of imprinted genes. Imprinting is mediated by imprinting control regions (*ICR*) located in the vicinity of the imprinted loci, often at a distance of several 100 kb. These regions are often methylated on one allele and have little or no methylation on the other allele, and hence designated differentially methylated regions (DMR). Hypomethylation of the methylated allele of a *DMR* could vitally

alter the regulation of genes controlled by the *ICR*; this could lead to loss of imprinting (LOI) as expression or silencing of both alleles. In this fashion, hypomethylation of *IGF2* leads to frequent loss of imprinting in colorectal cancer [Cui et al, 2003]. Similarly hypomethylation of *DMR-LIT1* initiated reduction in the level of expression of *CDKNIC* in esophageal cancer cell lines [Jelinic and Shaw, 2007; Cui et al, 2002] and bladder cancer cells [Hoffmann et al, 2005].

There are only a limited number of genes reported as activated by DNA hypomethylation in cancer. One example is the oncogene *HOX11.* Expression of *HOX11* in T-cell acute lymphoblastic leukemia correlated well with hypomethylation of its promoter whereas methylation of the promoter was observed in non-expressing cells [Watts et al, 2000]. In particular, hypomethylation appears to increase the transcription of many genes that are involved in invasion and metastasis. Studies on the gene encoding the plasminogen activator, uPA, suggested that it is methylated and silenced in normal prostate and breast cells but becomes expressed in prostate carcinoma and breast tumors. This expression correlated with hypomethylation of the promoter [Pakneshan et al, 2004]. Similarly, there are numerous reports establishing a relationship between hypomethylation and activation of the inhibitor of extracellular proteases *MASPIN* in many cancers [Kisseljova and Kisseljov 2005].

The best investigated genes regulated by hypomethylation are cancer-testis antigens. These genes, exemplified by *MAGE-A1*, are normally expressed exclusively in male germ cells and their promoters are methylated in all somatic cells. Their reexpression in melanoma cells (hence melanoma antigen, MAGE) was linked to hypomethylation of the promoters [De Smet et al, 1996]. There are, e.g. reports of hypomethylation and expression of *MAGE-A1* and five other family members in gastric tumors [De Smet et al, 2004]. In many tumors, hypomethylation of the *CAGE-1* promoter is associated with its expression [Cho et al, 2003]. MAGE genes are also overexpressed in bladder cancer [Fradet et al, 2005], but it has not been investigated whether this is associated with hypomethylation.

1.5 Bladder cancer

Bladder cancer is the fourth most common cancer in men and the most prominent genitourinary tumor affecting both genders. The risk increases with advancing age, most cases being diagnosed in patients between 65 and 84 years. In developed countries most cases present as urothelial carcinoma (synonymous with transitional cell carcinoma of the urinary tract) whereas in some Middle Eastern countries, squamous cell carcinoma of the bladder has

a higher incidence rate [Mitra and Cote 2009]. Although the bladder is the main site, urothelial cancers can also manifest in the renal pelvis, ureter and prostate.

At the time of diagnosis, bladder tumors are staged according to their level of invasion as the basis for determining the appropriate treatment. The TNM ('tumor, node, and metastasis') system is commonly used for this purpose. The prospects of the patient differ dramatically between cases that are restricted to the superficial layers of the bladder (urothelial epithelium and the mesenchymal lamina propria) or those having invading the underlying muscular layers. The most frequent subtype is the papillary type that if restricted to the urothelium is staged as pTa. Together, superficial bladder cancers (Ta, T1 and Tis, a malignant dysplasia still restricted to the epithelial layer) account for 75% to 80% of the cases. Invasive bladder cancers (staged T2-T4) have a strong tendency to metastasise and an according high mortality. Tumors are graded by the degree of cellular atypia and disturbance of urothelial differentiation, where grade1 indicates well differentiated tumors and grade 3 indicates poorly differentiated tumors.

Superficial bladder cancer patient are treated by transurethral removal of the tumor, often followed by adjuvant therapy with cytotoxic drugs like mitomycin or with a bacillus Calmette- Guérin preparation eliciting an immune reaction against the tumor cells. Although many patients are cured, more than half experience recurrences at least once with occasional progression to the invasive stage. Invasive bladder cancer patients are treated by cystectomy with adjuvant chemotherapy or radiotherapy in some cases. Despite radical treatment about half will progress to the metastatic stage [Sánchez-Carbayo and Cordon-Cardo, 2007]. Because of the frequent recurrences, difficult diagnostic procedures and elaborate treatments, bladder cancer is the most costly cancer type in developed countries.

1.5.1 Pathogenesis of bladder cancer

The pathogenesis of transitional cell carcinoma of bladder cancer can be linked to genetic alterations that occur sequentially, starting with chromosomal alterations and point mutations that lead to carcinogenesis, followed by loss of cell cycle control and altered apoptotic regulation enhancing tumor proliferation and finally development of novel cellular properties enabling metastasis. Accumulation of these molecular defects rather than a single defect determines the tumors phenotype. The non-invasive tumors are characterized by changes thought to result in activation of the Ras-MAPK pathway, whereas the invasive tumors are characterized by alterations in *p53* and in the pRB1 regulatory system that controls cell cycle and differentiation [Mitra and Cote 2009].

Low-grade noninvasive tumors are the most common type of bladder tumors characterized by expansion of tumor cells in the urothelial layer that displace the normal cells. Genetic alterations affecting this group of tumors are mainly mutations of certain oncogenes such as FGFR3*, HRAS, PIK3CA* as well as overexpression of *CCND1* and *MDM2*. Deletions of chromosome 9 are the most consistent chromosomal change in bladder tumors and in pTa tumors can represent the only detectable one. Deletions on 9p affect the *CDKN2A* locus that encodes regulators of Rb and p53 such as p16 and p14 tumor suppressor proteins, respectively [Knowles 2006; Schulz 2006]. Tumor suppressor genes with altered function as a result of deletions on 9q include *PTCH*, *DBC1* and *TSC1*. It is not yet understood in detail how suppression of these tumor suppressor genes in bladder cancer favors the expression of the malignant phenotype [Knowles 2008].

In contrast to pTa tumors, muscle-invasive urothelial carcinomas exhibit genomic instability and changes in DNA copy number in many regions of the genome. One target of gene amplifications is the *c-MYC* gene that favors cellular growth and proliferation. Another frequent amplification on 6p22.3 leads to overexpression of the pro-proliferative E2F3 transcription factor along with other genes in the region [Hurst et al, 2008; Wu et al, 2005 and Oeggerli et al, 2004]. Mutations inactivating *p53* represent a major difference between this group and low grade pTa tumors. Increased p53 expression, reflecting accumulation of mutant protein, is related to higher risk of disease recurrence and lower chances of patients' survival [Cote et al, 1998]. Other common features of invasive tumor include overexpression of *MDM2* in some cases and loss of CDK inhibitors like p21 and p57. Inactivation of *RB1* by internal deletions in the locus, allelic loss and altered expression of its protein occurs in up to half of patients with advanced stage urothelial carcinomas. Another region often affected by LOH is 10q; this region encodes the PTEN, a major negative regulator of PI3K signaling. In bladder cancer, these deletions are believed to have the most significant effect on the invasive characteristics of the tumor cells [de Vere White 2008]. Deletions of the short arms of chromosomes 3 and 8 are also common in high grade, muscle-invasive tumors [Gallucci et al, 2005].

One of the most important issues in bladder cancer research is which genetic and epigenetic changes are characteristic of superficial tumors, especially high grade noninvasive papillary tumors (pTaG3) and tumors extending into the lamina propria (pT1). These may to various extent harbor changes also found in invasive cancers, especially p53 mutations. The frequency of mutations in the tyrosine kinase receptor FGFR3 appears to decrease gradually

in tumors with increasing grade and stage. [Hernandez et al, 2006]. While the frequency of mutations in *FGFR3* decreases that of *P53* mutations increases during this critical transition and their combination may yield a good estimate of the risk of progression within this heterogeneous group of tumors [Bakkar et al, 2003; van Rhijn et al, 2004].

1.5.2 Biomarkers in bladder cancer

Tumor biomarkers are urgently needed for a number of applications in the management of bladder cancer, such as identification of individuals with high risk, screening for early stages of the disease as well as diagnosis, prognosis and prediction of therapeutic response [Duffy et al, 2007]. Perhaps the most important need exists for markers that allow (1) stratifying patients with superficial tumors by risk of recurrence and progression and (2) detecting recurrences early without the need for cystoscopy.

DNA methylation is emerging as a very promising tumor marker. Many genes that play critical roles in bladder tumor development or progression can be repressed by promoter DNA methylation. Hence genes that are methylated during the early stages of bladder tumorigenesis could be used as diagnostic markers while those that undergo methylation during progression of bladder tumor could be used as prognostic markers [Duffy et al, 2009]. There are several reasons why DNA methylation markers may be particularly well suited for this purpose. First, DNA hypermethylation is a pathological process and affects CpG-islands that are never methylated in healthy tissues. Therefore, the specificity of assays detecting this change is in theory excellent. In practice, the specificity is limited by partial methylation in ageing and preneoplastic tissue, a problem very relevant in bladder cancer (see below). Secondly, the sensitivity of modern assays using PCR techniques with fluorescence detection of products is very high meaning that minute amounts of DNA from tumor cells shed into urine or circulating in serum are sufficient to detect hypermethylated DNA. Thirdly, assays using DNA are more robust because of the superior stability of this nucleic acid and of methylation modifications in comparison to RNA and proteins. Fourthly, promoter methylation is restricted to specific genomic regions, making it easy to design primers that interrogate these regions of interest and easily determine the methylation status of the promoters of a select number of genes. By comparison, mutations in genes like *p53* and *APC*, which are also being studied as cancer biomarkers, are often distributed over many sites necessitating the designing of multiple primers thereby increasing the financial burden and limiting the sensitivity [Hainaut and Hollstein, 2000].

A prerequisite for such studies, however, is a good, if not comprehensive knowledge of the methylation changes in the cancers of interest and the frequency of their occurrence in various stages and subtypes. There are already a number of studies aiming at detection or classification of bladder cancers by DNA methylation assays (see examples below). Importantly, to achieve practically useful sensitivities and specificities, recent studies investigate 10-12 different DNA segments.

Christoph et al, 2006 used quantitative methylation-specific real-time PCR to demonstrate that hypermethylation of the promoter region in tumor samples was common for *APAF-1* (100%), *DAPK-1* (74%) and *IGFBP-3* (66%), but not for *CASP-8* (3.6%). Hypermethylation occurred less frequently in the normal urothelium group. The *APAF-1* methylation levels significantly correlated with tumor stage and tumor grade, also *APAF-1* and *IGFBP-3* methylation levels were able to separate tumors with higher recurrence risk from low-risk A limitation of the study is that all controls came from patients not at risk for urothelial cancer. Furthermore, the high methylation frequency of *APAF-1* was not replicated in other studies.

Similarly, Yates et al, 2007 used, quantitative methylation-specific PCR to show that promoter hypermethylation of *RASSF1A*, *E-cadherin (CDH1)*, *TNFSR25*, *EDNRB* and *APC* seems a reliable predictor of tumor progression in bladder cancer. It is associated with aggressive tumors and could be used to identify patients with either superficial disease requiring radical treatment or a low progression risk suitable for less intensive surveillance.

In another study, methylation-specific PCR showed that the methylation of *LAMA3* and *LAMB3* were correlated significantly with several parameters of poor prognosis (tumor grade, growth pattern, muscle invasion, tumor stage, and ploidy pattern), whereas methylation of *LAMC2* was associated with shortened patient survival. Also the methylation frequencies of *LAMA3* helped to distinguish invasive (72%) from noninvasive (12%) tumors. These suggest that methylation of Laminin genes has potential clinical applications in bladder cancers [Sathyanarayana et al, 2004]**.**

In other cancers, prominently breast cancer, the recent development of DNA microarrays for determining gene expression profiles has been applied to distinguishing subtypes with distinct clinical course and response to therapy [Alexe et al, 2007]. These successes have led to attempts at applications in the management of bladder cancer as well. A number of studies have compared gene expression in bladder cancer in comparison to the normal tissue counterpart or between different stages or histological subtypes of bladder cancer to identify individual (prognostic) markers or expression patterns that correlate with the clinical outcome.

Sanchez-Carbayo et al, 2003, used cDNA microarrays to elucidate the gene expression profiles of early stage bladder tumor in comparison to advanced stage bladder tumor to identify changes in gene expression during bladder cancer progression. In particular, the microarray results were able to segregate carcinoma in situ (CIS) from papillary superficial lesions and identified further subgroups within early-stage and invasive tumors. Another microarray study on 40 bladder tumors samples revealed clinically vital subgroups of bladder carcinoma. The microarray analysis classified the tumors into pTa, pT1, and pT2-4 and also identified further subgroups within the pTa tumors. Furthermore, using another panel of 68 tumors, a 32-gene molecular classifier was used in this study to segregate benign and muscle-invasive tumors with close correlation to pathological staging [Dyrskjot et al, 2003].A microarray study from this institution by Modlich et al, 2004, comparing 20 invasive and 22 superficial bladder tumors obtained from 34 patients with known outcome regarding disease recurrence and progression, was able to classify tumor samples according to clinical outcome as superficial, invasive, or metastasizing tumors. Also, they were able to identify several distinct clusters of genes that were specific to the superficial or the invasive tumors.
Although intriguing, the results from these different studies are quite divergent and – other than in breast cancers- there are to date no definitive gene expression profiles that could be used in practice to classify bladder cancers.

1.6 Selected genes from microarray studies

As a result of microarray studies conducted prior to the start of this thesis (described below, see also [Dokun et al., 2008, Modlich et al. 2004]) several genes seemed of interest for a detailed analysis of their expression and DNA methylation in bladder cancer. Some information on these follows.

1.6.1 *S100A4* and *S100A9*

The products of the *S100A4* and *S100A9* genes belong to the same calcium-binding family of S100 proteins with twenty well recognized members in humans. Each protein is encoded by a different gene, of which 16 are clustered on chromosome 1q21. These proteins range from 10-12 kDa and exist only in vertebrates. Structurally, they are capable of forming homodimers, heterodimers and oligomers. They possess both intracellular and extracellular functions in a tissue-specific manner. Intracellular functions include calcium homeostasis, regulation of protein phosphorylation and modulation of enzyme activities. Among the known extracellular roles are leukocyte chemoattraction, activation of macrophages and

regulation of cell proliferation. Some S100 proteins have tumor suppressor properties and others act as tumor promoters [Salama et al, 2008]. A summary of the functions discussed for S100 proteins is given in Figure 1.2.

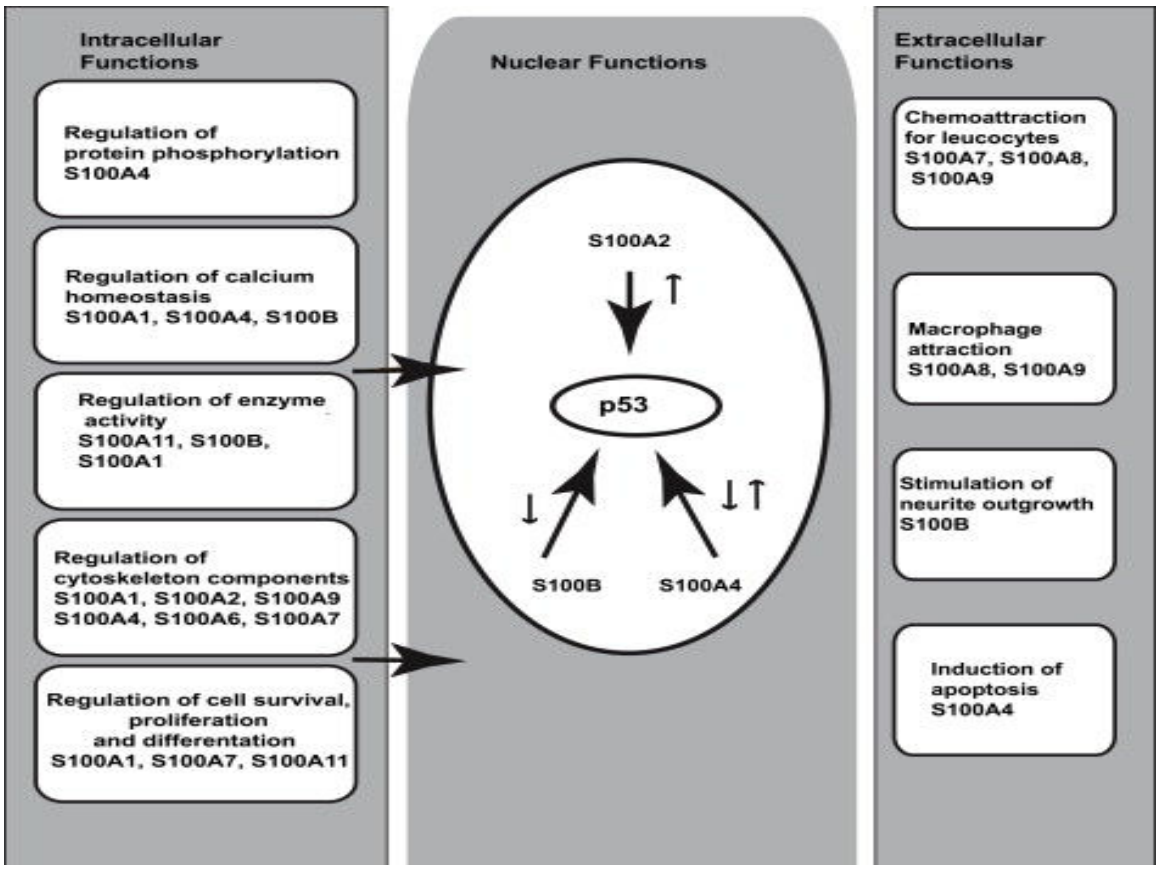

Fig. 1.2: S100 proteins and their functions as depicted by Salama et al, 2008

S100A4, also known under various other names, including metastasin (*Mst1*), calvasculin, and *CAPL*, has been shown to interact with a number of targets like methionine aminopeptidase, *p53* as well as proteins that function in cytoskeletal rearrangement and cell motility such as F-actin and the heavy chain of nonmuscle myosin II. The interaction of these proteins with S100A4 is calcium dependent suggesting that S100A4 relays effects of changes in the intracellular calcium concentration to its interaction partners. S100A4 regulates p53 by engaging with its C-terminal region and thereby blocking phosphorylation of p53 by protein kinase C (PKC). In this fashion it prevents *p53* from binding to its DNA recognition sequence. Expression of S100A4 favors the selection for an invasive phenotype, likely because of its interaction with targets like cytoskeletal proteins [Sarah et al, 2006; Sherbet 2008].

When S100A4 is present extracellularly, it regulates different aspects of tumor progression, including stimulation of cell motility, angiogenesis, induction of matrix metalloproteinases, and regulation of tumor-specific transcription factors [Helfman et al, 2005]. S100A4 has been reported to be more strongly expressed in invasive bladder cancers and has been ascribed a critical role in the pathogenesis of the disease [Davies et al, 2002; Matsumoto et al, 2007]. Of note, studies using immunohistochemistry have reported that the expression is highly heterogeneous, though [Agerbaek et al, 2006]. S100A4 is also strongly expressed in other types of cancers. It is upregulated in breast carcinoma in comparison to benign breast tumors and the upregulation correlates significantly with a poor prognosis for the patients [Wang et al, 2000]. In thyroid carcinomas S100A4 is highly upregulated and likewise linked to thyroid tumor invasion and metastasis [Zou et al, 2005].
S100A9 forms a heterodimer complex with S100A8. The two proteins are up-regulated in many cancers including gastric, prostate and colorectal cancer. They function in the regulation of cell proliferation and also act as chemo-attractants which facilitate the homing of tumor cells to pre-metastatic sites within the lung parenchyma [Salama et al, 2008]. S100A9 is highly expressed in prostate cancer and has been proposed to be involved in early events in prostate tumor development as well as progression of prostate carcinomas [Hermani et al, 2005]. Similarly, S100A9 contributes to important aspects of the malignant phenotype such as invasion, migration and proteinase expression in gastric cancer cells [Yong and Moon, 2007].

1.6.2 *SNCG*

The product of the *SNCG* gene at chromosome 10q23, γ-synuclein, belongs to the Synuclein family of neuronal proteins, which also includes α-synuclein and β-synuclein. They have numerous structural characteristics in common and share sequence homologies. The γ-synuclein has a different C-terminus from α-synuclein and β-synuclein and it is believed that this difference dictates the different subcellular localization of *SNCG* from the other members. The C-terminus of α-synuclein and β-synuclein confers nuclear localization, while that of the γ-synuclein determines a cytosolic localization [Ahmad et al. 2007]. Synucleins have been implicated in the pathogenesis of neurodegenerative diseases and cancer. Expression of *SNCG* is usually tissue-specific and has been described as being restricted to the nervous system, but *SNCG* is highly expressed in advanced-stage breast and ovarian cancers, hence the alternative name of the protein, breast cancer-specific protein 1 (*BCSG1*).

When overexpressed, *SNCG* stimulates cancer cell proliferation and metastasis. It is believed that demethylation of the CpG island encompassing the gene promoter region could be a reason for the abnormal gene expression [Yanagawa et al 2004]. *SNCG* has been reported to be highly expressed in most tumors from liver, oesophagus, colon, gastric, lung, prostate, cervical, and breast, but rarely expressed in tumor-matched nonneoplastic adjacent tissues [Liu et al, 2005]. Studies directed at discovering the mechanisms responsible for the oncogenic effects of *SNCG* showed that upregulation of *SNCG* in breast cancer cells initiated a more malignant phenotype with increased cell motility, enhanced resistance to drugs and an enhanced rate of chromosomal instability [Guo et al, 2007].

1.6.3 *LCN2*

Lipocalin-2 (*LCN2*), also known as 24p3, NGAL, belongs to a family of soluble proteins. LCN2 exists in three different forms, a 25 kDa monomer, a 46 kDa disulfide-linked homodimer and a 135 kDa disulfide-linked heterodimer with neutrophil gelatinase-B. Lipocalin-2 binding of gelatinase-B prevents its degradation. The protein also functions in iron transport. After binding iron ions, it binds to two cell surface receptors, 24p3R and megalin-cubulin, which facilitate its entry into the cell via endocytosis. Subsequently the iron dissociates from *LCN2* and is used by the cell. Some evidence supports the view that *LCN2* also functions in apoptosis via a converse mechanism. When *LCN2* has entered the cell, it accepts intracellular irons from siderophores and subsequently transports it to the extracellular surface. The ensuing intracellular shortage of iron signals the cell to undergo apoptosis [Rubinstein et al, 2008].

LCN2 has been implicated in the progression of breast cancer and high expression of *LCN2* correlated with invasive breast cancer. Also, overexpression of *LCN2* in breast cancer cells increased the expression of mesenchymal marker while suppressing the expression of epithelial markers. LCN2 was also found to increase cell motility and invasiveness. Accordingly, knockdown of the protein lead to reduced cell migration and reversion of the mesenchymal phenotype [Yang et al, 2009].

1.7 Aim of study

Bladder cancer is one of the most prominent urogenital cancers with an incidence rate of 357,000 and a mortality rate of 145,000 annually worldwide. A radical therapy, cystectomy is currently being used to treat patients with muscle-invasive bladder cancer, but still about half of such patients eventually develop metastasis and die within a few years after surgery. Also, contemporary chemotherapies are poorly efficacious despite having severe adverse effects. Current studies focus on elucidating the etiological factors and mechanisms involved in the development and progression of bladder cancer in order to reveal molecular biomarkers and molecular targets which could be used in the diagnosis, stratification and treatment of bladder cancer patients.

DNA methylation, an epigenetic mechanism, has been highlighted as a critical factor in the establishment and maintenance of many biological processes, including the regulation of gene expression. Alterations in DNA methylation patterns have been implicated in the pathogenesis and progression of many human diseases including cancers [Schulz and Dokun, 2009]. In cancers both DNA hypermethylation and genome-wide DNA hypomethylation exist, are well detectable and are often characteristic of particular subtypes and stages of the disease. These characteristics have brought DNA methylation into the spotlight as a potential epigenetic marker which could be exploited in the screening, diagnosis, prognosis and treatment of many cancers. Concurrently, the advent of cDNA microarrays has found a lot of applications in the study of carcinogenesis, especially in the identification of novel genes or groups of genes preferentially upregulated in cancers in comparison to their normal counterparts. There are already numerous elegant reports on the use of such applications for detection of cancer biomarkers and identification of pathological mechanisms. Profiling of gene expression using microarray technology has likewise helped in the better classification of several cancer types. The utilisation of cDNA microarrays to screen for potential epigenetic markers is relatively new in the field of cancer research and holds promises as well as challenges.

Hence, the aim of this study was to use the new state-of-the-art techniques in the field of molecular and cell biology to identify novel candidate genes or clusters of genes which are differentially expressed in bladder tumors in comparison to normal bladder that could be used as tumor markers in the diagnosis and prognosis of bladder cancer. In particular, hypermethylation of individual genes and hypomethylation of retroelement sequences are well established in this type of cancer, whereas there were essentially no studies on DNA hypomethylation of individual genes in bladder cancer. Thus, the project aimed primarily at

identifying genes that are activated in invasive bladder cancers by DNA hypomethylation. Moreover, in other cancer types, many candidate genes of that kind are associated with cancer progression and metastasis (see 1.6 for examples and [Hoffmann & Schulz 2005] for a review). Therefore, methylation patterns of such genes might provide particularly good markers for identifying bladder cancers with a high risk of progression.

MATERIALS AND METHODS

2.1. Tissues, Cells and Materials

2.1.1 Bladder and Prostate cancer cell lines

Thirteen bladder cancer cell lines (Table 2.1) and two prostate cancer cell lines (Table 2.2) were used derived from urothelial or prostate cancers of various pathologic stages and grades. The patients' ages ranged from 51 to 84 years. The fibroblasts from human foreskin were also used in some experiments. All cell lines were cultured by standard cell culture procedures (Section 2.9.1). RNA and DNA were extracted from these cell lines and stored at -80^{o}C and 4^{o}C respectively.

Table 2.1: Bladder cancer cell lines (Neveling et al, 2007)

Name	Grade/stage of tumor	Sex of patients	Age of patients
UM-UC3	UC	M	-
BFTC909	UC, G3	M	64
647v	UC, G2 pT1	M	59
RT112	UC, G2 papillary	F	-
5637	UC	M	58
639v	UC, G3	M	69
BFTC905	UC, G3 papillary, pTa	F	51
HT-1376	UC, G3 pT2	F	58
J82	UC, poorly differentiated, papillary	M	58
RT4	UC, G1 pT2	M	63
SD	UC	-	-
SW1710	UC, G3 papillary	F	84
VMCub1	UC, G3 papillary	M	-

Table 2.2: Prostate cancer cell lines

Name	Grade/stage of tumor	Sex of patients	Age of patients
PC3	Grade IV, adenocarcinoma	M	62
LNCaP	Lymph node metastasis	M	50

2.1.2 Bladder Tissue samples

Normal bladder and bladder tumor specimens were obtained from the tissue bank of the Dept of Urology of the University Clinic Duesseldorf, Germany (Table 2.3). Prior to transurethral resection and cystectomy, patients consent was obtained by a standard form approved by the ethics committee of the Medical Faculty. After surgery, the tissue specimens were sent to pathologist for histological staging and grading. Subsequently, the samples were stored in liquid nitrogen until needed for downstream applications. Prior to utilization of any tissue sample, they were subjected to internal quality control procedures.

In this study, samples were from 10 females and 40 males with ages ranging from 55 to 95 years were used. Overall 50 samples were used comprising 18 normal tissues and 32 bladder tumors. All tumors were classified as urothelial carcinoma. Predominantly advanced histological stages were available; pTa and pT1 were represented by one and two samples respectively. The remainder, 29 samples were from invasive stage cases, comprising 9 pT2, 15 pT3 and 5 pT4. Most of the tumors were graded as G3 except for 9 graded as G2. Among the invasive tumors, 19 showed no traces of metastasis (N0, M0) while the remaining 10 had metastasized to the lymph nodes (N1 or N2).

RNA and/or genomic DNA were extracted from these tissues with the aid of a Mikro-Dismembrator. For each extraction, 100 mg of the frozen tissue was measured and fixed in the Dismembrator following the manufacturers' recommendation; a shaking frequency of 2500 rpm for 30 s was used to ensure an efficient grinding of the tissue to powder. Subsequently, the powder produced was either used immediately for RNA/DNA isolation or stored at -70^{o}C until needed.

Table 2.3: Clinical characteristics of bladder tissues used in this project. Staging and grading were performed according to the UICC 1997 classification.

Patient			Tumor		
No	**Sex**	**Age**	**Stage**	**Lymph node**	**Grade**
15	m	70	normal	--	--
18	m	71	normal	--	--
32	m	61	normal	--	--
112	m	66	normal	--	--
127	f	55	normal	--	--
207	m	70	normal	--	--
253	m	60	normal	--	--
257	f	76	normal	--	--
259	f	63	normal	--	--
273	m	68	normal	--	--
274	m	66	normal	--	--
357	f	57	normal	--	--
363	m	75	normal	--	--
365	m	65	normal	--	--
726	m	69	normal	--	--
3	m	75	pT3b	N0	G2
12	m	70	pT3a	N0	G3
41	f	54	pTa	Nx	G2
52	f	87	pT3b	N0	G3
54	m	73	pT4a	N1	G3
61	m	75	pT3b	N0	G3
64	m	74	pT3b	N2	G3
67	f	94	>pT2	Nx	G3
69	m	77	pT3b	N0	G3
104	m	61	pT1	N0	G2
109	m	68	pT4a	N0	G3
114	f	66	pT1	N0	G2-3
115	m	74	pT3a	N2	G3
120	m	66	pT2	N0	G2
150	f	78	pT3a	N2	G3
168	m	64	pT3a	N2	G3
172	m	72	pT3a	N0	G3
205	f	65	pT2	N0	G2
212	m	73	pT2a	N1	G2
224	m	65	pT2a	N0	G2
231	m	95	>pT2	Nx	G2
246	m	61	pT4a	N2	G3
320	m	67	pT2a	N1	G3
322	m	70	pT4a	N0	G3
356	m	54	pT3b	N0	G3
360	m	76	pT4a	N0	G3

2.2 Chemicals and Regents

REAGENTS	COMPANY	LOCATION
Agarose	Sigma Aldrich	Steinheim
Ampicillin	Sigma Aldrich chemical	Taufkirchen
Aprotinin	Calbiochem	USA
6X loading buffer	Fermentas	St-Leon-Rot
5-Aza-2-deoxycytidine (5-Aza-dC)	Sigma Aldrich chemical	Taufkirchen
Collagen IV solution	Sigma Aldrich	Steinheim
Dimethyl sulfoxide (DMSO)	Sigma Aldrich chemical	Taufkirchen
DNA ladder	Fermentas	St-Leon-Rot
dNTP mix	Fermentas	St-Leon-Rot
EcoRI	Fermentas	St-Leon-Rot
4-(2-hydroxyethyl)-1-piperazineethane sulfonic acid (HEPES)	Sigma Aldrich chemical	Taufkirchen
Oligo(dT)	Roche	Mannheim
Protein-loading buffer	Fermentas	St-Leon-Rot
Protein-markers	PeqLab	Erlangen
TRIzol Reagent	Invitrogen	Mannheim
Trypsin/EDTA	Biochrom	Berlin
Trypsin inhibitor	Sigma Aldrich chemical	Taufkirchen

2.3 Enzymes and antibodies

Proteinase K	Qiagen	Hilden
Ribonuclease Inhibitor	Fermentas	St-Leon-Rot
Superscript III	Invitrogen	Mannheim
Anti-streptavidin antibody (goat) biotinylated	Vector laboratories	UK
Goat IgG	Sigma Aldrich	Steinheim

2.4 Kits

Blood and cell culture-DNA kit	Qiagen	Hilden
EZ DNA methylation Gold kit	Zymo research	Freiburg
Fast plasmid mini kit	Eppendorf	Hamburg
RNeasy kit	Qiagen	Hilden
One Shot TOP 10	Invitrogen	Mannheim
One-cycle target labelling kit	Affymetrix	UK
TOPO TA cloning kit	Invitrogen	Groningen

2.5 Growth media, buffers and solutions

DEPC-H_20	Fermentas	St-Leon-Rot
Dulbecco's Modified Eagle's Medium (DMEM)	Invitrogen	Mannheim
RPMI medium 1640	Invitrogen	Mannheim
Minimum essential medium (MEM)	Invitrogen	Mannheim
Keratinocyte Serum Free Medium (KSFM)	Invitrogen	Mannheim
Trypsin / EDTA	Sigma	Steinheim
Phosphate buffered saline (PBS)	Biochrom	Berlin
Penicillin/streptomycin (P/S)	Biochrom	Berlin
Luria Agar	Becton, Dickinson	USA
Luria Broth base	Invitrogen	Mannheim
Hanks Balanced Salt Solution (HBSS)	Invitrogen	Mannheim
Versene	Invitrogen	Mannheim

DEPC-H_20

0.1% (v/v) Diethylpyrocarbonate in H_20

LB medium

25 g Luria broth base

in 1000 ml of H_2O

LB Agar

30.5 g LB Agar base and 1mg/ml Ampicillin

in 1000 ml of H_2O

DMEM + GlutaMax-1 (Bladder cancer cell line culture medium)

+ 4.5 g/L glucose

+ 10% Fetal Calf Serum

+ 1% Penicillin/Streptomycin

RPMI 1640 + Gluta Max-1 (Prostate cancer cell line culture medium)

+ 4.5 g/L glucose

+ 10% Fetal Calf Serum

+ 1% Penicillin/Streptomycin

MEM Medium (Fibroblast culture medium)

+ 10% Fetal Calf Serum

+ 1% Penicillin/Streptomycin

Keratinocyte Serum Free Medium (Primary urothelial cells culture medium)

+ 2.5 µg Epidermal Growth Factor

+ 25 mg Bovine Pituitary Extract

+ 1% Penicillin/Streptomycin

Trypsin / EDTA

+ 0.5 g porcine trypsin

+ 0.2 g Tetrasodium.EDTA/L HBSS

Penicillin/Streptomycin

+ 10,000 U penicillin

+ 10 mg streptomycin

per 1 ml in 0.9% NaCl

PBS

+ 137 mM NaCl

+ 2.7 mM KCl

+ 4.3 mM Na_2HPO_4

+ 1.47 mM KH_2PO_4

Transport medium

HBSS

+ 10 mM HEPES (pH 7.4)

+ 2 KU Aprotinin

Washing buffer

+ 0.1 ml aprotonin (Calbiochem, 100 KU/ml)

+ 0.5 ml 1 M HEPES

+ up to 50 ml versene

Versene

+ PBS

+ 0.1% EDTA

Trypsin inhibitor

1 mg/ml in KSFM

12X MES Stock buffer

For 1000 ml

+ 64.61 g MES hydrate

+ 193.3 g MES sodium salt

+ 800 ml H_2O

2X Hybridization buffer

For 50 ml

+ 8.3 ml 12X MES stock buffer

+ 17.7 ml 5M NaCl

+ 4 ml 0.5 M EDTA

+ 0.1 ml 10% Tween-20

+ 19.9 ml H_2O

Wash buffer A

For 1000 ml

+ 300 ml of 20X SSPE

+ 1 ml 10% Tween-20

+ 699 ml of H_2O

Wash buffer B

+ 83.3 ml 12X MES stock buffer

+ 5.2 ml 5M NaCl

+ 1 ml 10% Tween-20

+ 910.5 ml H_2O

2X Stain buffer

For 250 ml

+ 41.7 ml 12X MES stock buffer

+ 92.5 ml 5M NaCl

+ 2.5 ml 10% Tween-20

+ 113.3 ml H_2O

10 mg/ml Goat IgG stock

50 mg resuspended in 5 ml of 150 mM NaCl

SAPE stain solution

2X stain buffer

50 mg/ml BSA

1 mg/ml Streptavidin Phycoerythrin (SAPE)

+ 270 µl H_2O

Antibody solution mix

2X stain buffer

50 mg/ml BSA

10 mg/ml Goat IgG stock

0.5 mg/ml biotinylated antibody

2.6 Oligonucleotide primers and PCR assays

2.6.1 Oligonucleotide primers

Oligonucleotides were routinely purchased from MWG Biotech, Ebersberg. Quantitect assays were obtained from Qiagen, Hilden. TaqMan assays were acquired from Applied Biosystems, Darmstadt. All primers and assays used are listed in Table 2.4

2.6.2 PCR reagents

QuantiTect SYBR Green PCR Kit	Qiagen	Hilden
HotStarTaq-DNA polymerase	Qiagen	Hilden
LightCycler Faststart DNA Master SYBR Green 1	Roche	Mannheim
TaqMan universal PCR Master Mix	Roche	Mannheim
LightCycler Taqman Master	Roche	Mannheim

Table 2.4: Oligonucleotide primers and PCR assays

	Annealing (°C)	Cycles
Bisulfite sequencing primers		
S100A4 prom forward: 5′-GTTGAGTTATGTATATTGGGTGGTG-3′ S100A4 prom Reverse: 5′-TACCAATCAAACCAACACAACTCAC-3′	59	38
S100A4 Intron Forward: 5′-TGTTTTTGAGATGTGGGTTTG-3′ S100A4 Intron Reverse: 5′-CACAATTACCTTCTACCTTTC-3′	58	38
S100A9 prom forward: 5′-TGAGTGGTGTTAGAGGAGTAGT-3′ S100A9 prom Reverse: 5′-CCACACAAAATATTTACCAAAACTATAC-3′	58	38
SNCG prom forward: 5′-GGTTGAGTTAGTAGGAGTTTA-3′ SNCG prom Reverse: 5′-CCTACCATACCCCACTTACCC-3′	58	38
LCN2 prom forward: 5′-TTGGGATTTAGTTGAGTAGG-3′ LCN2 prom Reverse: 5′-CACTTAACAAAATTTCTACACCT-3′	53	38
RT-PCR primers		
S100A4 forward: 5′-AGCTTCTTGGGGAAAAGGAC-3′ S100A4 reverse: 5′-CCCCAACCACATCAGAGG-3′	59	40
SNCG forward: 5′-ATGGATGTCTTCAAGAAGGG-3′ SNCG reverse: 5′-CTAGTCTCCCCCACTCTGGG-3′	59	40
LCN2 forward: 5′-CTCCACCTCAGACCTGATCC-3′ LCN2 Reverse: 5′-ACATACCACTTCCCCTGGAAT-3′ Universal Probe Library, Probe #84	60	45
GAPDH forward: 5′-TCC CAT CAC CAT CTT CCA-3′ GAPDH reverse: 5′-CAT CAC GCC ACA GTT TCC-3′	59	40
RT-PCR assays		
S100A9: Quantitect Primer Assay QT00018739	55	40
DEPDC1: Quantitect Primer Assay QT00069230	55	40
TBP: Quantitect Primer Assay QT00000721	55	40
JMJD1A: Quantitect Primer Assay QT00088879	55	45
H2AFY: Quantitect Primer Assay QT00059143	55	45
PCAF: Quantitect Primer Assay QT00092267	55	45
MYST4: Quantitect Primer Assay QT00008638	55	45
CBX7: Quantitect Primer Assay QT00051149	55	45
SIRT1: Quantitect Primer Assay QT00051261	55	40
DDX58: TaqMan Gene Expression Assays Hs00204833_m1	60	40
KLF4: TaqMan Gene Expression Assays Hs00358836_m1	60	40
SIRT7: TaqMan Gene Expression Assays Hs00213029_m1	60	40
LOXL2: TaqMan Gene Expression Assays Hs00158757_m1	60	40
TBP: TaqMan Gene Expression Assays Hs00427620_m1	60	40

2.7 Equipments and materials

AbiPrism 7900	Applied Biosystems	Darmstadt
Agilent Chip	Agilent technologies	Waldbronn
ELISA easy Reader	SLT labinstruments	Austria
Electrophoresis system	Owl Scientific	USA
Gel Print 2000i	MWG-Biotech	Ebersberg
Gel Electrophoresis system	Biometra	Göttingen
MWG Human 30K Array	MWG Biotech	Ebersberg,
HG U133A 2.0 Array	Affymetrix	UK
GeneChip Scanner 3000	Affymetrix	UK
Light Cycler II	Roche	Mannheim
LightCycler capillaries	Roche	Mannheim
Nanodrop	Nanodrop technologies	Wilmington, USA
Photometer	Eppendorf	Köln
pH meter	WTW	Weilheim
T3 Thermocycler	Biometra	Göttingen
Trio Thermoblock	Biometra	Göttingen
Mikro-Dismembrator	B.Braun International	Melsungen, Germany
Nikon ECLIPSE E400	Nikon	Duesseldorf
Nikon ECLIPSE TE400-S	Nikon	Duesseldorf

2.8 Softwares and databases

Genesis 1.0

Microsoft Office 2007

Lucia G version 4.80

NIS-Elements D 2.30

SPSS

Ensembl genome-wide MeDIP data

GeneChip Operating software (version 1.3, Affymetrix)

www.ncbi.nlm.nih.gov

www.ensembl.org

2.9 Cultivation of human cells

2.9.1 Culture of cancer cell lines and fibroblasts

Human bladder cancer cell lines previously stored in liquid nitrogen were thawed and cultured in T75 flasks containing 12 ml of DMEM medium (4.5 g/L glucose + 10% FCS + 1% P/S) at 37°C with 5% CO_2. Cells were allowed to grow until 70% confluent before they were passaged. When the desired cell density was attained, the culture medium was aspirated; cells were washed with 4 ml of PBS, followed by addition of 2.5 ml of trypsin-EDTA solution. The trypsinization was for 2 min at room temperature for cells that detached easily from the flask. For cells that formed a more adherent monolayer, the flask was kept in the incubator for 2 min. After the cells have fully detached from the flask, serum-containing culture medium was added to inhibit the trypsin activity. Cells were subsequently seeded into new flasks at a ratio of one to ten. Twenty-four hours after the passage the medium was changed and then every three days afterwards until the desired cell density was reached and the cells were passaged again. For human fibroblast culture, the MEM Medium (10% FCS + 1% P/S) was used. Human prostate cancer cell lines were culture with RPMI 1640 + GlutaMax Medium (10% FCS + 1% P/S) and passaged as described above.

2.9.2 Preparation of primary urothelial cells from human ureters

On the first day, after obtaining patients consent, healthy ureters from nephrectomies were quickly transferred into transport medium at room temperature. The transport medium was aspirated followed by washing of the ureter in washing buffer. Subsequently, the ureter was transferred to a 10 ml dish containing washing buffer. The connective tissues and fat pads were removed. The ureter was then washed in a new 10 ml dish with washing buffer. It was then cut open horizontally across its two outlets, inverted with the epithelial side facing down in the washing buffer and then preserved overnight at 4°C. A mixture of 12 ml of PBS and 300 µl of collagen IV solution was prepared in one or two 75 cm^2 cell culture flasks to facilitate the adhesion of the urothelial cells to the bottom of the flask; for small ureter segments, a 25 cm^2 cell culture flask was used. In either case the flask was stored overnight at 4°C.

On the second day, the washing buffer was aspirated; the ureter was gently washed with KSFM medium with or without supplements. The epithelial cells were gently stripped off from the connective tissues with the aid of two sterile Pasteur pipettes; taking extra caution to ensure no connective tissue cells were stripped off along. The stripped off urothelial cells came off as flakes. A 10 ml glass pipette was used to carefully transfer these flakes to a sterile 50 ml conical tube. This was followed by centrifugation at 1000 rpm for 5 min to collect the cell pellet. The mixture of PBS and collagen was removed from the 75 cm^2 cell culture flask, followed by washing of the flask with PBS; 10 ml of complete KSFM (+ EGF + BPE + 1% P/S) was transferred into the flask. Immediately after pelleting the urothelial cells, the supernatant was aspirated and the cell pellet was gently resuspended in 5-10 ml of complete KSFM and seeded into the cell culture flasks to obtain 50% confluency.
On the third day, the medium containing unattached cells was aspirated, the flask was washed once with PBS and fresh medium was added. Three to seven days later, after the cells had grown to near confluency, they were washed with PBS once, followed by addition of 10 ml versene at room temperature for one minute. After aspiration of the versene, 3 ml of trypsin was added to the flask and left for a minute to remove the residual fibroblasts growing on top of the urothelial cell layer. The flask was gently swirled, and the detached fibroblasts were removed. Another 3 ml of trypsin was added to the flask, which was incubated at 37^oC for 3 min. The flask was briefly checked under the microscope to ensure that the urothelial cells had detached. Then immediately, 6 ml of trypsin inhibitor was added to the flask to neutralise the trypsin. The cell suspension was transferred to a 50 ml conical tube; the flask was washed with 10 ml of KSFM to remove the remaining cells from the flask, which was then added to the 50 ml tube. This was followed by a centrifugation at 1000 rpm for 5 min at room temperature. Following centrifugation the supernatant was aspirated and the cell pellet was resuspended in fresh complete medium and seeded as required for the particular experimental set-up.

2.9.3 Treatment of cultured cells with demethylating agent

In order to investigate the effect of DNA methylation on gene expression, cells were cultured in T75 flasks until about 70% confluency. Then they were seeded and cultured in duplicates in 10 cm tissue culture plates. One of the plates was treated with the demethylating agent 5-aza-2-deoxycytidine (5-aza-dC) at 2 µM in fresh medium every 24 hr for three days while the other received only fresh medium. The cells were cultured over 3 days and the medium was replaced for both plates everyday. After 3 days the cells were harvested and RNA extracted.

2.10 Preparation of nucleic acids from human cells

2.10.1 RNA isolation from cultured cells and frozen tissues

The RNeasy mini kit was used for the extraction of RNA from cultured cells. As a rule, when cells had attained a confluency of about 70%, the culture medium was removed and 1 ml of QIAzol lysis reagent was added to each flask and mixed until a viscous solution was obtained. Subsequently the solutions were transferred to the collection tubes and kept at room temperature for 5 min. One hundred µl of chloroform was then added to each tube, vortexed for 15 s and then kept at room temperature for an additional 3 min. This was followed by centrifugation at 12,000 g for 15 min at 4^{o}C. The centrifugation separated the sample into three phases; the upper aqueous phase was transferred to a collection tube. An equal volume of 70% ethanol was added to the collection tube. The tube was immediately vortexed. Subsequently 700 µl of each sample was added to an RNeasy spin column followed by centrifugation at 8000 g for 15 s at room temperature. This was followed by addition of 700 µl of Buffer RW1 and a centrifugation step at 8000 g for 15 s. After this, 500 µl Buffer RPE was added and the centrifugation step was repeated. Finally the RNA was eluted into a new tube by the addition 30 µl of RNase-free water to the spin column and centrifugation at 8000 g for one minute. For RNA extraction from frozen tissues, the tissues were initially converted to powder (Section 2.1.2). 1 ml of QIAzol lysis reagent was added to the powder and the rest of the procedure was performed in the same way as the RNA extraction from cultured cells.

2.10.2 Genomic DNA isolation from cultured cells

High molecular weight genomic DNA was isolated from cultured cells using the Qiagen Genomic DNA kit. Required buffers were in advance prepared following instructions from the kit handbook. Cells were cultured until about 70% confluency and then harvested by trypsinization. Cell pellets were obtained after centrifugation at 15,000 g for 10 min at 4^{o}C. The pellets were subsequently washed in 4 ml of cold PBS and then recentrifuged at 15,000 g for 10 min at 4^{o}C. The supernatant was removed and the cells were resuspended in PBS. To each sample a mixture of 19 µl of RNase A stock solution and 9.5 ml of Buffer G2 was added. The samples were homogenized and later transferred to a 50 ml screw-cap tube. Proteinase K solution was subsequently added and thoroughly mixed with the homogenate. The homogenate was incubated overnight at 50^{o}C.

After incubation the samples were centrifuged at 15,000 g for 10 min at 4°C to remove any debris or particles. QIAGEN Genomic-tips were equilibrated with Buffer QBT and the samples were added to the tips. This was followed by washing of the tips twice with 7.5 ml of Buffer QC. Five ml of Buffer QF was used to elute the genomic DNA. The eluted DNA was precipitated by adding 3.5 ml of isopropanol. The tube was inverted 10-20 times, followed by spooling of the DNA with a plastic rod. The spooled DNA was transferred to a fresh tube containing 200 µl of TE. This was followed by incubation at 55°C for 1 hr. The genomic DNA concentration was measured on the nanodrop while the quality was determined by running an aliquot on a 1% agarose gel.

2.11 Cloning of PCR products

2.11.1 Ligation

The TOPO TA Cloning kit was used for the ligation. A mixture of 2 µl of fresh PCR product, 2 µl of sterile water, 1 µl of salt solution and 1 µl of TOPO vector was prepared and mixed gently, followed by incubation at room temperature for about 20 min. After the incubation the reaction mix was stored at -20°C until needed.

2.11.2 Transformation

Two µl from the previously performed TOPO Cloning reaction was added to a vial of one shot chemically competent E. coli, the mixture was mixed gently and then incubated on ice for 20 min. After the incubation period the cells were quickly transferred to a water bath for a 30 s heat-shock at 42°C. After the heat-shock the tubes were rapidly put on ice followed by addition of 250 µl of S.O.C medium at room temperature. The tubes were capped tightly and then kept on a shaker at 200 rpm for 1 h at 37°C. Two different volumes of 50 µl and 200 µl from each transformation were spread on prewarmed LB plates containing ampicillin to ensure that at least one plate had an appropriate colony density. The plates were incubated overnight at 37°C. About 4-10 colonies were selected from each plate and grown overnight in 2 ml of LB medium containing 2 µl of ampicillin to yield a concentration of 100 ng/µl.

2.11.3 Plasmid purification

After an overnight bacterial culture, the FastPlasmid Mini kit was used for plasmid purification. An aliquot of the culture was transferred to 2 ml tubes and centrifuged briefly for a minute at about 13,000 rpm to obtain the bacterial pellet. The supernatant was removed

by gentle decantation. Four hundred µl of ice-cold complete lysis solution made up of a mixture of lysis solution plus the RNase/lysozyme mix was added to the bacterial pellets. This was immediately followed by vortexing the tubes at the highest speed for about 5 min. The lysate was then incubated at room temperature for about 3 min, before being transferred to a spin column. The columns were subsequently centrifuged at the highest speed for one minute. Following centrifugation, the filtrate was discarded and the column reassembled, to each column 400 µl of diluted wash buffer was added. The wash buffer had been previously diluted with 100% isopropanol at a ratio of 1:2.1. Immediately the columns were centrifuged for a minute. The spin columns were transiently removed from the centrifuge to get rid of the filtrate, after decanting the filtrate the columns were returned to the centrifuge for a further centrifugation at maximum speed for one minute to ensure that the spin column was dried. Subsequently the columns were placed in a new 1.5 ml collection tubes to collect the DNA. For this purpose, 50 µl of sterile water was added to the column filter followed by centrifugation at maximum speed for a minute. Lastly, the spin column was removed and the 1.5 ml collection tube with the eluted DNA was quickly stored at -20^{o}C until needed.
After elution of the DNA the concentration was determined by photometry at 260 nm. The plasmids were then analysed for inserts by restriction analysis using 1 µl of *Eco*RI enzyme, 2 µl of *Eco*RI buffer, 12 µl of sterile water and 5 µl of the plasmid. This mixture was incubated at 37^{o}C for 1 h. After incubation, 2 µl of loading buffer was added to each mixture and run on 2% agarose gel about 40 min at 120 V. Subsequently the samples were sent to the central sequencing facility, BMFZ, for sequencing by standard methods.

2.12 RT-PCR

2.12.1 Reverse transcription

Reverse transcription of RNA to cDNA was performed as follows (Tables 2.5-6). Two mastermixes A for denaturation and B for reverse transcription were prepared with the following constituents.

Table 2.5: Mastermix A for reverse transcription

REAGENT	VOLUME
Oligo(dT) [0.5 µg/µl]	1 µl
dNTP-Mix [10 mM]	1 µl

Table 2.6: Mastermix B for reverse transcription

REAGENT	VOLUME
5X Forward Strand Buffer	4 µl
Dithiothreitol [0.1 M]	2 µl
RNase Inhibitor [40 U/µl]	1 µl
Superscript II reverse	1 µl

Two µg of RNA from the sample was diluted in a total volume of 10 µl of water in a 500 µl tube. To every tube 2 µl of Mastermix A was added and the mixture was then transferred to the heating block for 5 min at 65°C. It was subsequently kept on ice and 8 µl of Mastermix B was added to each tube. The tubes were transferred to the heating block for 2 min incubation at 42°C. This was followed by a programme of 50 min at 42°C, 15 min at 70°C and paused at 4°C. After reverse transcription the cDNAs synthesized were stored at -20°C until needed.

2.12.2 Quantitative PCR

The mRNA expression level of the selected genes in a series of urothelial carcinoma cell lines and tissues were quantified with Real time RT-PCR using the LightCycler II apparatus or ABI Prism 7900 HT (Table 2.4). LightCycler-FastStart DNA Master PLUS SYBR Green I kit, LightCycler-Taqman Master (Roche, Mannheim, Germany), Quantitect SYBR Green kit (Qiagen, Hilden, Germany) and TaqMan Gene Expression Assays (Roche, New Jersey, USA) were used as deemed best for the analysis of different genes of interest.
The expression analysis of *SNCG, S100A4* and *GAPDH* in the bladder cell lines and tissues was done with the LightCycler-FastStart DNA Master PLUS SYBR Green on the Lightcycler II apparatus (Table 2.7-8). In all cases the PCR was first optimised to determine the best PCR programme to be used. For the three genes the annealing temperature used was 59°C.

Table 2.7: The PCR program for LightCycler-FastStart DNA Master PLUS SYBR Green

	TEMPERATURE	TIME
denaturation	95°C	15 min
amplification 40 cycles	95°C	15 s
	59°C	10 s
	72°C	10 s
melting curve	65°C	20 s
cooling	40°C	30 s

The PCR Mastermix consisted of water, the primer pairs, SYBR-Green enzyme mix and the diluted cDNA, typically at 1:5 or 1:10 dilution. After the measurement of the expression of the gene of interest the normalization of the expression data was done with *GAPDH*.

Table 2.8: The Mastermix for LightCycler-FastStart DNA Master PLUS SYBR Green

COMPONENT	END CONCENTRATION
H_20	Up to 10 µl
Forward primer	10 pmol
Reverse primer	10 pmol
5X SYBR-Green Enzyme mix	1X
cDNA 1:10 dilution	1 µl

For quantification of *LCN2* expression, the LightCycler-Taqman Master was employed and the PCR was performed on the LightCycler (Tables 2.9-10). The probe end concentration in the PCR reaction was 100 nM and the cDNA was diluted at a ratio of 1:10.

Table 2.9: The Mastermix for LightCycler-Taqman Master

COMPONENT	END CONCENTRATION
H_20	Up to 10 µl
Forward primer	0.75 µM
Reverse primer	0.75 µM
5X Enzyme mix	1X
Probe (10 µM)	100 nM
cDNA 1:10 dilution	1 µl

The annealing temperature used was 60^{o}C. The amplification step was repeated for 45 cycles. The *GAPDH* was used to normalize the expression data from *LCN2*.

Table 2.10: The PCR program for LightCycler-Taqman Master

	TEMPERATURE	TIME
denaturation	95°C	15 min
amplification 45 cycles	95°C	10 s
	60°C	30 s
	72°C	1 s
cooling	40°C	30 s

Quantification of the expression of many of the genes used in this thesis was carried out with appropriate Quantitect primer assays designed by Qiagen.

Table 2.11: The PCR program for Quantitect primer assay on the LightCycler

	TEMPERATURE	TIME
denaturation	95°C	15 min
amplification 40 cycles	94°C	15 s
	55°C	20 s
	72°C	20 s
melting curve	70°C	20 s
cooling	40°C	30 s

The primer assays for *S100A9, DEPDC1, TBP* and *SIRT1* were used on the LightCycler, for these genes the PCR program was as above (Table 2.11), the annealing temperature was 55°C and the amplification was for 40 cycles. Similarly the same Mastermix composition was as specified below (Table 2.12).

Table 2.12: Mastermix for Quantitect primer assay on the LightCycler

COMPONENT	END CONCENTRATION
H_20	Up to 10 µl
10X Quantitect Primer Assay	1X
2X Quantitect SYBR Green	1X
cDNA 1:10 dilution	1 µl

Expression analysis of *CBX7, JMJDIA, H2AFY, PCAF* and *MYST4* were done on the ABI Prism 7900 HT. The PCR program and mastermix are shown below (Tables 2.13-14)

Table 2.13: The PCR program for Quantitect primer assays on the ABI Prism 7900 HT

	TEMPERATURE	TIME
denaturation	95°C	15 min
amplification 45 cycles	94°C	15 s
	55°C	30 s
	72°C	30 s
melting curve	95°C	15 s
	60°C	15 s
	95°C	15 s

The total volume of the master mix was 25 µl, and the cDNA samples used were diluted 1:20.

Table 2.14: Mastermix for Quantitect primer assays on the ABI Prism 7900 HT

COMPONENT	END CONCENTRATION
H_20	Up to 25 µl
10X Quantitect Primer Assay	1X
2X Quantitect SYBR Green	1X
cDNA 1:20 dilution	2 µl

The expression levels *of DDX58, KLF4, SIRT7* and *LOXL2* were quantified with TaqMan Gene Expression Assays on the ABI Prism 7900 HT (Tables 2.15-16). The normalization of these genes was to the results of the TBP TaqMan Gene Expression Assay.

Table 2.15: The PCR program TaqMan Gene Expression Assays

TEMPERATURE	TIME	NUMBER OF CYCLES
95°C	10 min	1
95 °C	15 s	40
60 °C	1 min	

The Mastermix was prepared following the manufacturers recommendation.

Table 2.16: Mastermix for TaqMan Gene Expression Assays

COMPONENT	END CONCENTRATION
TaqMan Gene Expression Assays	1 µl
2X TaqMan universal PCR master Mix	17 µl
cDNA 1:20 dilution	2 µl

2.13 Analysis of modified DNA

2.13.1 Bisulfite treatment of DNA

The EZ DNA methylation-Gold kit was used for the bisulfite treatment. 130 µl of CT conversion reagent was added to 1 µg of genomic DNA in a volume of 20 µl of water. The samples were mixed, placed on a thermal cycler and the following reaction was performed (Table 2.17).

Table 2.17: Incubation program for bisulfite treatment of DNA

TEMPERATURE	TIME
98^{o}C	10 min
64^{o}C	2.5 hr
4^{o}C	Up to 20 hr

After the reaction, the Zymo-Spin IC columns were assembled on the collection tubes, to each column 600 µl of M-Binding buffer was added, followed by a sample. Each tube was closed and inverted several times followed by centrifugation at full speed for 30 s. The filtrate was discarded. This was followed by addition of 200 µl of M-wash buffer to each column; the tubes were then centrifuged at full speed for 30 s. Two hundred µl of M-Desulphonation buffer was then added at room temperature for about 20 min and this was followed by spinning at full speed for 30 s. 200 µl of M-wash buffer was added to each column followed by centrifugation at full speed for 30 s. This step was repeated twice. Finally, 50 µl of M-Elution buffer was added to the centre of the column, the columns were placed in new 1.5 ml collection tubes and subsequently centrifuged at high speed to elute the DNA. The eluted DNA was stored at -20^{o}C until needed.

2.13.2 PCR analysis of bisulfite treated DNA

After the genomic DNA extraction (Section 2.9.2) and subsequent bisulfite treatment with EZ DNA methylation-Gold kit (Section 2.12.1), PCR was performed using specific primers with Hotstar Taq Master Mix Kit on T3 Thermocycler (Table 2.4). Primers were designed to amplify specific CpG-rich regions within the regulatory regions or intronic sequence of interest in the genes. The PCR program and mastermix used are shown below (Table 2.18-19).

Table 2.18: PCR programme for bisulfite treated DNA

TEMPERATURE	TIME	NUMBER OF CYCLES
94^{o}C	15 min	1
95 ^{o}C	30 s	37
53^{o}C-59^{o}C	30 s	
72^{o}C	45 s	
72^{o}C	10 min	1
4^{o}C	∞	

The annealing temperature used for the *S100A4* promoter region was 59^{o}C, whereas 58^{o}C was used for the *S100A4* intronic region and the regulatory regions for both *SNCG* and *S100A9*. In all PCR reactions for methylation analysis performed the amplification lasted for 38 cycles.

Table 2.19: PCR Mastermix for bisulfite treated DNA

COMPONENT	END CONCENTRATION
dNTP (10mM)	150 µM
Forward Primer	0.3 µM
Reverse Primer	0.3 µM
10X PCR Buffer (Qiagen)	1 X
Hot star Taq polymerase (Qiagen)	1 U
Converted DNA	2 µl
H_20	up to 50 µl

Subsequently the PCR product was checked by electrophoresis on 2% agarose gels to verify that the amplicon was of the right size. Afterwards, the PCR product was cloned as previously described (Section 2.10.1-3).

2.14 Microarray experiments

2.14.1 Microarray I

The microarray was performed by Dr Andrea Florl prior to the beginning of this thesis; a fuller description has been published [Dokun et al, 2008]. In brief, three cultures were prepared from the papillary part of a urothelial carcinoma and three normal urothelial cultures from the ureteral tissue of the same 61 year old patient. RNA was extracted from each sample followed by reverse transcription and differential labelling. The labeled cDNA were hybridized to MWG Human 30K Arrays A. Following prehybridization and denaturation the slides were washed, scanned and images were developed and normalized. The analysis was repeated with a dye swap. Finally, statistically significant differentially expressed genes were identified. The list of genes differentially expressed in this microarray study is shown in the appendix 1.

2.14.2 Microarray II

This microarray expression analysis was performed on HG-U133A (Affymetrix) oligonucleotide chips using 2 independent primary cultures of 5-aza-dC treated or untreated normal urothelial cells (UP159 and UP160), and 5-aza-dC treated or untreated VMCub1 and UMUC3 cells. Triplicates of each of the 8 samples were used with one-cycle target labeling assay for expression analysis on the microarrays. Two µg of high-quality total RNA was isolated from each of the bladder carcinoma cell lines and normal urothelial cells using TRIzol and QIAGEN RNeasy mini kit were used for the preparation of pure RNA. The quantity of RNA was measured on the nanodrop and the integrity of the RNA samples was determined by capillary electrophoresis on the Agilent 2100 Bioanalyzer. The Poly-A RNA control stock was diluted with Poly-A control Dil buffer according to the protocol.
The cDNA synthesis kit was used to generate the first and second strand cDNA as shown below (Table 2.20-21). The RNA sample was added to the diluted Poly-A controls and the T7-Oligo (dT) primer and the mixture was subsequently incubated using the following programme on a thermal cycler.

Table 2.20: First-Strand cDNA synthesis with the One-Cycle cDNA Synthesis kit

TEMPERATURE	TIME
70°C	10 min
4°C	∞
42°C	2 min
42°C	60 min
4°C	∞

During the first pause step, a first strand master mix comprising 5X 1st Strand reaction mix, DTT and dNTP was added to the RNA/T7-Oligo (dT) primer mix. The new mixture was incubated for 2 min at 42°C followed by the addition of SuperScript II and the rest of the programme was completed.

The second strand master mix consisting of RNase-free water, 5X 2nd strand reaction mix, dNTP, DNA Ligase, DNA polymerase 1 and RNase H was prepared and added to the first strand synthesis sample, this was then incubated with the following programme recommended in the kit

Table 2.21: Second-Strand cDNA synthesis with the One-Cycle cDNA Synthesis kit

TEMPERATURE	TIME
16°C	120 min
4°C	Pause
16°C	5 min
4°C	Pause

The double stranded cDNA was purified by sequentially adding cDNA binding buffer and cDNA in wash buffer to the double stranded cDNA following the instruction in the kit. The cDNA was finally eluted with cDNA elution buffer.

The GeneChip IVT labeling kit was used for the synthesis of biotin-labeled cRNA. For the IVT reaction a mixture consisting of RNase-free water, 10X IVT labeling buffer, IVT labeling NTP mix and IVT labeling enzyme mix was prepared and incubated at 37°C for 16 h. Subsequently 5X fragmentation buffer and RNase-free water were added to the cRNA for fragmentation with incubation at 94°C for 35 min.

For the hybridization step, a hybridization cocktail consisting of fragmented cRNA, control oligonucleotide B2, 20X eukaryotic hybridization controls, herring sperm DNA, BSA, 2X hybridization buffer, DMSO and H_20 was heated at 99°C for 5 min. Subsequently, the array chamber was filled with 1X hybridization buffer and incubated at 45°C for 10 min. Following incubation the hybridization buffer was removed and replaced with hybridization cocktail containing the labeled RNA. Subsequently, the probe array was incubated at 45°C for 16 h. After 16 h hybridization, the hybridization cocktail was removed and replaced with wash buffer A. The arrays were stained using SAPE solution mix consisting of 2X stain buffer, BSA, Streptavidin Phycoerythrin (SAPE) in H_20, followed by antibody solution mix comprised of stain buffer BSA Goat IgG stock, biotinylated antibody and H_20. After the washing and staining procedure the probe array was scanned on the GeneChip Scanner 3000. GeneChip Operating Software (GCOS, version 1.3, Affymetrix) was used to develop the images and this was followed by total intensity normalization.

RESULTS

3.1 Results of microarray I

In an experiment performed prior to the beginning of this thesis (see description in Section 2.13.1), oligonucleotide microarrays were used to investigate the gene expression profiles of three independent primary cultures each from a papillary bladder carcinoma and normal urothelial cells from the ureter of a 61 year old male patient. According to the data 82 genes were differentially upregulated in a statistically significant manner in the tumor cells in comparison to the normal urothelial cells. Conversely, in the normal urothelial cells 130 genes had a higher expression than in the tumor cells (See appendix 1). Genes from all chromosomes were present at the expected frequency, but a higher fraction of genes from chromosome 9q was downregulated (Table 3.1). Genes from chromosome 1q were overrepresented among those upregulated. Deletion of chromosome 9q is very frequent in bladder cancer and this seems consistent with the microarray data.

Table 3.1: Chromosomal locations of genes up- or downregulated in bladder tumor cells

	Upregulated genes		Downregulated genes	
	p	**q**	**p**	**q**
1	5	7	6	4
2	1	-	4	8
3	1	2	1	4
4	-	1	1	7
5	1	1	-	5
6	4	-	3	5
7	-	2	5	3
8	-	-	1	2
9	-	4	1	11
10	-	6	2	4
11	3	7	2	6
12	2	2	5	3
13	-	1	-	2
14	-	3	-	7
15	-	1	-	3
16	2	2	-	5
17	1	4	1	3
18	-	1	1	2
19	5	5	-	1
20	1	1	-	3
21	-	3	-	3
22	-	2	-	1
X	-	2	3	1
Y			-	2

The microarray investigation revealed differences in the expression pattern of genes that are critical in specific biological processes. The 10 most differentially upregulated genes in the tumor cells were *SPINK1, IQSEC1, KRT13, UPK1A, LSP1, PSMB10, TJP3, RARRES3, KRT15* and *IVL* (See appendix 1). Overall, there was a marked upregulation of genes encoding cytokeratins such as *KRT13* and *KRT15* and related genes such as IVL (*involucrin*) which like *KLF5* is known as an epidermal differentiation marker. Interestingly, in the carcinoma cells genes for urothelial differentiation markers such as *ELF3, UPK1A* and *UPK1B* were upregulated. The tumor cells also showed higher expression of genes encoding proteins that function as complement factors and antigen presenting proteins. In contrast, in tumor cells, genes encoding adhesion proteins such as *CTNNAL1, CD44* and *TSLC1* as well as several genes encoding proteins that function in signaling and apoptosis were downregulated.

The 10 most strongly expressed genes in the normal urothelial cells were *VIM, SRGN, AREG, TFPI2, EFEMP1, TNC, LAMA3, STAT4, STK17A* and *VEGFC* (see appendix for full list). This list indicated a higher expression of genes encoding proteins that function in extracellular matrix biosynthesis (like the products of the *EFEMP1, TNC, LAMA3* genes Fibulin-2, Tenascin-C and Laminin A3) in the normal urothelial cells. Another notable group of genes expressed more strongly in the normal urothelial cells encoded growth factors like amphiregulin (*AREG*) and inhibin β functioning in the growth stimulation of urothelial cells whereas in the cancer cells higher expression of two *TGFβ*-related growth factor genes (*TGFβ4*, placental *TGFβ/GDF15*) and the gene encoding endothelin-1 was observed.

To identify DNA hypomethylation induced genes in bladder cancer, we first examined the promoter region of the upregulated genes. Selected results from this analysis are shown in Table 3.2. According to a usual definition of CpG-islands, at least 40 CpG sites should be contained in a 1 kb segment. Most upregulated genes had few CpG sites, although around 50% of all human genes harbor CpG-islands around their start site. From the genes in the table, only IQSEC1 and to a lesser degree LSP1 and TJP3 would meet the definition.

Table 3.2 Number of CpG sites in selected upregulated genes in tumor cells

HGNC Symbol ID	Gene name	Number of CpG sites (-1000 bp upstream)
SPINK1	serine peptidase inhibitor, 1	4
IQSEC1	IQ motif and Sec7 domain 1	59
KRT13	keratin 13	13
UPK1A	uroplakin 1A	20
LSP1	lymphocyte-specific protein 1	33
PSMB10	proteasome (prosome, macropain) subunit, beta type, 10	9
TJP3	tight junction protein 3	31
KRT15	keratin 15	24
IVL	involucrin	5
CYP4B1	cytochrome P450 4B1	3
ELF3	E74-like factor 3	10

Some members of the S100 calcium binding protein family were upregulated in the carcinoma cultures, prominently *S100A9* and *S100B. S100A9* has been variously reported as overexpressed and implicated in the progression of many carcinomas including prostate cancer, breast cancer and gastric cancer [Hermani et al, 2005; Yong and Moon, 2007; Salama et al, 2008]. *S100A9* has been reported as overexpressed in bladder cancer too [Yao et al, 2007], but there is no report on the methylation of *S100A9* in any cancers. Hence the relationship between the expression and methylation of *S100A9* in the context of bladder cancer was addressed in this thesis.

Although *S100A4*, another member of the S100 calcium-binding protein family, was not on the list of the upregulated genes, many studies have indicated that it is upregulated in various cancers including breast cancer [Wang et al, 2000] and thyroid cancer [Zou et al, 2005]. In several instances, this upregulation has been ascribed to hypomethylation of the gene, especially of a region in the first intron containing 4 CpG sites. *S100A4* has been proposed to play a role in the pathogenesis of bladder cancer, but its methylation in this cancer had not yet been studied [Davies et al, 2002]. Therefore, we decided to determine if overexpression of *S100A4* in bladder cancer occurs and is a result of DNA hypomethylation. Since no one has studied the actual 5' regulatory region, we studied both the intronic region as well as the regulatory region at the transcriptional start site.

SNCG was upregulated by 4.7 fold in the tumor cell cultures. *SNCG* has been reported as upregulated in many cancers in relation to metastasis [Liu et al, 2005]. Furthermore DNA hypomethylation has been proposed as the mechanism responsible for the abnormal gene expression [Yanagawa et al 2004].
Similarly, *LCN2* was upregulated by 13.3 fold in the tumor cells according to the microarray data. There are reports linking increased *LCN2* expression to breast cancer development [Yang et al, 2009]. Also, a study on pancreatic cancer reported *LCN2* as a gene activated by hypomethylation [Sato et al, 2003]. Expression of *SNCG* and *LCN2* had not been investigated in bladder cancer before. Hence the two genes were selected for closer analysis.

3.1.1 Expression analysis of hypomethylation candidate genes

The expression of these genes was evaluated in a panel consisting of three independent primary cultures of normal urothelial cells, thirteen bladder cancer cell lines and fibroblasts. Subsequently the expression of the genes was measured in cells treated with the DNA methyltransferase inhibitor 5-aza-2-deoxycytidine (5-aza-dC) to assess if their expression was regulated by DNA methylation. Following the expression analysis in the panel of cell lines, the study was extended to a panel consisting of 18 normal and 32 tumor tissues.

3.1.2 Expression analysis of *SNCG*

A heterogeneous pattern of *SNCG* expression was observed in the bladder cancer cell lines (Fig 3.1). Among the three normal urothelial cell cultures one exhibited markedly higher expression of the gene than the others. Compared to all normal urothelial cell lines, RT112, BFTC905, HT-1376, RT4, SD and VMCub1 had equal or higher expression of the gene, whereas the highest expression of the gene was witnessed in RT112 and SD. Expression of *SNCG* in the remaining bladder cancer cell lines was very low and no expression was detected in UM-UC3, 639v, J82 and SW1710. Similarly, a very low expression of *SNCG* was observed in fibroblasts.

Treatment of the cell lines with the DNA methylation inhibitor 5-aza-dC led to the induction of *SNCG* in some previously non- or low expressing cells (Fig 3.1). Notably the gene was slightly induced in fibroblasts, BFTC909, 647v, 5637, J82, whereas the highest induction was witnessed in BFTC905, HT-1376 and RT4. Among the urothelial cells only one 5-aza-dC treated culture was available for analysis; in these cells, a moderate upregulation of the gene was observed. Unexpectedly, treatment with 5-aza-dC lead to downregulation of the gene in

some of the strongly expressing cell lines in comparison to their untreated counterpart, notably in the case of RT112 and SD.

Since the results were unexpected in view of the published data on other cancers, we additionally examined the expression of *SNCG* in normal prostate epithelial cells (PrEC) and prostate cancer cell lines (Fig 3.1). The expression of *SNCG* in PrEC was at a similar level to most of the normal urothelial cell cultures, whereas the expression of *SNCG* was not detectable in the prostate cancer cell lines PC3 and LNCaP. Expression in these cell lines was however induced after treatment with 5-aza-dC.

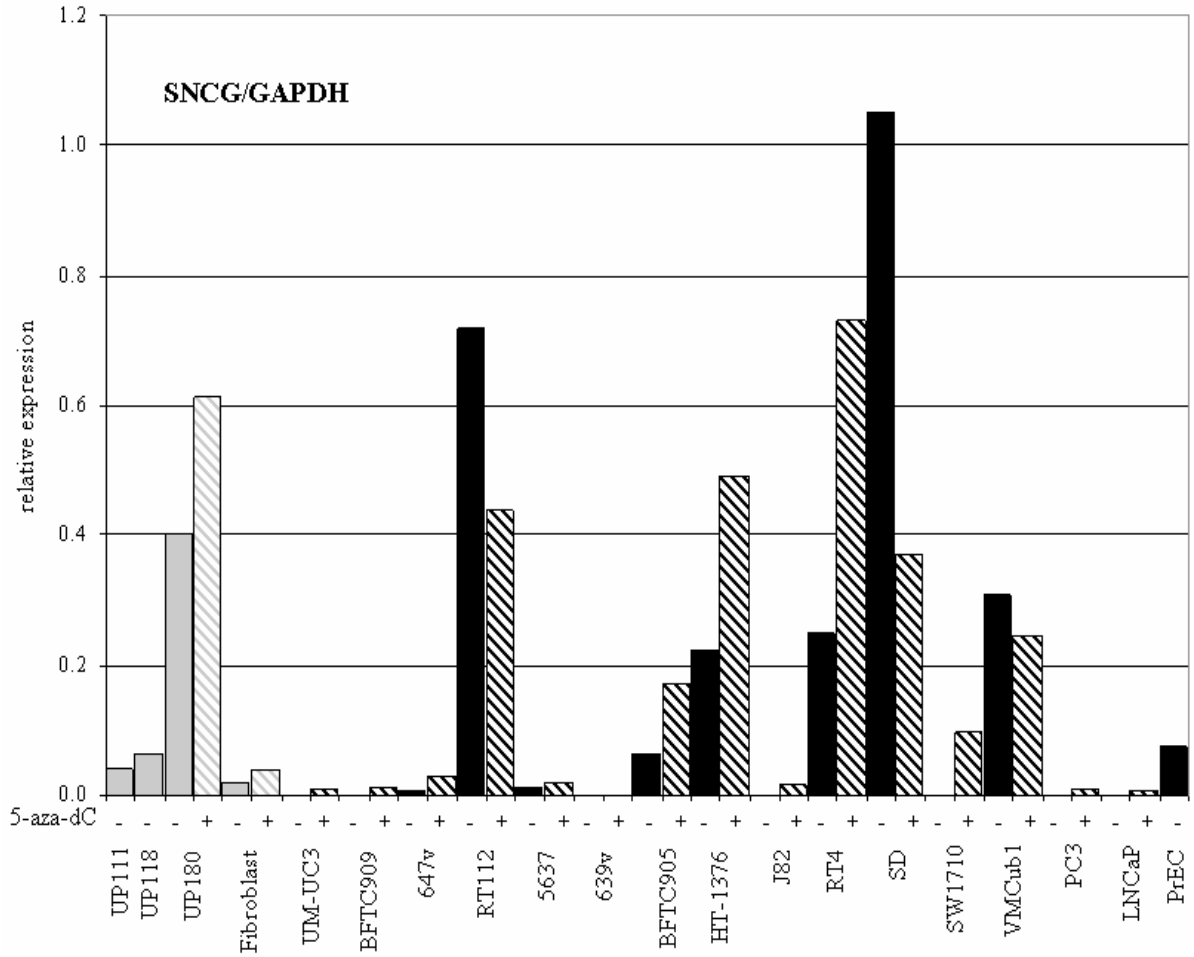

Fig. 3.1: Expression of SNCG relative to GAPDH in normal urothelial cells, prostate epithelial cells, fibroblasts, bladder carcinoma cell lines and prostate carcinoma cell lines as quantified by RT-PCR. 5-aza-dC treated cells are depicted as striped bars and the untreated cells are represented by solid bars. Normal urothelial cells or fibroblasts are represented in grey bars and bladder or prostate cancer cell lines are represented in black bars. The minus [-] and plus [+] symbols indicate without or with 5-aza-dC treatment respectively.

3.1.3 Expression analysis of *S100A4*

The majority of the bladder cancer cell lines examined for the expression of *S100A4* displayed an equal or higher level of expression in comparison to the normal urothelial cells, whereas approximately the same level of expression as in urothelial cells was observed in 647v, BFTC909, 5367, J82, RT4, SD and BFTC905 (Fig. 3.2). Increased expression was seen in RT112 and HT-1376. Similarly the expression of *S100A4* was very high in fibroblasts. Notably, no expression of the gene was detected in UM-UC3, 639v and VMCub1.

Treatment with 5-aza-dC induced the expression of *S100A4* in almost all bladder cancer cell lines (Fig. 3.2). A remarkable induction was observed in BFTC909, BFTC905, HT-1376, J82, RT4, SD and SW1710. Similarly, upregulation of the gene by 5-aza-dC treatment was observed in the UP80 culture. Fibroblasts and RT112 had the highest expression of the gene among all cell lines investigated, independent of 5-aza-dC treatment.

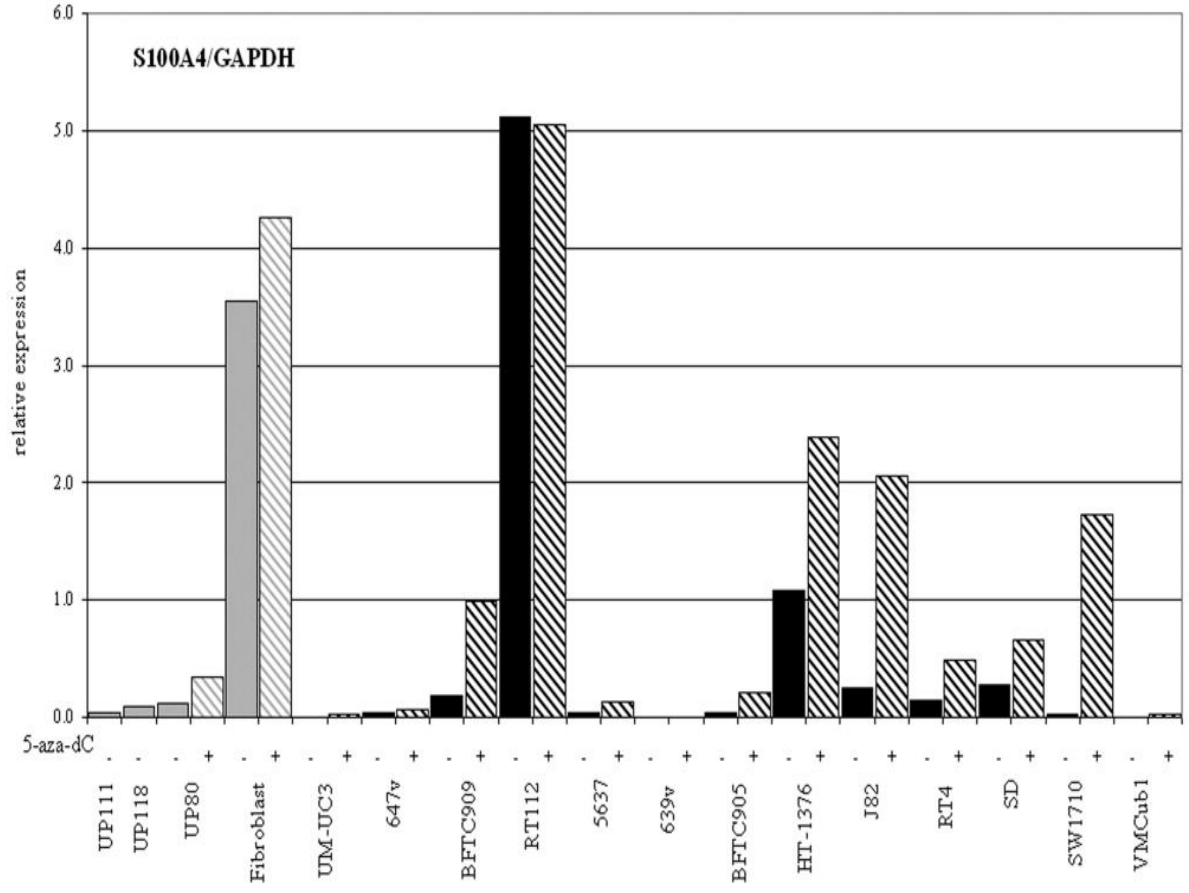

Fig. 3.2: Expression of S100A4 relative to GAPDH in normal urothelial cells, fibroblasts and bladder carcinoma cell lines as quantified by RT-PCR. 5-aza-dC treated cells are shown as striped bars and the untreated cells are represented by solid bars. Normal urothelial cells or fibroblasts are represented in grey bars and bladder cancer cell lines are represented in black bars. The minus [-] and plus [+] symbols indicate without or with 5-aza-dC treatment respectively.

3.1.4 Expression analysis of *S100A9*

Expression of *S100A9* in most of the bladder cancer cell lines was low or undetectable (Fig. 3.3). No expression of the gene was seen in the cancer cell lines UM-UC3, BFTC909, 639v, HT-1376, SW1710, VMCub1 and J82. Moderate expression of *S100A9* was noticeable in RT112 and BFTC905. In contrast, RT4 and SD had high expression of the gene. The highest expression in the whole panel was observed in 5637. In the normal urothelial cells, expression of the gene was well detectable. Overall, the expression pattern of *S100A9* in the bladder cancer cell lines was remarkably heterogeneous.

Treatment with 5-aza-dC had very little or no effect on *S100A9* expression in UP80, 647v, BFTC909, 639v, HT-1376, J82, SW1710 and VMCub1 (Fig. 3.3), but led to its induction in selected bladder cell lines like RT112 and BFTC905, whereas a decrease was observed in 5637, RT4 and SD.

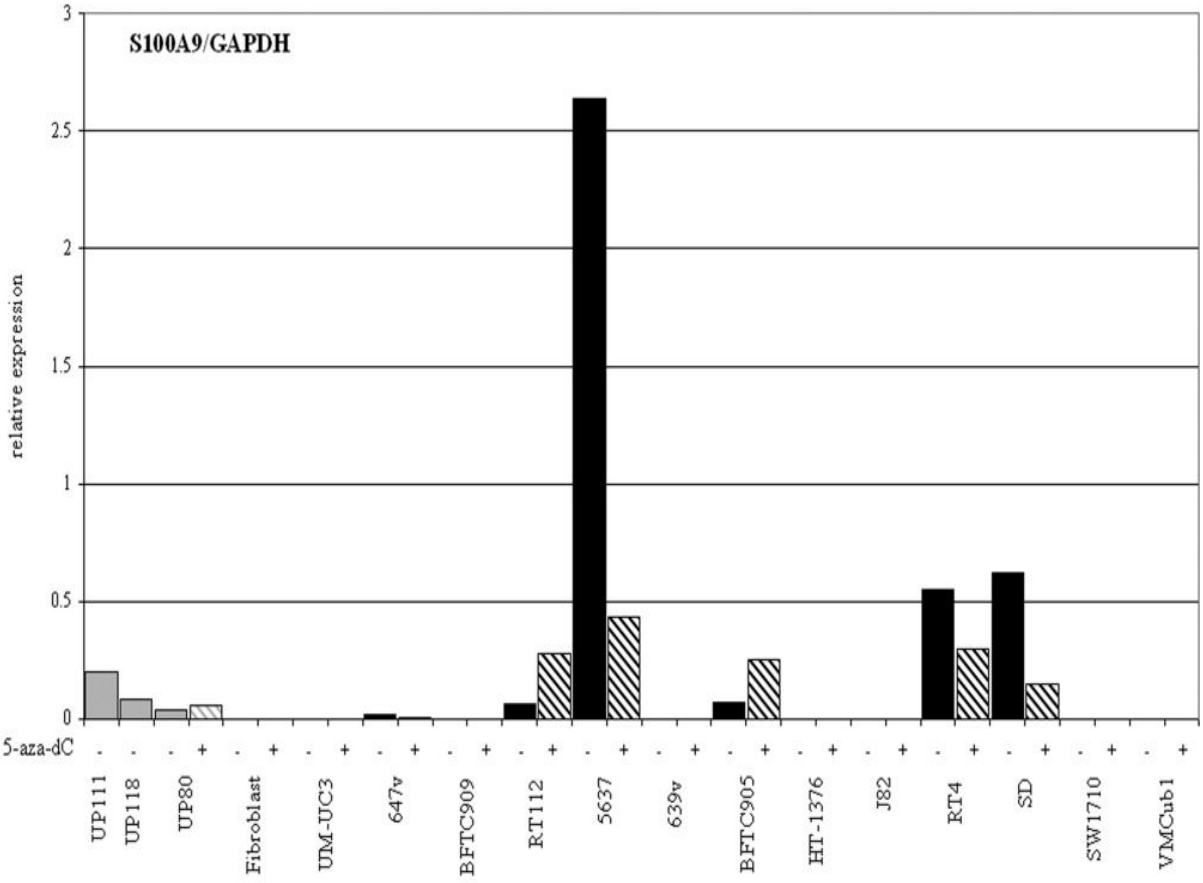

Fig. 3: Expression of S100A9 relative to GAPDH in normal urothelial cells, fibroblasts and bladder carcinoma cell lines as quantified by RT-PCR. 5-aza-dC treated cells are shown as striped bars and the untreated cells are represented by solid bars. Normal urothelial cells or fibroblasts are represented in grey bars and bladder cancer cell lines are represented in black bars. The minus [-] and plus [+] symbols indicate without or with 5-aza-dC treatment respectively.

3.1.5 Expression analysis of *LCN2*

There was a high expression of *LCN2* in two of the three primary cultures of normal urothelial cells. Its expression in these urothelial cells cultures was much higher than its expression in all the bladder cancer cell lines except for SD (Fig. 3.4). No expression of *LCN2* was detected in fibroblasts, SW1710, BFTC909, HT-1376, 5637 and J82. There was very low expression in 639v, and VMCub1, whereas high expression was observed in BFTC905, RT4, UM-UC3, RT112, 647v and SD. Treatment with 5-aza-dC induced the gene in several cell lines and in particular in the UP80 culture.

Treatment with 5-aza-dC had no effect on *LCN2* expression in fibroblasts, HT-1376 and VMCub1 (Fig. 3.4), which maintained the same very low level of *LCN2* expression. In contrast, upregulation of *LCN2* as a result of 5-aza-dC treatment was pronounced in SW1710 and 5637, both of which had shown no expression of the gene. Similarly cell lines which previously expressed the gene like BFTC905, RT112 and SD all showed an upregulation of the gene, but notably the level of *LCN2* was downregulated in some previously expressing cells like 639v, RT4, UM-UC3 and 647v.

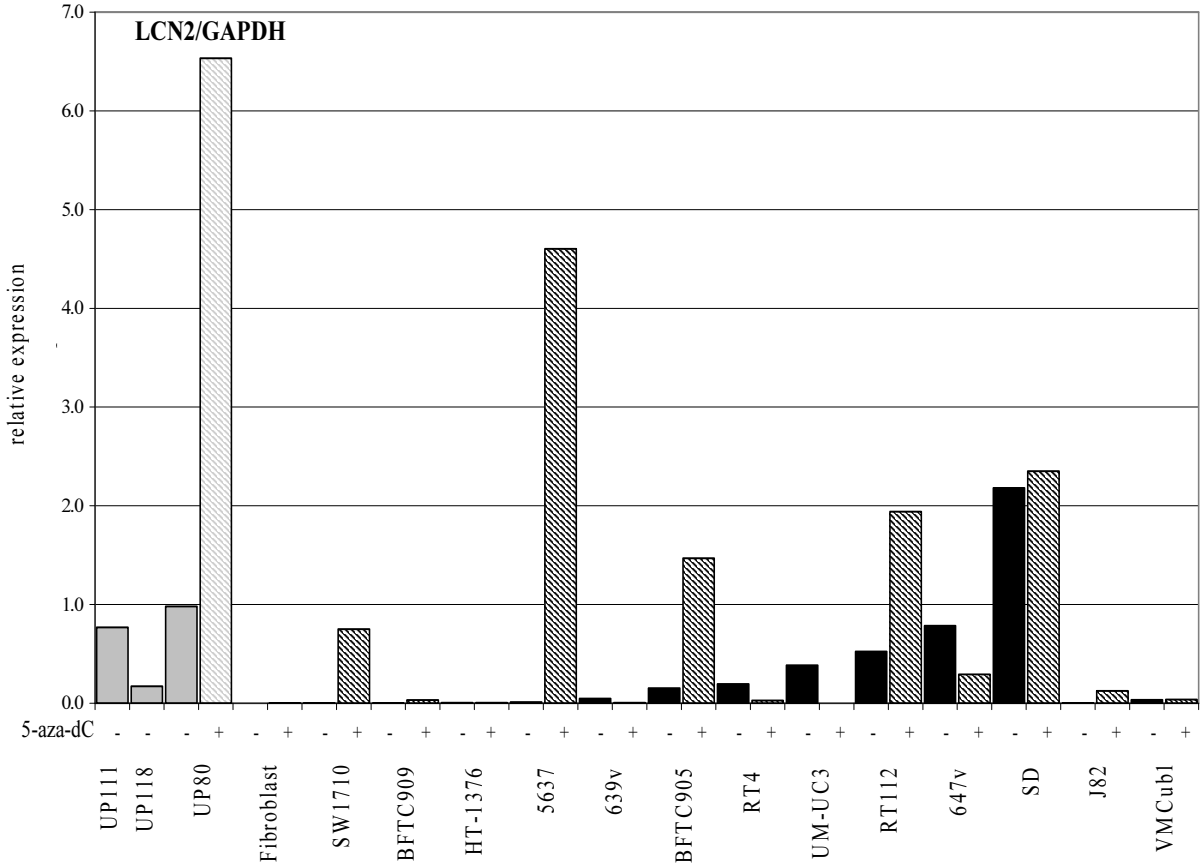

Fig. 3.4: Expression of LCN2 relative to GAPDH in normal urothelial cells, fibroblasts and bladder carcinoma cell lines as quantified by RT-PCR. 5-aza-dC treated cells are shown as striped bars and the untreated cells are represented by solid bars. Normal urothelial cells or fibroblasts are represented in grey bars and bladder cancer cell lines are represented in black bars. The minus [-] and plus [+] symbols indicate without or with 5-aza-dC treatment respectively.

3.1.6 Expression analysis of *SNCG, S100A4, S100A9* and *LCN2* in normal bladder and tumor tissue samples

Subsequently, the expression of the 4 genes was assessed in a set of tissues comprising 18 normal bladder tissue samples and 32 bladder tumor samples (Fig. 3.5). There was no significant difference in the expression of *SNCG* and *S100A4* between tumor and normal tissues. Overall, the expression of these genes in the tumor tissues tended to be lower than in normal tissues. However, there were some outliers among the tumor samples with expression levels considerably above those witnessed in the normal tissues. The lowest relative unit value for *SNCG* in the tumor tissues was 0.004, whereas the lowest unit for normal tissues was 0.07. Similarly, the lowest relative units for *S100A4* observed were 0.02 and 0.35 in tumors and normal tissues respectively.

Overall, a comparison of the expression analysis of the *SNCG* and *S100A4* in the panel of bladder cancer cell lines and urothelial cells on one hand and the panel of normal bladder and bladder tumor on the other hand showed that *SNCG* and *S100A4* can be overexpressed or underexpressed in individual cancerous cell lines or tumors in comparison to normal urothelial cells or bladder tissues.

In contrast to *SNCG* and *S100A4* expression of *S100A9* and *LCN2* in the panel of tissue samples revealed upregulation of each gene in tumor tissues by about 2-fold on average (Fig. 3.5). The Mann-Whitney test confirmed that the increases were statistically significant ($p < 0.05$). Again, there were outliers among the tumor tissues with expression levels approximately five fold higher than the median of the tumor tissues.

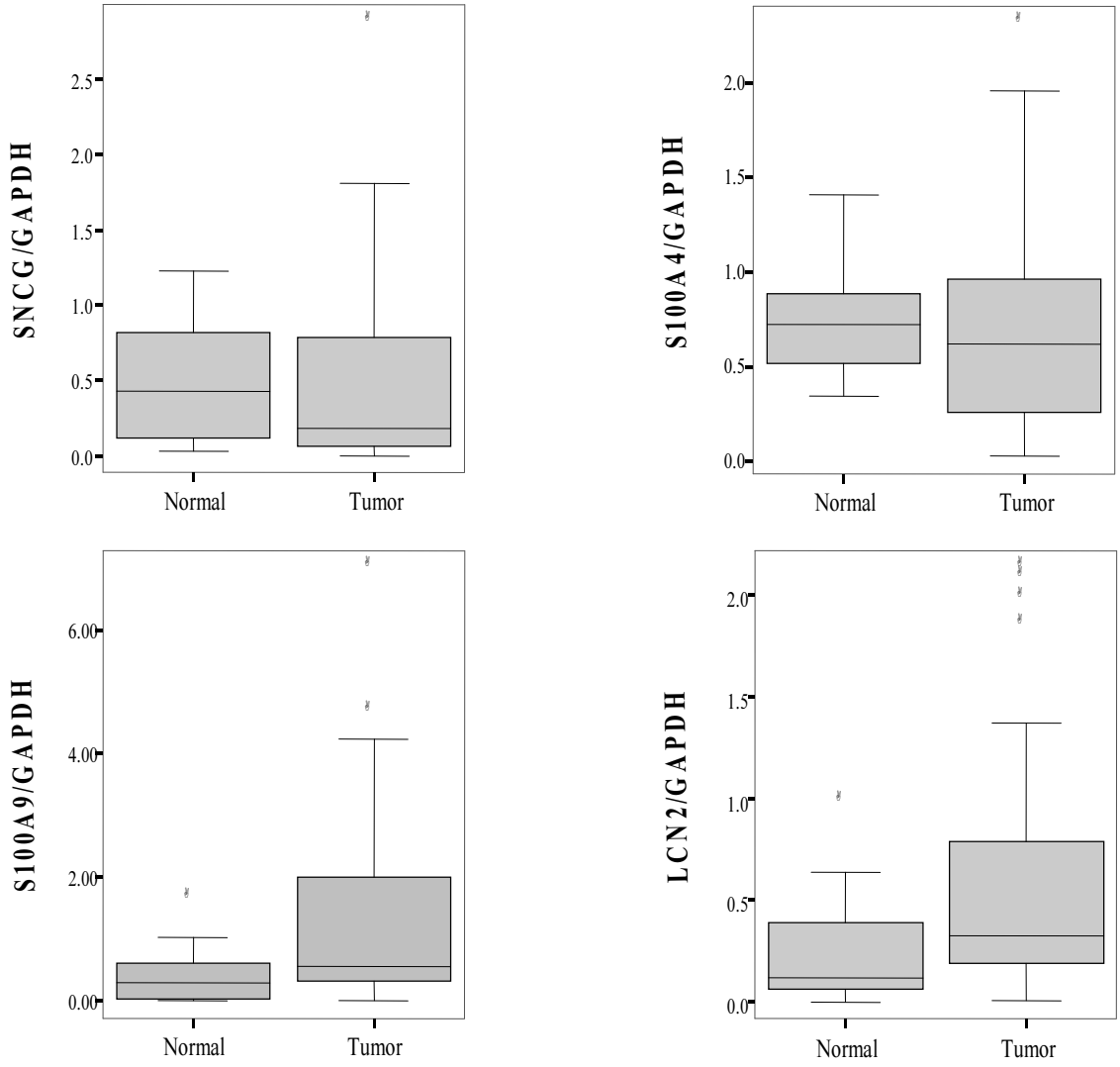

Fig. 3.5: Box plots depicting the expression of SNCG, S100A4, S100A9 and LCN2 relative to GAPDH in 32 bladder tumors and 18 normal tissues as determined by real-time RT-PCR.

3.1.7 Methylation analysis of the regulatory regions of *SNCG, S100A4, S100A9*, *LCN2* and an intronic regulatory region of *S100A4*

In order to elucidate the relationship between expression of these four genes and their DNA methylation status, their regulatory regions were investigated for methylation. For this purpose cell lines with high or low expression of the genes were selected for bisulfite sequencing. In the case of *SNCG*, 14 CpG sites within the proximal promoter were assessed for methylation. Regarding *S100A4*, 4 CpG sites in the first intronic region and 8 CpG sites in the promoter were selected for analysis. Five and 6 CpG sites from the promoters of *LCN2* and *S100A9*, respectively, were analyzed.

For cell lines with homogeneous methylation, four clones each were studies, for cell lines with heterogeneous methylation, the number of clones analysed was increased to eight. Methylation was considered dense, if at most 2 CpG sites were unmethylated in one sequence, and lacking, if at most one site was methylated. All other patterns were considered partial.

To analyze the correlation between the expression of these genes and their respective methylation status, at least two bladder cancer cell lines with high expression of the gene and at least two bladder cancer cell lines with the low expression of the gene were selected. Hence, the selection of bladder cancer cell lines used for each gene varied accordingly.

Urothelial cancers are not homogeneous in their cell composition, but rather consist of different quantities of carcinoma cells and non-carcinoma cells such as fibroblast stromal cells, endothelial cells and immune cells. Therefore, to get an impression of the DNA methylation status in stromal cells, we investigated fibroblasts and in some cases dissected connective tissue from a ureter used for preparation of normal urothelial cells. Thus, overall, the normal controls used consisted of two independent normal urothelial cultures, fibroblasts, ureter connective tissue and two blood leukocyte samples.

3.1.8 Methylation analysis of *SNCG*

Methylation analysis on *SNCG* involved 3 different panels of samples, the first panel comprised of 2 blood leukocyte samples, 2 urothelial cell samples and one each from fibroblasts and ureteral connective tissue. The second panel consisted of bladder cancer cell lines namely, BFTC909, HT-1376, UM-UC3, RT4, RT112, SW1710, SD and VMCub1, and the last panel consisted of cells of prostatic origin, namely PrEC, LNCaP and PC3 (Fig 3.6).
In DNA from the two normal urothelial cell samples no methylation was observed whereas partial methylation occurred in the two blood leukocyte samples, fibroblasts and ureter. The normal urothelial cells and to a much lower extent the fibroblasts expressed *SNCG*. Similarly, four of the bladder carcinoma cell lines expressing the gene were unmethylated in the *SNCG* promoter, namely HT-1376, RT4, RT112, SD and VMCub1. In contrast BFTC909, UM-UC3 and SW1710 lacking *SNCG* gene expression were all densely methylated in the promoter.
Furthermore assessment of the methylation pattern of *SNCG* in the prostatic cells revealed dense methylation in the prostate cancer cell lines, i.e. LNCaP and PC3 (Fig 3.6), whereas the normal prostate epithelial cells (PrEC) were unmethylated. Analogous to the urothelial cells, the normal PrEC had expression of the gene whereas no expression of the gene was seen in the prostate carcinoma cell lines.

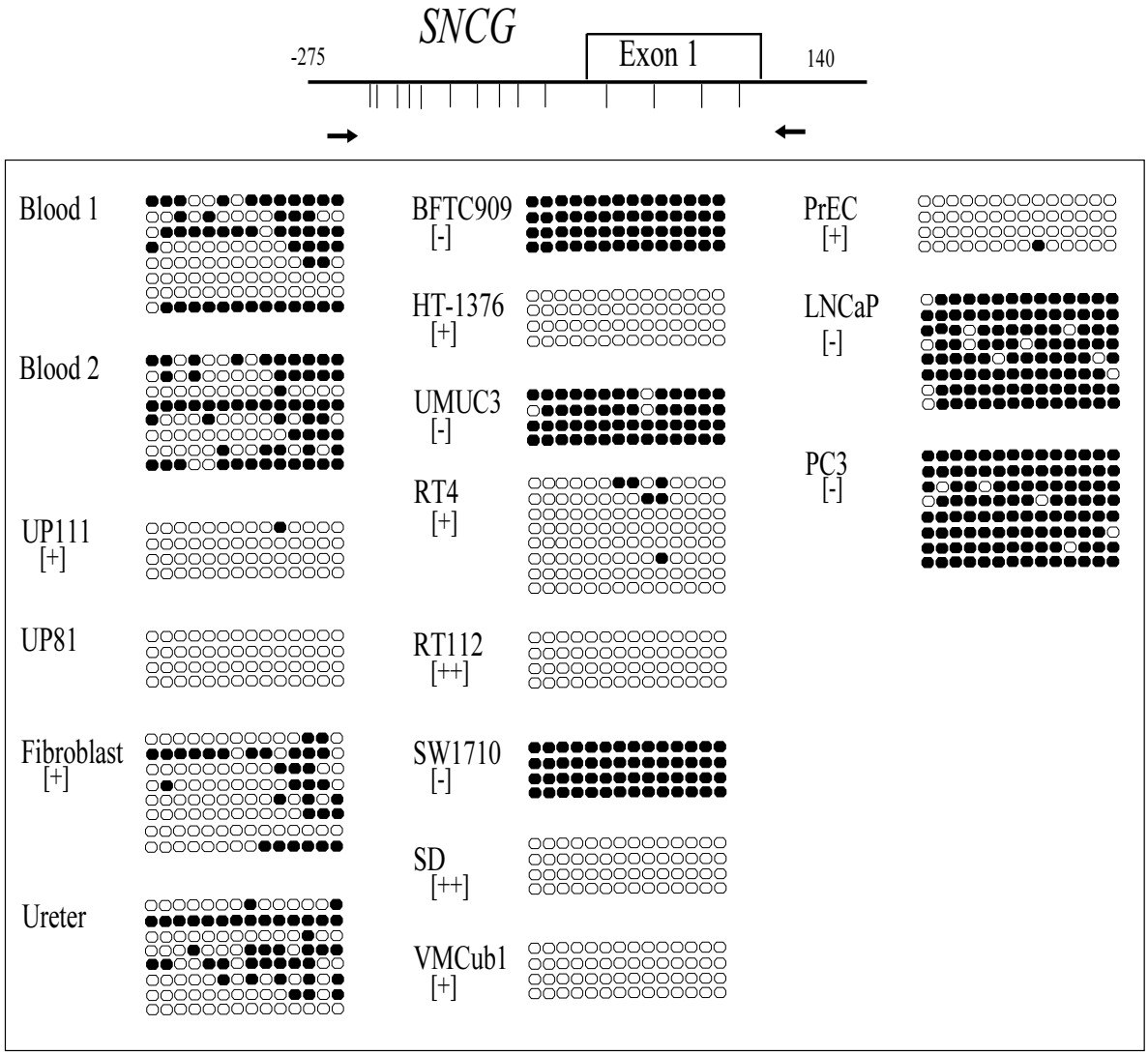

Fig.3.6: Bisulfite sequencing analysis of the SNCG regulatory region in selected cell lines and tissue samples. The upper sketch represents the location of the investigated 14 CpG sites relative to the transcription start site. The arrows show the direction and location of the bisulfite sequencing primers. In the lower panel, unmethylated CpG sites are indicated as white circles while the methylated CpG sites are represented as white circles. The samples used as normal controls are arranged on the left of the panel and comprised blood leukocytes, two independent cultures of urothelial cells, fibroblasts and ureter connective tissue. The middle panel consists of bladder carcinoma cell line, namely BFTC909, HT-1376, UM-UC3, RT4, RT112, SW1710, SD and VMCub1. The panel on the right includes the normal prostate epithelial cell culture and two prostate carcinoma cell lines, namely PC3 and LNCaP. The plus or minus symbol in parentheses represents the corresponding mRNA expression levels: [-] no or low expression, [+] moderate expression, [++] high expression.

3.1.9 Methylation analysis of *S100A4*

The methylation pattern of *S100A4* was investigated in a panel comprising one blood leukocyte sample, normal urothelial cells and bladder cancer cell lines 647v, HT-1376, RT112, VMCub1 as well as ureteral connective tissue (Fig 3.7). Previous studies by other investigators have suggested 4 intronic CpG sites regulating the transcription of this gene. We therefore analyzed these CpG sites and 8 additional CpG sites within the promoter of the gene.

The analyses of the intronic region revealed a weak and variable pattern of partial methylation. Blood leukocytes, normal urothelial cells and ureteral connective tissue were completely unmethylated. The bladder carcinoma cell lines 647v, HT-1376 and RT112 were weakly and partially methylated. Analysis of the promoter CpG sites showed partial methylation for blood leukocytes. This region was densely methylated in normal urothelial cells and especially the bladder carcinoma cell lines 647v, HT-1376, VmCub1 and RT112, whereas the ureter connective tissue was predominantly unmethylated.

Bladder cancer cell lines 647v, HT-1376, and RT112 all had moderate or high levels of expression but *S100A4* was not expressed in VMCub1. Notably, the gene was also expressed in normal urothelial cells

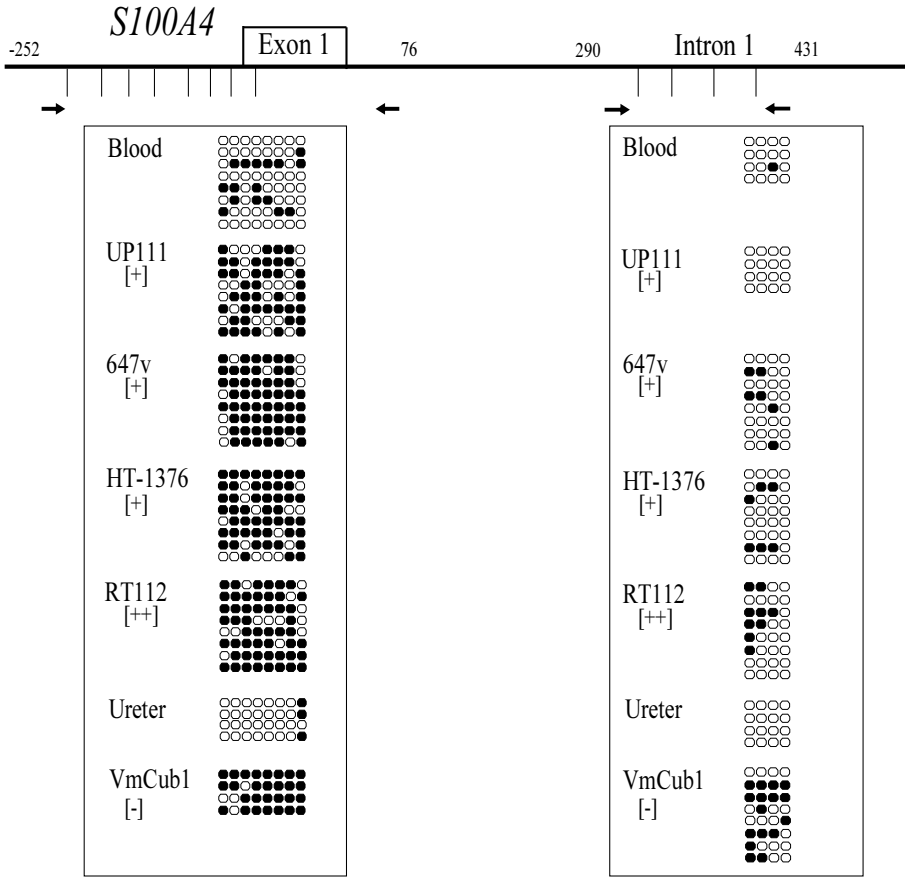

Fig. 3.7: Bisulfite sequencing of the S100A4 regulatory region and the first intron in selected bladder carcinoma cell lines and tissue samples. The upper sketch depicts the locations of the 8 CpG sites within the regulatory region as well as the 4 CpG sites in the first intron investigated. The panel on the right represents analysis of the intronic region while the panel on the left shows the analysis of the promoter region. The plus or minus symbol in parentheses represents the corresponding mRNA expression levels: [-] no or low expression, [+] moderate expression, [++] high expression.

3.1.10 Methylation analysis of *S100A9*

The promoter region of *S100A9* was unmethylated in one blood leukocyte sample and weakly methylated in the other (Fig 3.8). The fibroblasts were partly methylated, but the normal urothelial cells from the UP92 culture were completely unmethylated in this DNA segment. Of the bladder cancer cell lines selected both RT4 and 5637 were completely unmethylated, whereas partial methylation was seen in 639v and SW1710.

No expression of *S100A9* occurred in fibroblasts but there was expression in normal urothelial cells. The gene was also expressed in the bladder carcinoma cell lines RT4 and 5637 but no expression occurred in SW1710 and 639v.

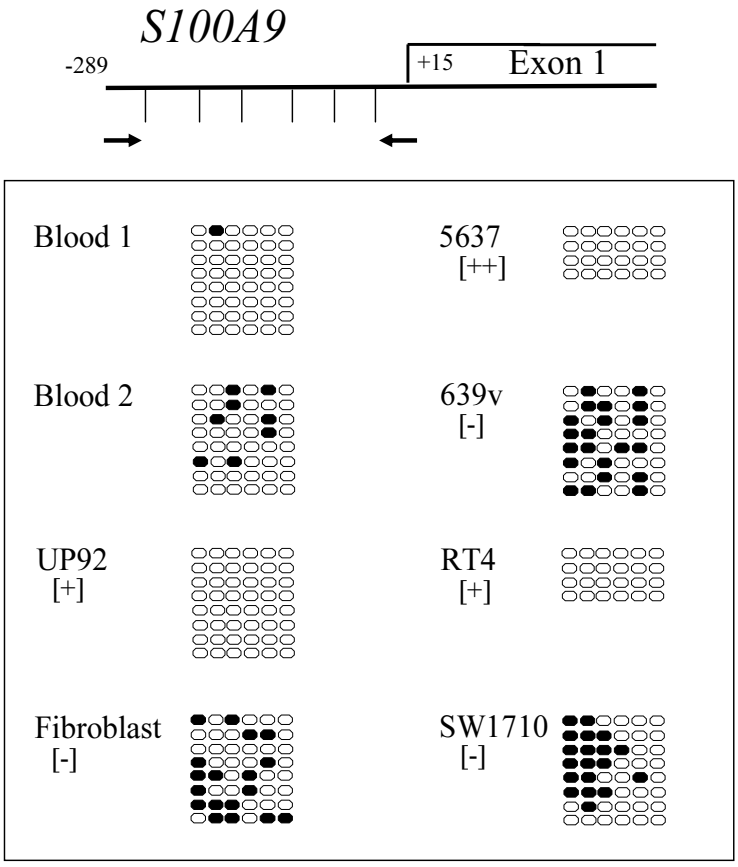

Fig. 3.8: Bisulfite sequencing analysis of 6 CpG sites in the regulatory region of S100A9, on the left are the normal controls and on the right are the bladder cancer cell lines. The plus or minus symbol in parentheses represents the corresponding mRNA expression levels: [-] no or low expression, [+] moderate expression, [++] high expression.

3.1.11 Methylation analysis of *LCN2*

Five CpG sites within the promoter of the *LCN2* gene were assessed for methylation in a series of DNAs from two different blood leukocytes samples, normal urothelial cells, fibroblasts and bladder cancer cell lines 5637, 647v, HT-1376, J82, RT112 and SD (Fig 3.9). Overall, the first two CpG sites seemed to be preferentially methylated in most cell lines, if any methylation occurred. Blood leukocytes were partially methylated; normal urothelial cells were predominantly unmethylated and fibroblast DNA was weakly methylated. Bladder cancer cell lines HT-1376 and J82 were both partially methylated, RT112 and SD were both weakly methylated, but 5637 and 647v were both unmethylated.

LCN2 was expressed in normal urothelial cells; similarly RT112, SD and 647v expressed the gene. *LCN2* was not detectable in J82, HT-1376, 5637 and fibroblasts.

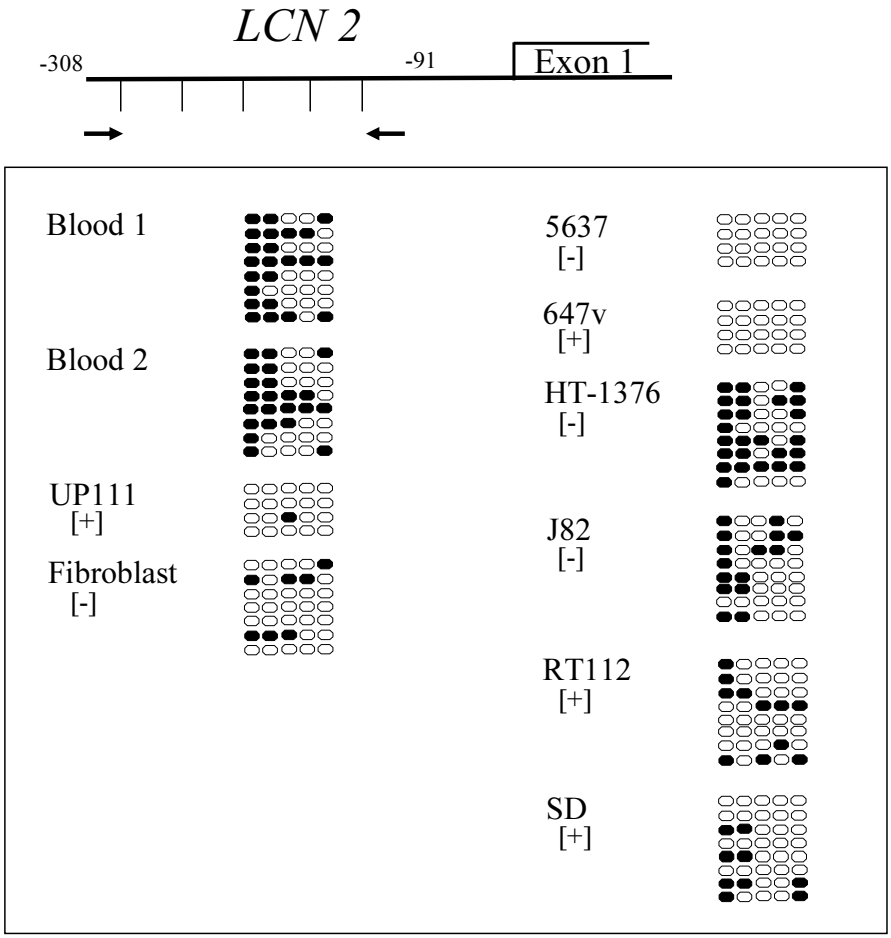

Fig. 3.9: Bisulfite sequencing analysis of 5 CpG sites in the regulatory region of LCN2, on the left are the normal controls and on the right are the bladder cancer cell lines. The plus or minus symbol in parentheses represents the corresponding mRNA expression levels: [-] no or low expression, [+] moderate expression, [++] high expression.

3.2 Results of microarray II

3.2.1 Design and general evaluation of microarray II

The first microarray study (Section 2.14.1) had compared the expression profiles of normal and malignant urothelial cells from one patient. Although it had yielded several candidates for genes that might be overexpressed in bladder cancer as a consequence of DNA hypomethylation, there was no specific selection in the approach for hypomethylation as opposed to other possible mechanisms leading to overexpression. In order to identify further candidates, a second microarray was performed using an approach more specifically designed to identify genes activated by DNA hypomethylation.

For this purpose, gene expression profiles were compared before and after treatment of two cultures of normal urothelial cells (UP159 and UP160) and two bladder cancer cell lines (VMCub1 and UM-UC3) with the DNA methylation inhibitor 5-aza-dC using HG-U133A (Affymetrix) oligonucleotide chips containing 22,283 identifiers (Section 2.14.2). Genes activated in cancer cells by hypomethylation specifically should emerge in this comparison as expressed more strongly in cancerous than normal cells AND induced by DNA demethylation in normal cells (because of being repressed by DNA methylation in these) AND not or weakly induced by 5-aza-dC treatment in cancer cells (because of being already hypomethylated and overexpressed).

Fig 3.10 shows the distribution of genes differentially expressed between the various treated and untreated cells by significance levels. Using a significance level of p=0.01, 2354 identifiers were significantly differentially expressed between the two different cultures of normal urothelial cells under basal conditions. Following treatment with 5-aza-dC, this number increased to 3087. Overall, 4413 identifiers were differentially expressed in the urothelial cells with or without 5-aza-dC treatment. Between the two bladder cancer cell lines, 5738 identifiers were expressed significantly different in the absence of treatment. After treatment with 5-aza-dC, the number increased to 6318 identifiers. A total of 4163 identifiers were differentially expressed in both cell lines as a consequence of 5-aza-dC treatment. In the absence of 5-aza-dC treatment, 8102 identifiers differed significantly between the urothelial cells and the bladder cancer cell lines.

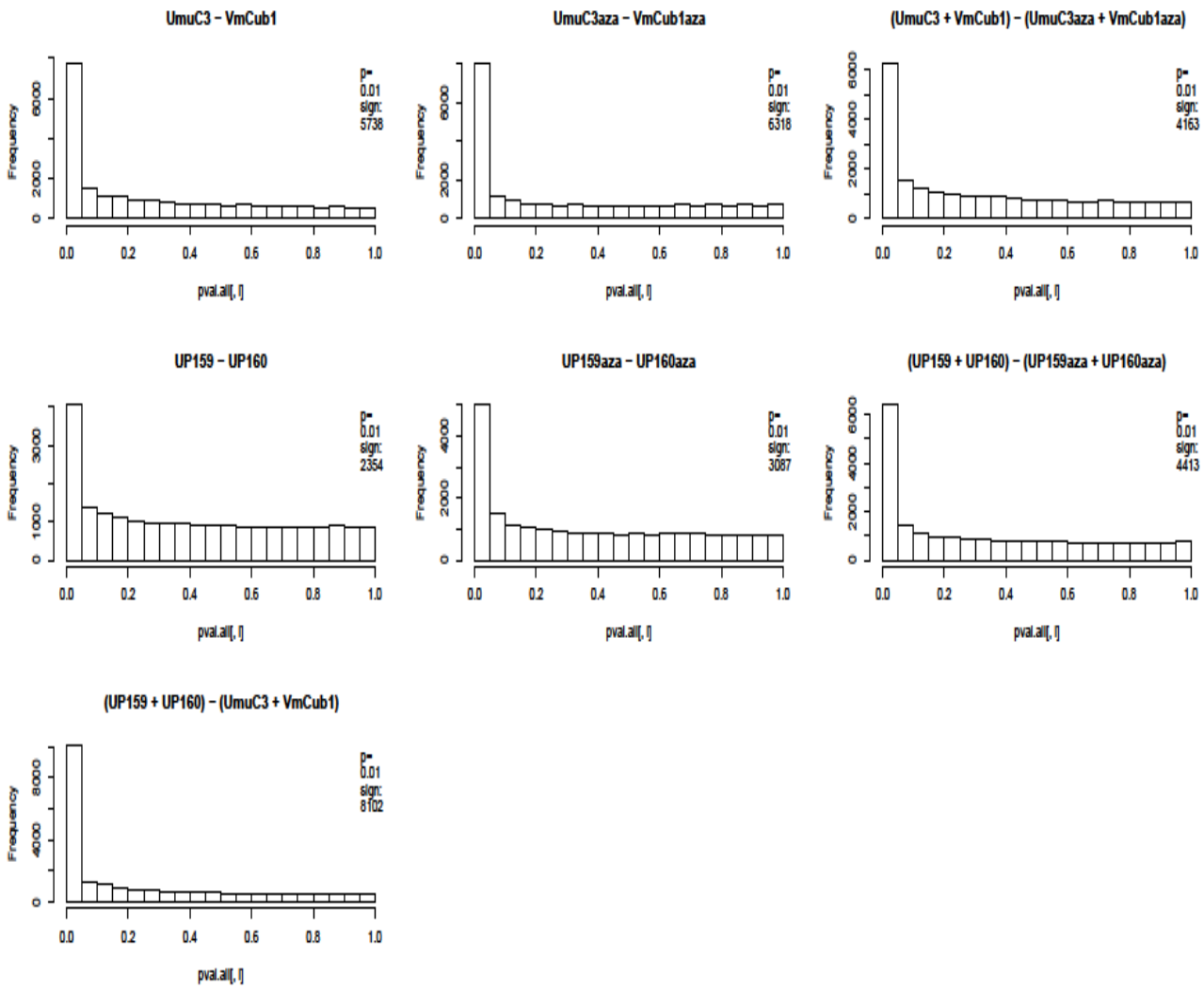

Fig. 3.10: Histogram of identifiers differentially expressed in normal urothelial cells and bladder cancer cell lines with or without 5-aza-dC treatment. The x-axis and y-axis represent the p-value and the frequency of identifiers respectively. Only identifiers with a significance level of p=0.01 were considered for further analysis.

To identify candidate genes upregulated in bladder cancer as a result of DNA hypomethylation we made three comparisons to define Group 1-3. Group 1 consisted of identifiers upregulated in the normal urothelial cells as a result of 5-aza-dC treatment, Group 2 contained identifiers upregulated in the bladder cancer cell lines in comparison to the normal urothelial cells and Group 3 consisted of identifiers upregulated due to the effect of 5-aza-dC treatment on the bladder cancer cell lines. From these three groups we selected identifiers present in Groups 1 as well as 2. From these results, we removed genes that were also present in Group 3. This procedure yielded an initial list of 838 identifiers. This was then reduced to a list of 205 genes by removing redundancies, i.e. genes represented by several identifiers, not annotated ESTs, and by requiring an at least 1.5-fold difference in the

comparisons. Furthermore, genes without annotations were excluded from this list. This list is shown in Appendix 2 and the genes are summarily called “candidates II” in the following.
As a positive control for the validity of the approach, the lists of significant genes were investigated for genes encoding cancer testis antigens, i.e. genes known to be expressed in solid tumors but repressed by DNA methylation in normal tissues (Section 1.4.2). Indeed, the selected genes included members of the MAGE family of proteins, *MAGEA3, MAGEA4, MAGE5, MAGEA6* and *MAGEB2*, of which the first two were retained following application of the stricter criteria.

3.2.2 Bioinformatic analysis of the candidate list of genes

Next, the “candidate II” gene list (Appendix 2) was analyzed for gene function, chromosomal localization and tissue-specific expression.
Ordering the genes by gene ontology (GO) groups revealed several significantly overrepresented categories, shown in red in Fig. 3.11 and 3.12. Fifteen genes were involved in cell communication by playing an active role in regulation of signal transduction and 5 genes were specifically involved in the regulation of Rho protein signal transduction. Overall, nineteen genes function as negative regulators of cellular physiological processes. Of special interest in the context of this study, 13 genes are involved in chromosome organization and biogenesis and 2 genes act as negative regulators of transcription factor activity. Eleven genes are involved in DNA packaging and establishment and maintenance of chromatin architecture. Similarly, 9 genes play a role in chromatin or nucleosome assembly. On a note of caution, the overrepresentation of these categories is largely a consequence of a number of histone genes from the HIST1 cluster on chromosome 6p, which contains histone genes expressed during cell proliferation. In addition two variant histone genes, *H2BFS* and *H2AFY* (encoding MacroH2A), and the *KAT2B* gene encoding the histone and protein acetylase PCAF were present. Moreover, inspection of the preliminary list selected by less strict criteria revealed many additional genes encoding chromatin factors, such as the histone deacetylases *SIRT1* and *SIRT7*. The overrepresentation of genes encoding immune response genes and chemokines in the list is typical of many studies involving 5-aza-dC (see discussion section 4.2). With respect to biochemical functions, the significantly overrepresented groups are dominated by a group of genes encoding proteins with ascorbic acid-dependent (hence: vitamin binding) oxidoreductase activity such as *P4HA1, PLOD2, PLOD1, LEPREL1, EGLN1* and by GTP exchange factors for Rho proteins.

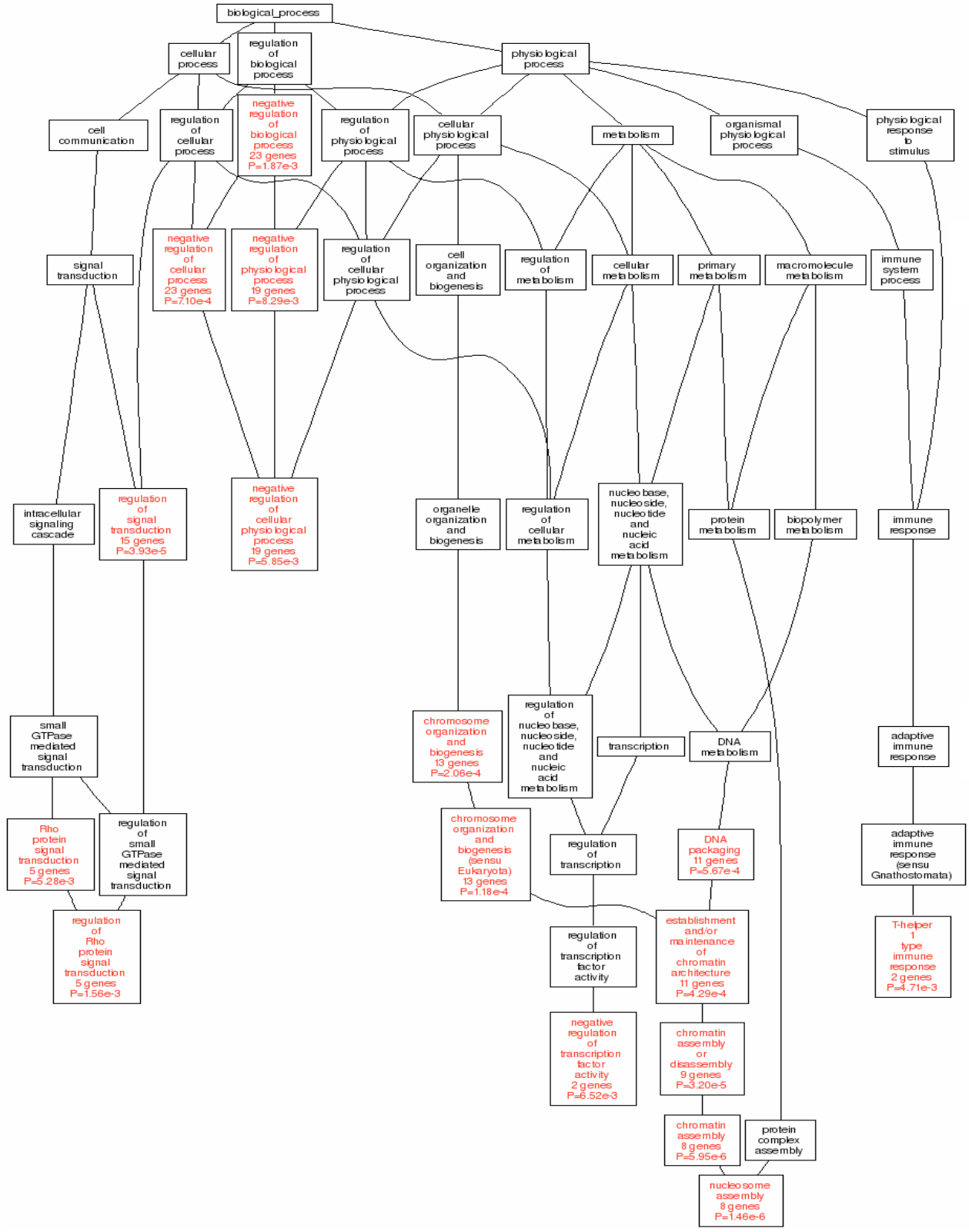

Fig. 3.11: DAG View of enriched GO categories. The enriched GO categories representing the biological process common to the list of 205differentially expressed genes are brought together and visualized as a Direct Acyclic Graph (DAG). Categories in red are enriched ones while those in black are non-enriched parents. Listed in the boxes are the name of the GO category, the number of genes in the category and the P-value indicating the significance of enrichment (GO database and WebGestalt software)

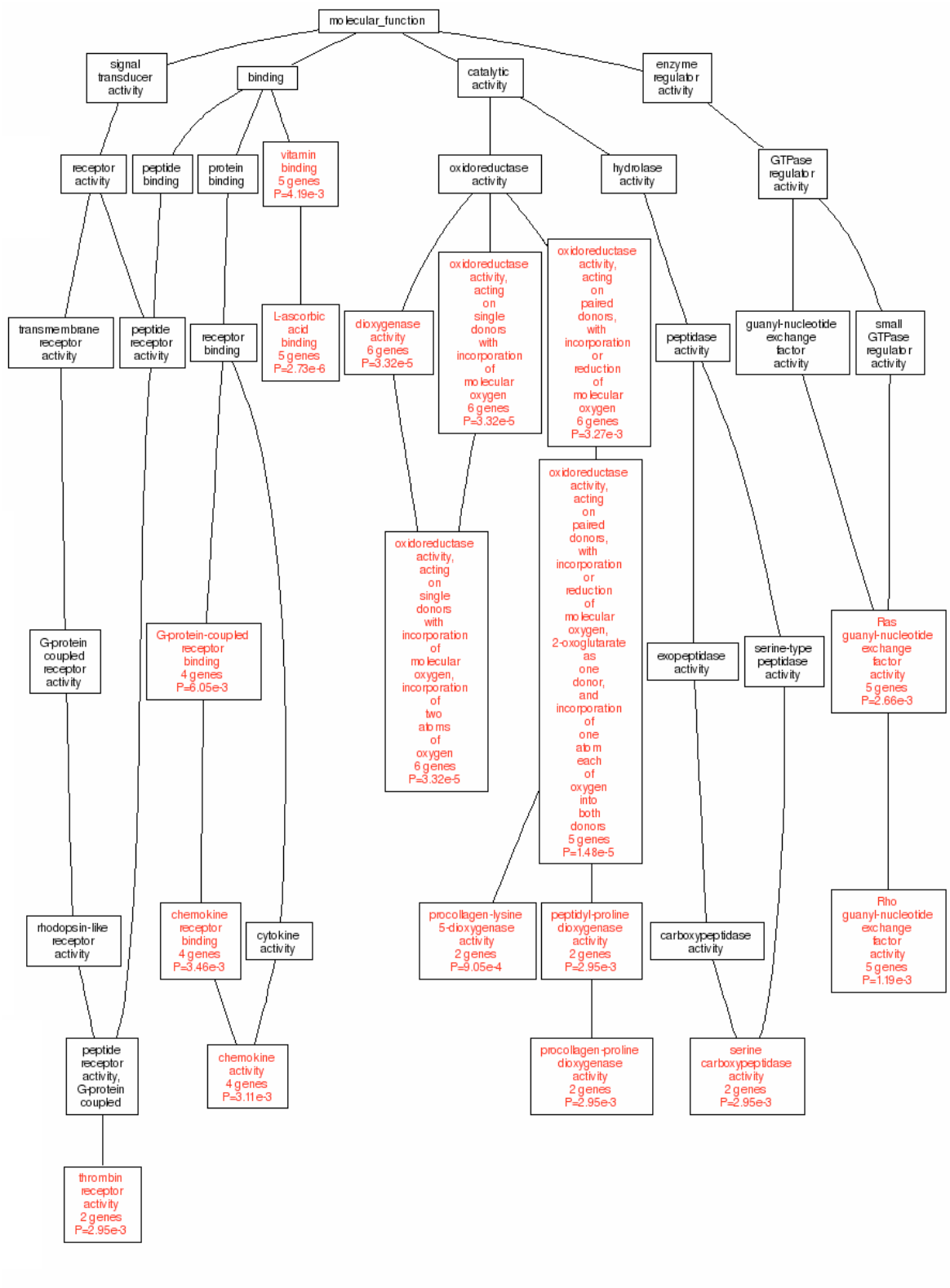

Fig. 3.12: DAG View of enriched GO categories. The enriched GO categories representing the molecular function common to the list of 205 differentially expressed genes are brought together and visualized as a Direct Acyclic Graph (DAG). Categories in red are enriched ones while those in black are non-enriched parents. Listed in the boxes are the name of the GO category, the number of genes in the category and the P-value indicating the significance of enrichment (GO database and WebGestalt software).

Concerning chromosomal locations, the (large and) gene-rich chromosomes 1 and 6 accounted for about 20% of the induced genes (Table 3.3). The highest numbers of genes were located on 1p and 6p. This finding brings to mind that the most frequent amplification in bladder cancer occurs around a region at chromosome 6p22, but it is mostly due to the presence of the 8 histone genes at 6p21.3 (Fig 3.13). Genes from all other chromosomes were represented, including chromosome 9. There was no gene contained from chromosomes 14p, 15p, 16p, 17p, 18p, 21p and 22p. The specific location of each gene on the chromosomes is shown in Fig 3.13.

Table 3.3: *Chromosomal locations of genes meeting strict selection criteria for hypomethylation candidates*

	Number of genes		
	p	**q**	**total**
1	14	4	18
2	6	6	12
3	3	9	12
4	1	7	8
5	2	7	9
6	13	10	23
7	3	8	11
8	6	5	11
9	3	6	9
10	1	8	9
11	6	5	11
12	3	8	11
13	4	3	7
14	0	12	12
15	0	4	4
16	0	1	1
17	0	5	5
18	0	4	4
19	4	2	6
20	3	6	9
21	0	6	6
22	0	5	5
X	2	8	10
Y	-	-	-

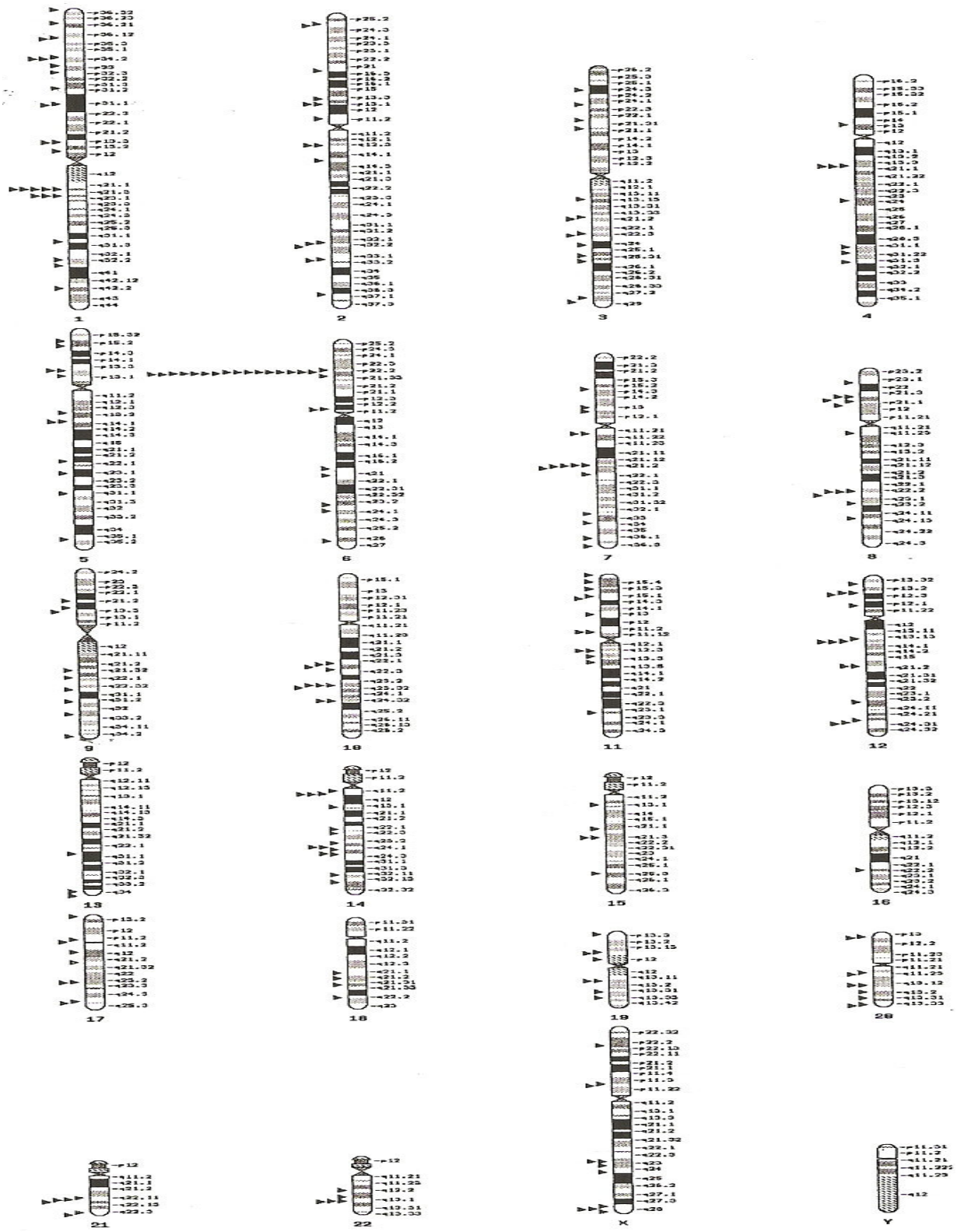

Fig 3.13: Diagrammatic representation of the precise chromosomal location of the genes meeting strict selection criteria for hypomethylation candidates

Further, a hierarchical clustering analysis was performed for the 205 genes that passed the filtering criteria (Appendix 2) with respect to their expression patterns in different tissues including cerebellum, amygdale, hypothalamus, liver, bone marrow, heart, skeletal muscle, thymus, testis, pituitary, adrenal gland, kidney, ovary, lymph node, pancreas, salivary gland, trachea, lung, placenta, thyroid, prostate and the uterus (Fig 3.14). This analysis was based on the data from the gene expression atlas. Unfortunately, the database does not cover gene expression in urinary bladder tissue.

Inspection of Fig 3.14 with respect to the tissues reveals that subsets of the candidate II genes tended to be particularly highly expressed in certain brain regions, like amygdala and hypothalamus, in the placenta, the thyroid gland, the testis, thymus and lymph nodes. More impressively, the genes clustered into several major groups, labelled A-F in the figure, with subdivisions in the A and F clusters. The cluster C consists of genes that are weakly expressed in all tissues, whereas the clusters D and even more so F2 are comprised of genes that are highly expressed in all tissues (i.e. “household genes”). The genes in cluster A1 show the most pronounced differences in expression between tissues, i.e. the cluster consists of “tissue-specific” genes. Similarly, the genes in clusters A2, B, E and F1 display considerable heterogeneity in their expression patterns in various tissues. The difference between them is that genes in the former two clusters tend to be weakly expressed overall, whereas those in the latter clusters tend to be strongly expressed in all tissues. Genes expected to be activated by hypomethylation in cancer would be expected among those that are expressed at low levels in all tissues or among those expressed in a tissue-specific manner. This means they should be contained in clusters A1 through C.

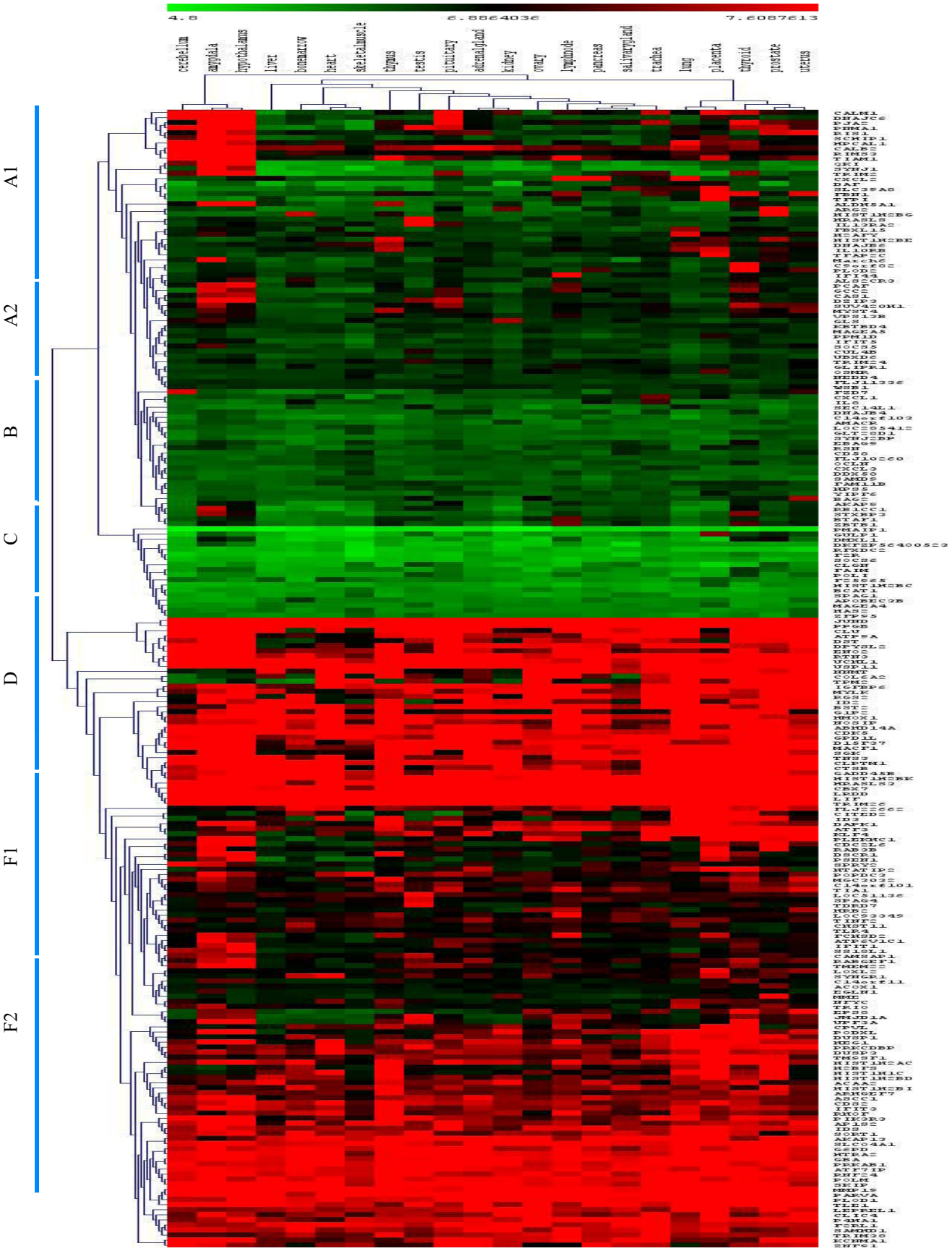

Fig 3.14: The hierarchical clustering analysis of tissue-specific expression for the candidate II genes

In order to further evaluate whether the candidate II genes might indeed represent genes activated by hypomethylation in cancer, they were investigated for “methylatibility”. The program [Bock et al, 2006] gives a likelihood of being unmethylated in normal tissues, which considers several factors, including DNA sequence, repeats and predicted DNA structure. The Fig. 3.15 shows a comparison of that likelihood for the candidate II genes against all genes in the genome. Unexpectedly, this analysis suggested that the candidate list was depleted of genes with a particular high likelihood of being methylated in their normal state.

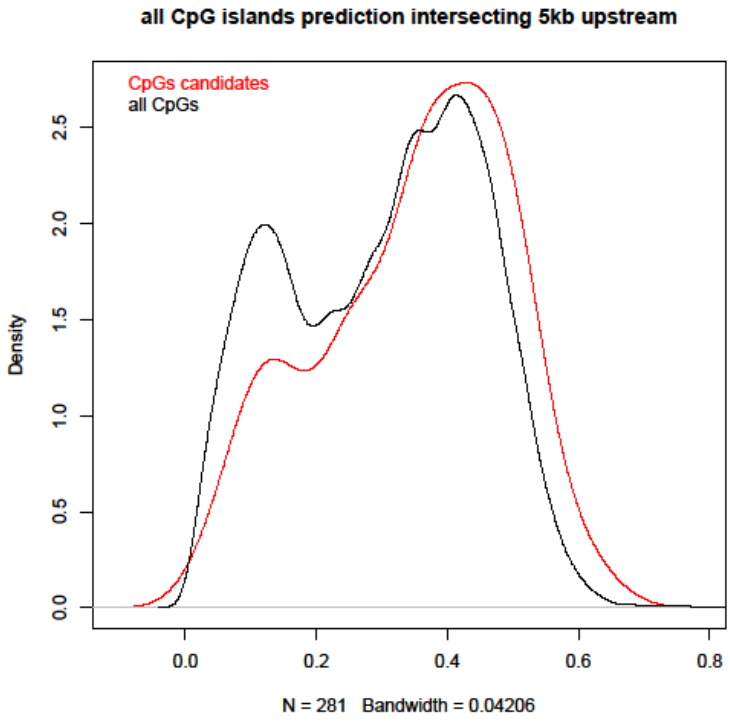

Fig. 3.15: Histogram of predicted methylation score, the x-axis represents the degree of methylatibility and the range 0 to 0.8 indicates the decreasing tendency of being methylated, the y-axis represents CpG density within 5 kb upstream of all candidate gene promoters. The N=281 is different from 205 genes, because the calculation program did not use all the genes due to insufficient information on them (resulting in a lower number), but considered alternative transcription start sites or first exons (resulting in an overall higher number).

In an attempt to verify if these expressed genes were truly hypomethylation candidate genes, 89 genes from cluster F1, A1 and some parts of cluster A2 in the Fig 3.14 were systematically searched on the ensembl genome-wide MeDIP data. These data shown by a visualization tool that has been integrated into the Ensembl genome browser for genome-wide identification and analysis of human tissue-specific differentially methylated regions. It is based on a study by Rakyan et al, 2008 who analyzed the genome-wide tissue-specific DNA methylation profiles for 12 normal tissues namely cervix, colon, liver, lungs, pancreas, placenta, prostate, rectum, skeletal muscle, sperm, uterus and whole blood. Among the 89 genes analyzed, 3 genes had no information available, 60 genes had at least one CpG island and 11 genes had 2 or more CpG islands. Eleven genes had a methylated region, of which 4 genes displayed homogenous methylation among all tissues; but none had a methylated region within the CpG island around the gene transcription start site. Overall, the data showed that there was no true DNA hypomethylation candidate gene among the 89 genes analyzed.

Considering the above analyses, 11 genes were selected for expression analysis consisting of 3 genes from a preliminary list selected by less strict criteria namely *DEPDC1, SIRT1* and *SIRT7* as well as 8 additional genes from the pool of 205 genes generated by strict filtering criteria, namely *DDX58, LOXL2, KLF4, H2AFY, PCAF, CBX7, JMJD1A and MYST4.* These selected genes have been various reported as critical regulators of cancer progression or as vital to the regulation of the chromatin structure (Table 3.4). Only *KLF4*, *CBX7* and *DEPDC1* have been investigated in bladder cancer so far but even they have not been studied yet to verify if their upregulation was due to DNA hypomethylation.

Table 3.4: List of selected genes, their function and expression in human cancers

Gene name	Protein name	cancer type	expression	references
LOXL2	LOXL2	esophageal head and neck	upregulated downregulated	Ban et al, 2005 Rost et al, 2003 Payne et al, 2007
DDX58	DDX58	Kaposi's sarcoma	upregulated	Livergood et al, 2007
DEPDC1	DEPDC1	bladder	upregulated	Kanehira et al, 2007
KLF4	KLF4	colorectal breast	downregulated upregulated	Zhao et al, 2004 Foster et al, 2000 Evans et al, 2007
SIRT1	SIRT1	prostate hepatic	upregulated downregulated	Hoffmann et al, 2007 Wang et al, 2008, Firestein el al, 2008
SIRT7	SIRT7	thyroid breast	upregulated upregulated	De Nigris et al, 2002; Frye 2002. Ashraf et al, 2006
MYST4	MYST4			Fraga et al, 2005 McGraw et al, 20073
PCAF	PCAF	Wilm's tumors central nervous system tumors	upregulated upregulated	Schiltz and Nakatani, 2000. Patel et al., 2004 Okumura et al., 2006, Armas-Pineda et al, 2007
JMJD1A	JMJD1A	renal	upregulated	Yamane et al, 2006 Loh et al, 2007 Okada et al, 2007 Beyer et al, 2008
CBX7	CBX7	follicular lymphoma bladder, thyroid	upregulated downregulated downregulated	Gil et al, 2004 Scott et al, 2007 Hinz et al, 2008 Pallante et al, 2008
H2AFY	MacroH2A			Heard and Disteche, 2006

3.2.3 Expression analysis of *H2AFY*

The mRNA expression of *H2AFY* (encoding the histone variant Macro-H2A) was measured in a panel of cell lines consisting of two independent primary cultures of urothelial cells, namely UP160 and UP159, and twelve urothelial carcinoma cell lines (Fig. 3.16). A high expression of *H2AFY* was observed in the normal urothelial cell cultures. Among the cancer cell lines, the highest expression occurred in the papillary tumor cell line RT4. High expression of *H2AFY* was also noticeable in RT112, SD and SW1710, whereas the remainder of the carcinoma cell lines expressed *H2AFY* at a moderate level, below those of normal urothelial cells. Overall, there was a higher level of expression in the urothelial cells in comparison to the urothelial carcinoma cell lines. In order to investigate whether the downregulation of *H2AFY* in some of the bladder cancer cell lines was due to DNA hypermethylation the cell lines were treated with 5-aza-dC. Subsequent treatment of the panel of cell lines with 5-aza-dC led to a slight induction of the gene in some of the cell lines, notably 639v and 647v (Fig. 3.16). However it had no effect or reduced expression in fibroblasts, UM-UC3, SD, RT4, SW1710 and RT112. It is therefore more likely that changes in *H2AFY* gene expression are not related to altered DNA methylation.

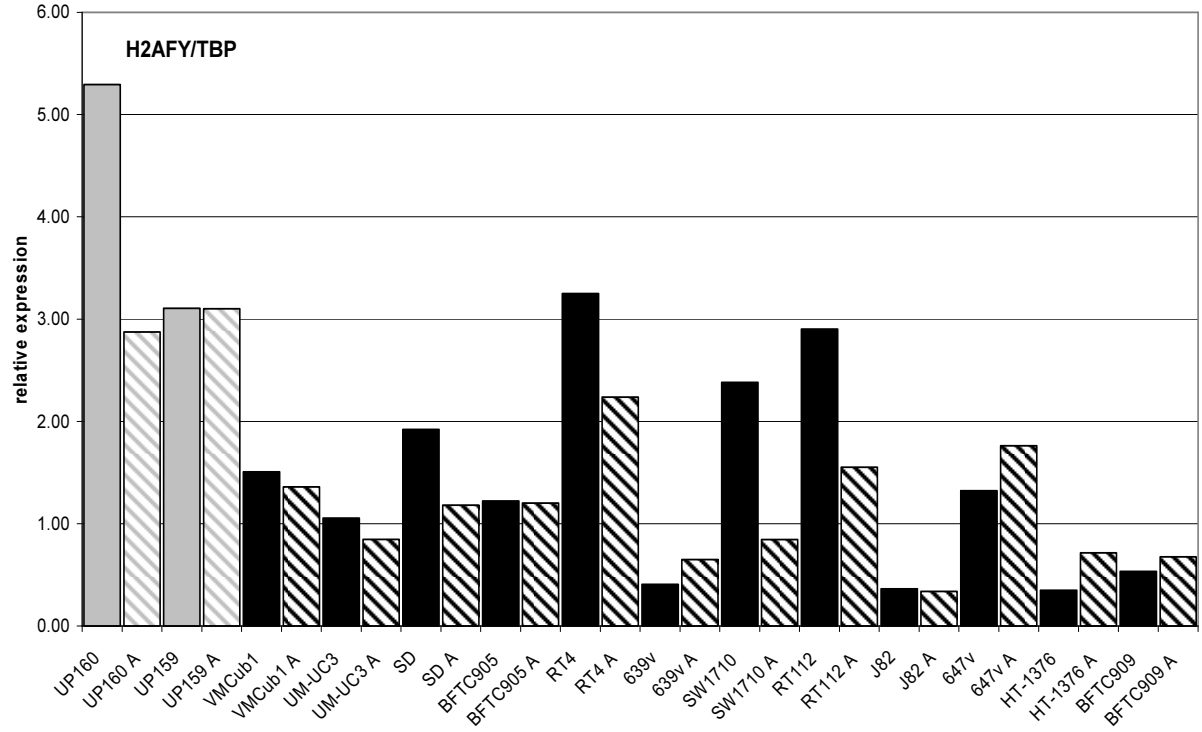

Fig. 3.16: Expression of H2AFY relative to TBP in normal urothelial cell cultures and bladder cancer cell lines as quantified by RT-PCR. 5-aza-dC treated cells are shown as striped bars and the untreated cells are represented by solid bars. Normal urothelial cells are represented in grey bars and bladder cancer cell lines are represented in black bars.

3.2.4 Expression analysis of *PCAF*

The expression of *PCAF* (encoding a major histone acetyltransferase) was highest in the normal urothelial cells from the UP160 culture, but there was also high expression in the other normal urothelial cells (Fig. 3.17). Among the cancer cell lines, VMCub1, UM-UC3, SW1710, RT4 and RT112 all had high expression of *PCAF* whereas cell lines such as SD, BFTC905, 639v, J82, 647v, HT-1376 and BFTC909 displayed moderate to low levels of expression. Overall, there was an heterogenous pattern of expression in the bladder cancer cell lines and normal urothelial cell cultures.

Treatment with 5-aza-dC led to higher *PCAF* expression in normal urothelial cells from one but not another culture (Fig. 3.17). Similarly, it led to induced *PCAF* expression in some bladder cancer cell lines especially with low expression such as SD, RT4, 639v and HT-1376, but to downregulation of *PCAF* in other cells such as VMCub1, UM-UC3, SW1710, RT112 with higher expression under basal conditions. Thus, PCAF expression may to some extent be affected by DNA methylation.

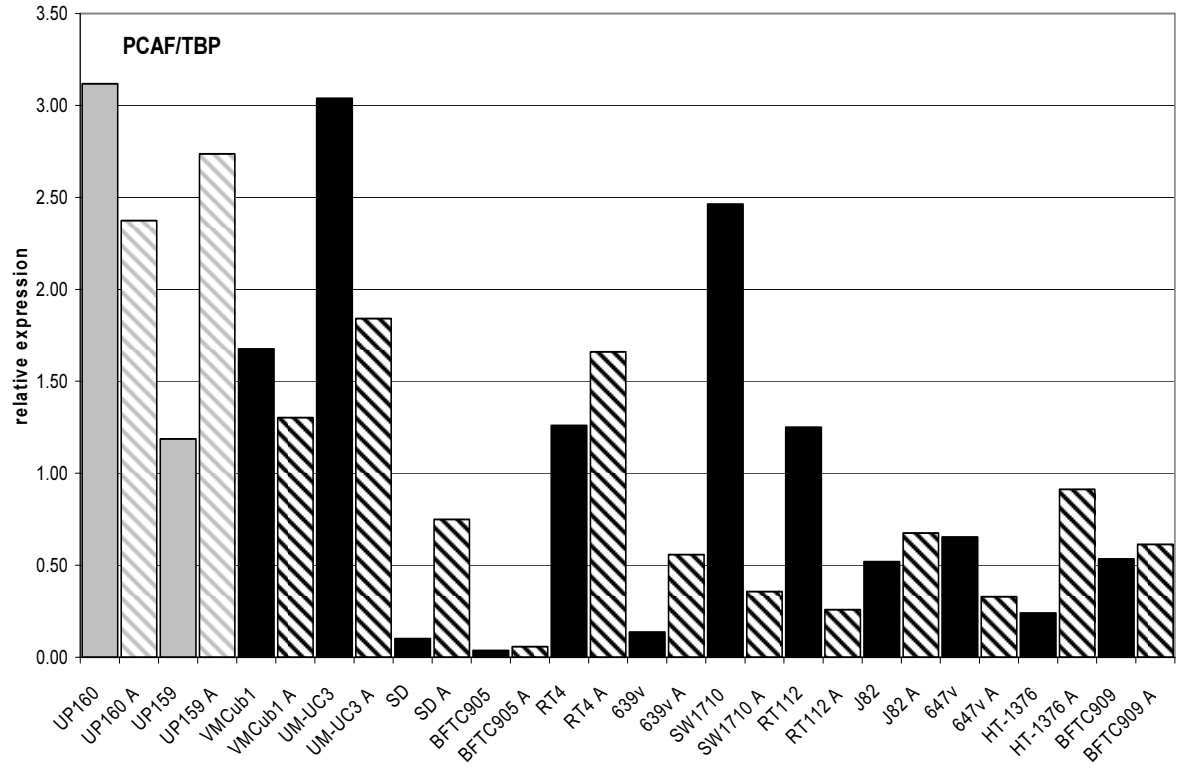

Fig. 3.17: Expression of PCAF relative to TBP in normal urothelial cell cultures and bladder cancer cell lines as quantified by RT-PCR. 5-aza-dC treated cells are shown as striped bars and the untreated cells are represented by solid bars. Normal urothelial cells are represented in grey bars and bladder cancer cell lines are represented in black bars.

3.2.5 Expression analysis of *MYST4*

MYST4 expression was quantified in both normal urothelial cell cultures and bladder carcinoma cell lines (Fig. 3.18). The gene encodes a prominent histone acetyltransferase. There was a high expression of *MYST4* in the normal urothelial cell cultures. Similarly, high expression of this gene was witnessed in bladder cancinoma cell lines UM-UC3, SW1710 and RT112. Remarkably there was a low expression of MYST4 in most of the bladder carcinoma cell lines including SD, BFTC905, RT4, 639v, J82, 647V, HT-1376 and BFTC909. The highest overall expression was seen in VMCub1.

There was a moderate induction of *MYST4* expression in some of the cell lines after 5-aza-dC treatment (Fig. 3.18). Notably the UP159 culture was slightly induced. In contrast, bladder cancer cell lines such as SD, BFTC905, 639v, J82, HT-1376 all were little affected by 5-aza-dC treatment and some cell lines actually had reduced expression of *MYST4*, namely the UP160 culture, VMCub1, UM-UC3, RT4, SW1710 and RT112. Overall, any effect of DNA methylation on gene expression seem subtle.

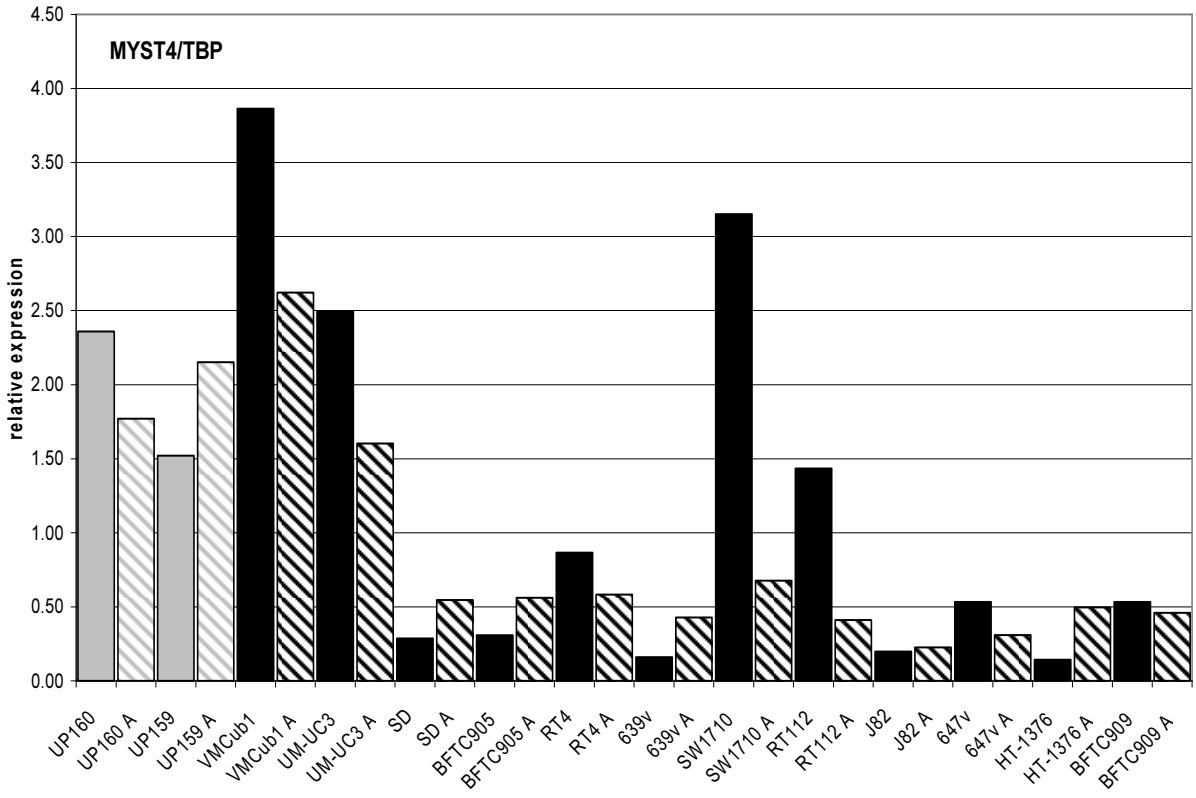

Fig. 3.18: Expression of MYST4 relative to TBP in normal urothelial cell cultures and bladder cancer cell lines as quantified by RT-PCR. 5-aza-dC treated cells are shown as striped bars and the untreated cells are represented by solid bars. Normal urothelial cells are represented in grey bars and bladder cancer cell lines are represented in black bars.

3.2.6 Expression analysis of *JMJD1A*

There was a heterogeneous level of expression of *JMJD1A*, which encodes a histone H3K9 demethylase, ranging over one order of magnitude in the panel of cells examined (Fig. 3.19). The gene had very high expression in the normal urothelial cell cultures. Among the bladder carcinoma cell lines, there was a high expression of the gene in VMCub1, UM-UC3, RT4, SW1710 and RT112, whereas the other bladder cancer cell lines had a moderate or low level of expression of *JMJD1A*.

The treatment with 5-aza-dC led to induction of *JMJD1A* expression in some of the cell lines such as SD, UP159, BFTC905, 639v, and HT-1376 (Fig. 3.19). It had little or no effect on most of the other cell lines. In fact, for some of the cell lines there was a marked reduction in the level of expression as in the case of UM-UC3, VMCub1, RT4, SW1710 and RT112. Thus, DNA methylation appears to have at most minor effects on this gene.

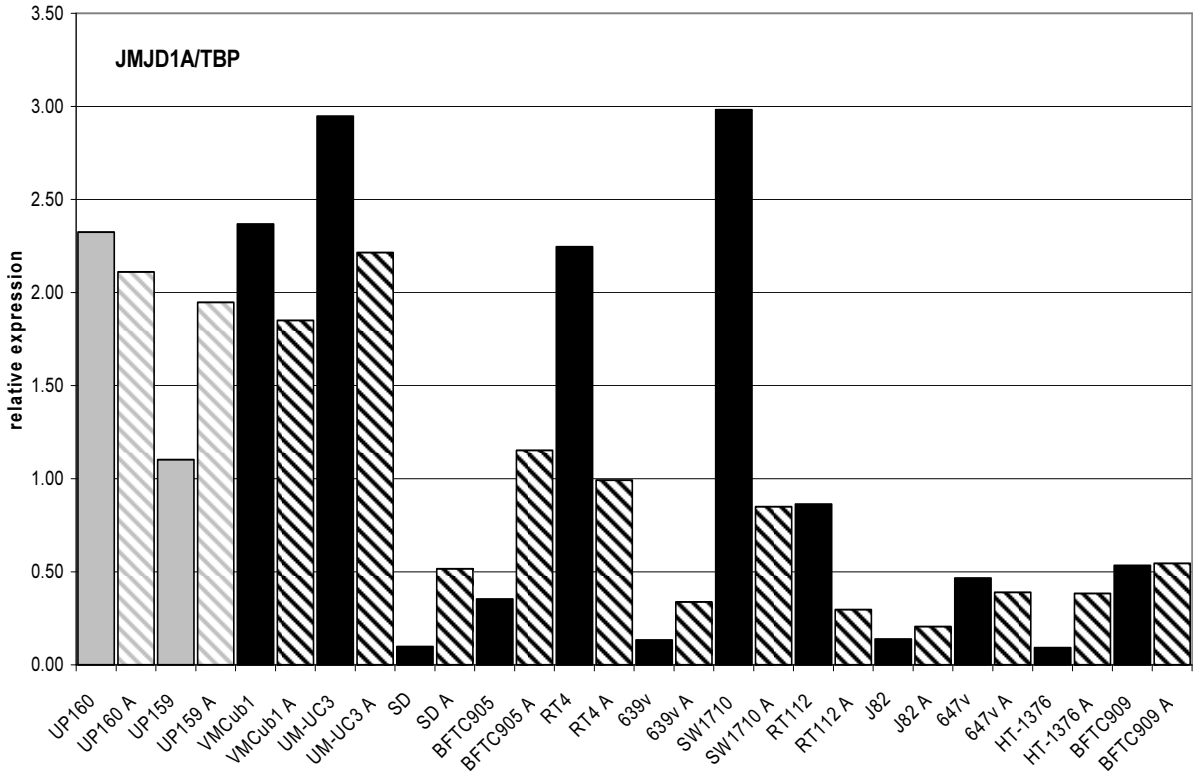

Fig. 3.19: Expression of JMJD1A relative to TBP in normal urothelial cell cultures and bladder cancer cell lines as quantified by RT-PCR. 5-aza-dC treated cells are shown as striped bars and the untreated cells are represented by solid bars. Normal urothelial cells are represented in grey bars and bladder cancer cell lines are represented in black bars.

3.2.7 Expression analysis of *MYST4, JMJD1A, H2AFY, PCAF* and *CBX7* in normal bladder and tumor tissue samples

The expression of *MYST4, JMJD1A, H2AFY, PCAF* and the polycomb factor *CBX7* was measured in a set of tissue samples consisting of 10 normal bladder tissue samples and 31 tumor samples (Fig. 3.20). The expression of *MYST4, PCAF* and *CBX7* was clearly higher in normal tissue samples in comparison to the tumor samples. All p-values obtained by Mann-Whitney test, $p = 0.026$ for *MYST4,* $p = 0.003$ for *PCAF* and $p < 0.001$ for CBX7 showed a statistically significant decrease in the cancer tissues. The lowest relative unit values for *MYST4, PCAF* and *CBX7* in the tumor samples were 0.49, 0.97 and non-detectable, respectively, whereas the lowest relative units for the *MYST4, PCAF* and *CBX7* in the normal tissues samples were 9.59, 74.84 and 16.30 respectively.

There was no statistically significant difference in the expression of *JMJD1A* in the tumor tissue samples in comparison to the normal tissues. The p-values according to Mann-Whitney test was $p = 0.463$. However the expression of *JMJD1A* in many tumor samples was remarkably low. The lowest relative unit value for *JMJD1A* in tumor tissues was 0.10 while the lowest relative unit value for normal tissues was 4.81.

Conversely, normal tissue samples presented lower relative unit values for *H2AFY* in comparison to the tumor samples, although, ranges overlapped. The lowest relative unit value for *H2AFY* in tumor tissues was 0.84 and the lowest relative value in normal tissues was 1.27. Nevertheless, the overall difference in expression between tumor and benign tissues was statistically different ($p = 0.039$).

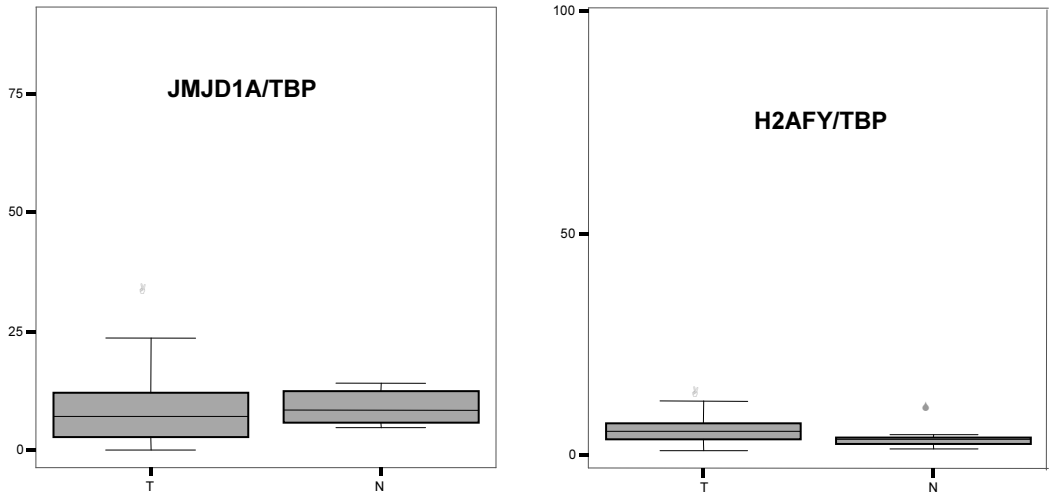

N=10 T=31

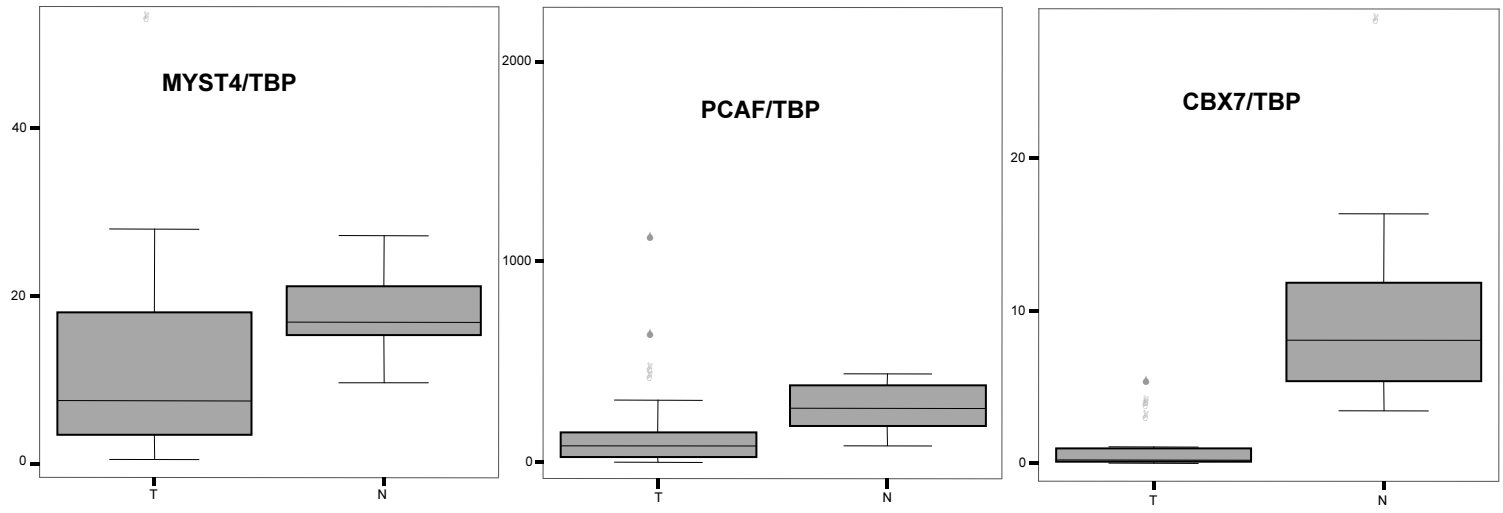

Fig. 3.20: Box plots depicting the expression of JMJD1A, H2AFY, MYST4, PCAF and CBX7 relative to TBP in 31 bladder tumors and 10 normal tissues as determined by real-time RT PCR. N represents normal tissue samples and T represents tumor samples. Two outliers in the normal tissues for JMJD1A and PCAF with the relative unit values of 89.5 and 2181 and an outlier in the tumor tissues for H2AFY with a relative unit value of 96.73 were omitted.

3.2.8 Expression analysis of *DDX58*

The expression of *DDX58* (also called *RIG-1*), encoding an interferon-inducible protein capable of detecting viral RNAs, was assessed in two independent cultures of normal urothelial cells and 13 bladder carcinoma cell lines (Fig. 3.21). The gene was expressed in the normal urothelial cell cultures at a comparable level with those of most bladder cancer cell lines. Particularly high expression of *DDX58* occurred in J82 and 647v. SW1710 also had very high expression of the gene. A moderate level of expression was seen in 5637, BFTC905, RT112 and SD whereas 639v, BFTC909, HT-1376, RT4, UM-UC3 and VMCub1 all expressed *DDX58* at a slightly lower level than the normal urothelial cell cultures. Overall the level of *DDX58* expression was elevated in 3 bladder cancer cell lines, but it was expressed at an equal or lower level in other bladder cancer cell lines in comparison to the normal urothelial cell cultures.

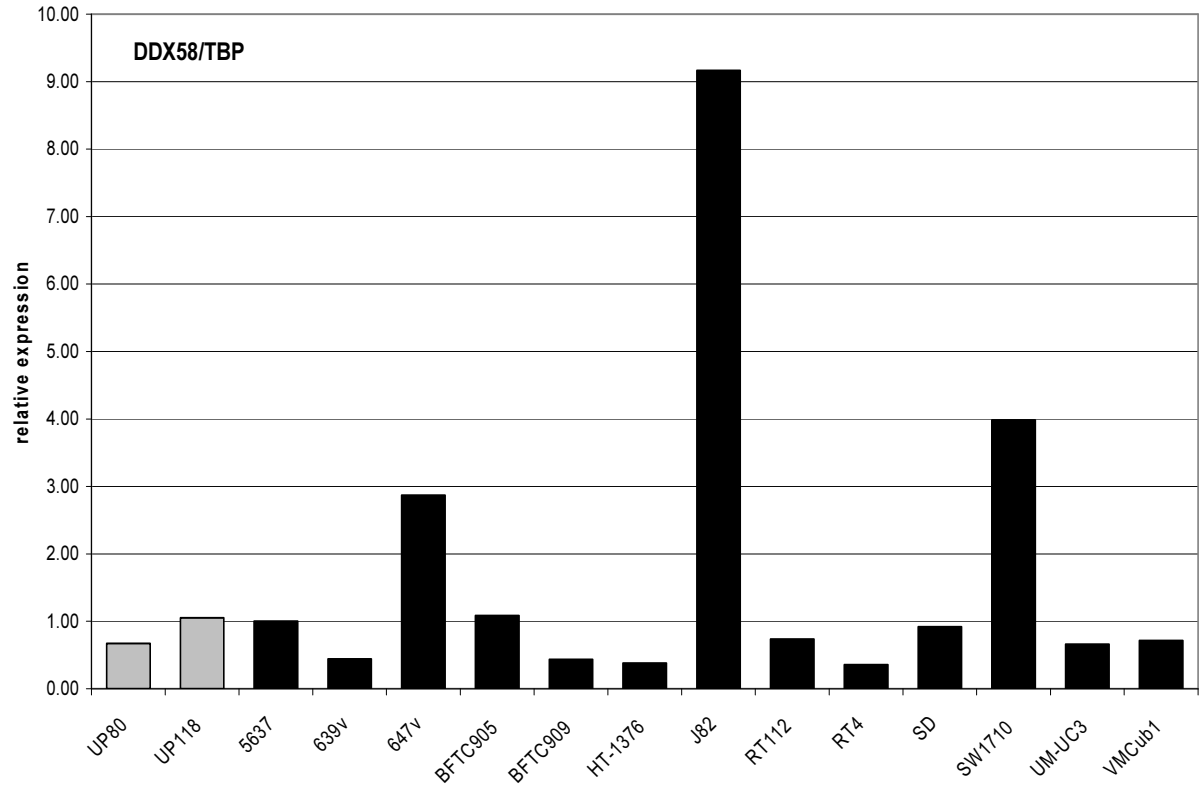

Fig. 3.21: Expression of DDX58 relative to TBP in normal urothelial cell cultures and bladder cancer cell lines as quantified by RT-PCR. Normal urothelial cells are represented in grey bars and bladder cancer cell lines are represented in black bars.

3.2.9 Expression analysis of *KLF4*

There was a low but detectable level of expression of *KLF4,* which encodes a transcription factor controlling cell differentiation, in the two independent cultures of normal urothelial cells investigated (Fig. 3.22). Most of the bladder cancer cell lines displayed a very high level of expression of *KLF4* with the exceptions of SW1710 and UM-UC3. The expression level in 639v, in contrast, was almost undetectable. The highest expression seen in HT-1376 was more than 20-fold higher than in normal cells. In a snapshot the pattern of expression of *KLF4* was variable in the bladder carcinoma cell lines with only few cell lines expressing *KLF4* at a low level similar to normal urothelial cell cultures; the remaining bladder cancer cell lines expressed *KLF4* at levels much higher than those seen in the normal urothelial cells.

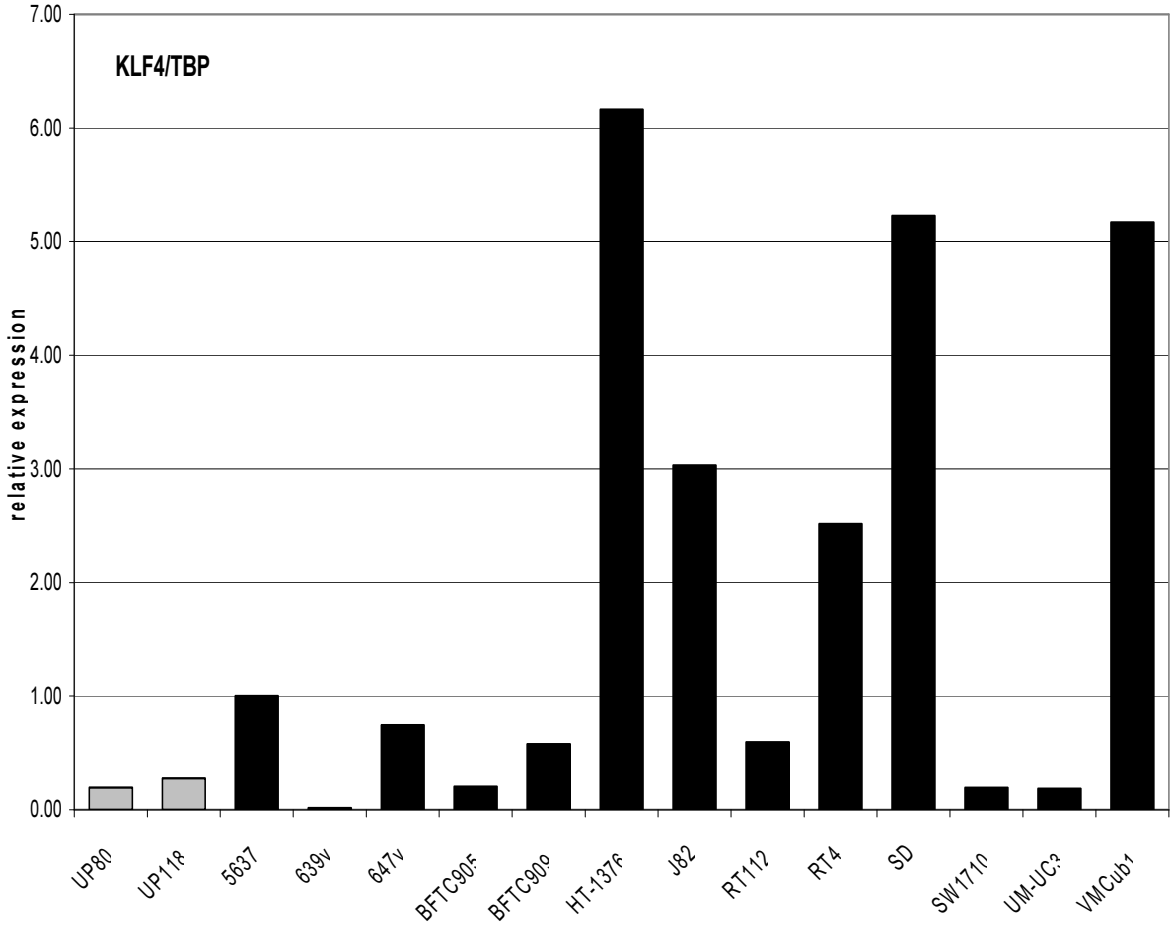

Fig. 3.22: Expression of KLF4 relative to TBP in normal urothelial cell cultures and bladder cancer cell lines as quantified by RT-PCR. Normal urothelial cells are represented in grey bars and bladder cancer cell lines are represented in black bars.

3.2.10 Expression analysis of *SIRT7*

Measurement of the *SIRT7* gene expression was performed in normal urothelial cell cultures and 13 bladder carcinoma cell lines (Fig. 3.23). The gene encodes an NAD^+-dependent protein deacetylase. The lowest level of expression of this gene was seen in the BFTC909 cell line, whereas the expression was high in 639v and RT4. All other cell lines had expression levels 1 - 2-fold those of the normal urothelial cell cultures. Thus expression of this gene tends to be increased in cancer cells, but moderately so, overall.

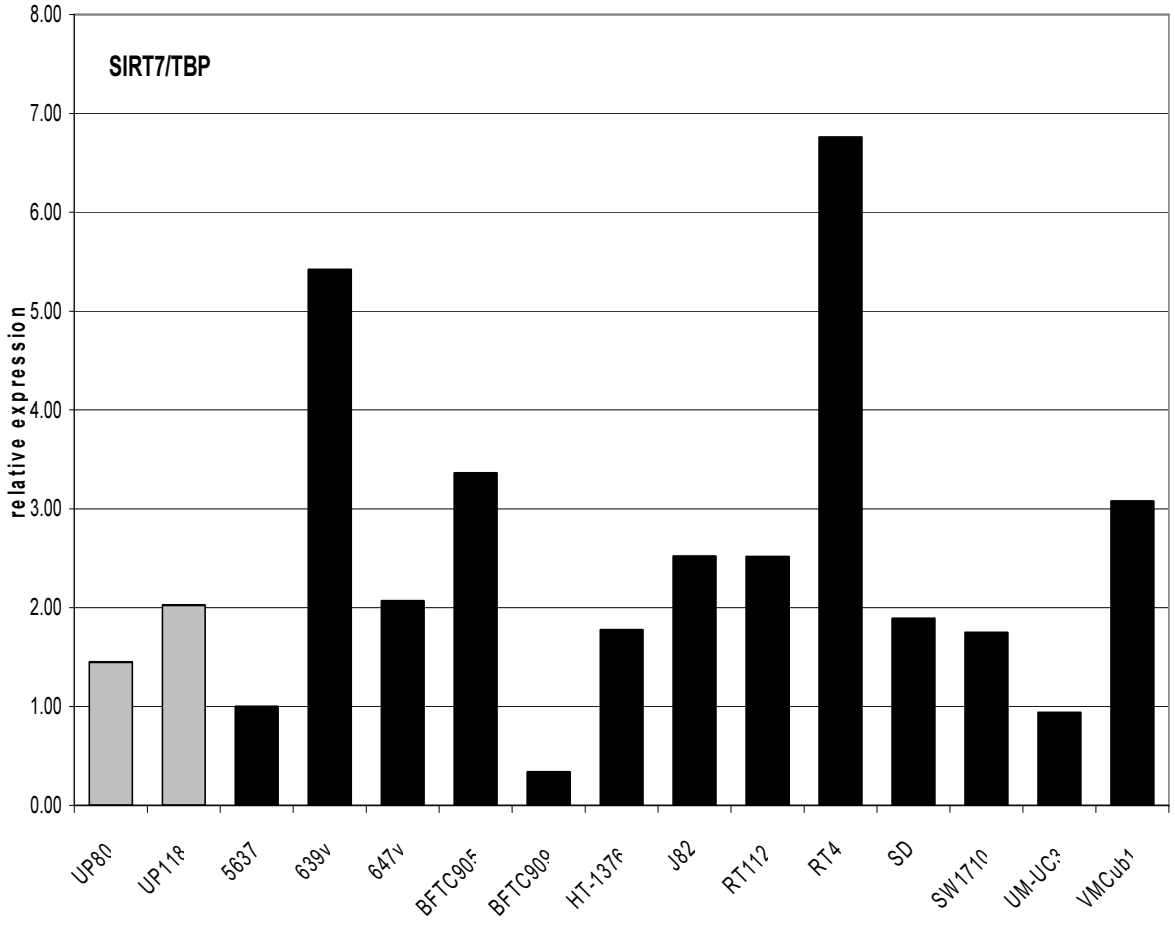

Fig. 3.23: Expression of SIRT7 relative to TBP in normal urothelial cell cultures and bladder cancer cell lines as quantified by RT-PCR. Normal urothelial cells are represented in grey bars and bladder cancer cell lines are represented in black bars.

3.2.11 Expression analysis of *LOXL2*

In the bladder cancer cell lines and normal urothelial cells examined, *LOXL2* encoding a protein hydroxylase implicated in metastasis, was the most variably expressed gene (Fig. 3.24). Interestingly, bladder cancer cell lines such as J82, UM-UC3, 647V, BFTC909 and SW1710 had high or very high expression of *LOXL2,* whereas other carcinoma cell lines the 2 independent cultures of normal urothelial cells either lacked the expression of the gene or expressed the gene at a low level. The difference between the highest level of expression in J82 and the average of the normal urothelial cells was almost 100-fold.

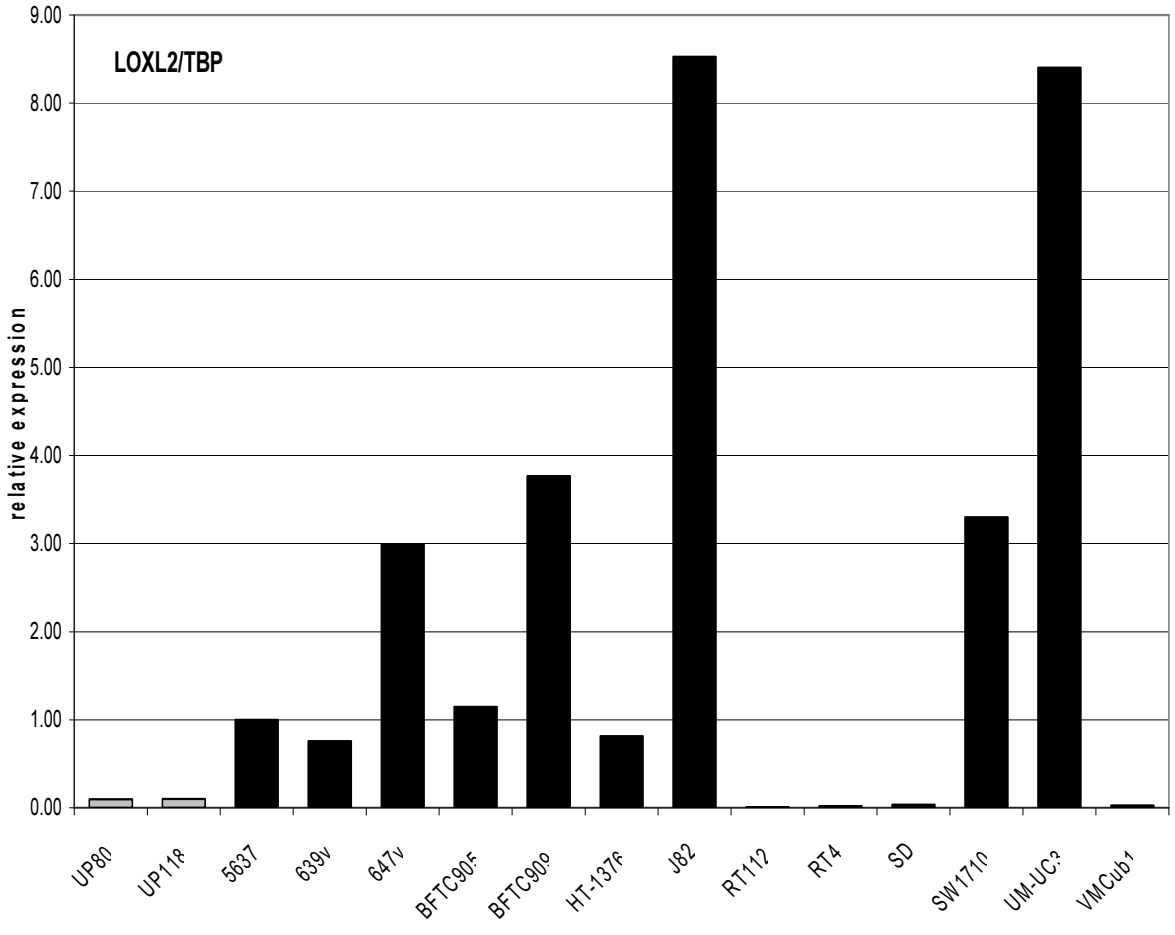

Fig. 3.24: Expression of LOXL2 relative to TBP in normal urothelial cell cultures and bladder cancer cell lines as quantified by RT-PCR. Normal urothelial cells are represented in grey bars and bladder cancer cell lines are represented in black bars.

3.2.12 Expression analysis of *SIRT1*

The expression of *SIRT1*, encoding the best characterized NAD^+-dependent protein deacetylase, was quantified in normal urothelial cells and bladder cancer cell lines (Fig. 3.25) and was well detectable in all cell lines examined. There was a heterogeneous pattern of expression in the cell lines used ranging over one order of magnitude. The expression of *SIRT1* was higher in the two independent primary cultures of normal urothelial cells than in several carcinoma cell lines including 5637, 639v, BFTC905, SD and UM-UC3. The highest expression was seen in SW1710, followed by 647v and VMCub1. The lowest expression occurred in UM-UC3. Overall, 5 bladder cancer cell lines had an expression level higher than those seen in the normal urothelial cells but the remaining bladder cancer cell lines had an expression level either equal to or lower than those of the normal urothelial cells.

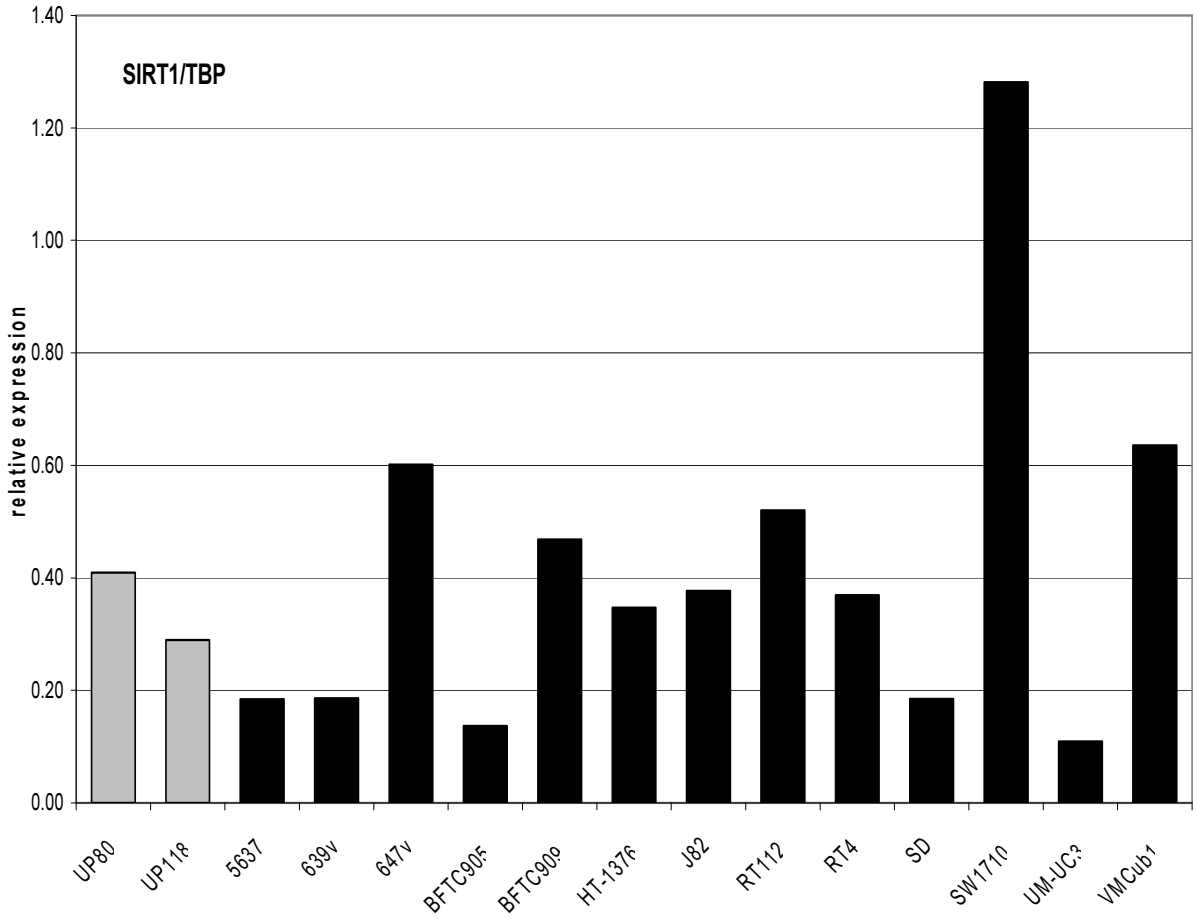

Fig. 3.25: Expression of SIRT1 relative to TBP in normal urothelial cell cultures and bladder cancer cell lines as quantified by RT-PCR. Normal urothelial cells are represented in grey bars and bladder cancer cell lines are represented in black bars.

3.2.13 Expression analysis of *DEPDC1*

DEPDC1, a gene with unclear function described as overexpressed in bladder cancer [Kanehira et al, 2007], was well detectable in all the cell lines examined (Fig. 3.26). The expression in the normal urothelial cell cultures was higher than in some but not all of the bladder cancer cell lines. The highest expression of the gene was witnessed in SW1710 followed by HT-1376 whereas the lowest expression occurred in the RT4, BFTC905 and UM-UC3. The expression of *DEPDC1* in the bladder cancer cell lines is therefore rather heterogeneous but overexpression does occur as reported by others [Kanehira et al, 2007].

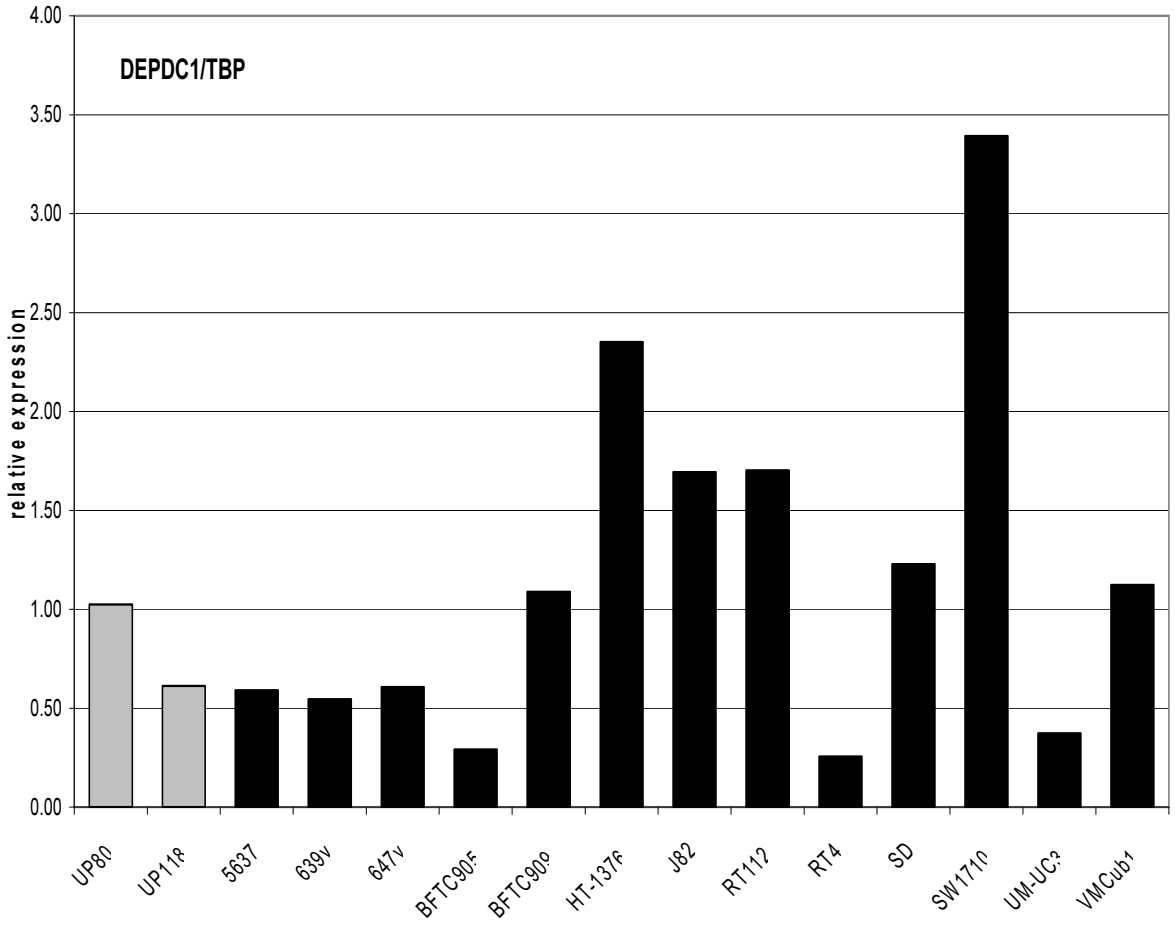

Fig. 3.26: Expression of DEPDC1 relative to TBP in normal urothelial cell cultures and bladder cancer cell lines as quantified by RT-PCR. Normal urothelial cells are represented in grey bars and bladder cancer cell lines are represented in black bars.

DISCUSSION

4.1 DNA methylation and expression of *SNCG, S100A4, S100A9* and *LCN2* in bladder cancer

4.1.1 Expression of *SNCG, S100A4, S100A9* and *LCN2* in human cancers

The analysis performed in this part of the thesis centered on investigating the possibility of DNA methylation as a mechanism responsible for the regulation of 4 genes selected following a microarray-based expression analysis of cultivated urothelial tumor cells. Recent reports from many investigators suggest that *SNCG, LCN2* and *S100A4* are upregulated in other types of cancer. Furthermore, this upregulation has been linked to DNA hypomethylation (see Introduction, section 1.6). Only *S100A9*, the fourth gene selected had not been previously studied for DNA methylation, but regulation by DNA methylation seemed a reasonable proposition due to its relationship with *S100A4.*

SNCG is upregulated prominently in advanced-stage breast and ovarian cancers, but overexpression has also been found in a large variety of other cancers. *SNCG* was reported to be highly expressed in most tumor tissues from liver, oesophagus, colon, gastric, lung, prostate, cervical, and breast cancer, but rarely expressed in tumor-matched nonneoplastic adjacent tissues [Liu et al, 2005]. Overexpression of γ-Synuclein has been shown to stimulate cancer cell proliferation and metastasis [Yanagawa et al 2004]. No study yet had been conducted in bladder cancer. The data from this thesis reveal no significant overall differences between bladder cancer and normal tissues. Similarly, the expression level found in cultured normal urothelial cells was intermediate in the sense that some bladder cancer cell lines had higher and several much lower expression than normal cells. A similarly strong variation was also seen in the tissue. These results contrast somewhat with the overall conclusion from studies on other tissues that γ-Synuclein is not expressed in the normal tissues and becomes upregulated in association with progression of cancers towards a metastatic state. However, the investigation of normal and cancerous prostate cells in the present study also revealed the same pattern as in the urothelial cells, namely expression in the normal epithelial cells, but a lack in cancer cell lines – which hardly fits with the report by Liu et al. 2005 on this cancer type. Obviously, more studies by independent groups on this matter are required.

Analysis of a panel of bladder tumor had revealed stronger expression of *S100A4* protein in the invasive tumors in comparison to the non-invasive tumors, thus suggesting a critical role for *S100A4* in the pathogenesis of bladder cancer, and also that it could be used to identify the group of patients at higher risk of progressing to the metastatic stage. Increased expression of

S100A4 protein correlated well with bladder cancer, pathologic stage and cancer-specific mortality [Davies et al, 2002].

Like *SNCG*, *S100A4* is highly expressed in breast carcinoma in comparison to benign tissues and significantly correlated with a poor prognosis for the patients [Wang et al, 2000]. At the protein level, S100A4 was expressed in both early and advanced breast cancer stages in comparison with normal tissue bolstering the evidence for its role in the progression of breast cancer [Ismail et al, 2008; Cabezon et al 2007]. Similarly, overexpression of *S100A4* is found in papillary thyroid tumours and associated with thyroid tumour invasion and metastasis [Zou et al, 2005]. *S100A4* is overexpressed at the mRNA and protein level in several other cancers including colorectal, gastric, lung and prostate cancer (see section 1.6.1).

An inverse correlation between *S100A4* expression and E-cadherin expression has been observed in melanoma and breast cancer suggesting that increased *S100A4* expression is associated with the phenomenon of the epithelial-mesenchymal transition (EMT). This transition is considered a critical step in tumor invasion and metastasis and might explain why overexpression of *S100A4* in all these cancers was related to metastasis and lower chances of survival [Salama et al, 2008]. A relationship between *S100A4* and the EMT fits with observation in the present thesis that expression was higher in fibroblasts than epithelial cells. However, the expression of *S100A4* by mesenchymal cells, from tumour stroma or from carcinoma cells having undergone EMT, can in principle complicate the determination of the actual expression level of the gene in tumor tissues. This complication could account for some discrepancies in the literature, including bladder cancer.

According to a previous microarray study from our institution comparing bladder carcinoma and normal tissues, *S100A4* was the most differentially upregulated gene [Modlich et al, 2004]. On the contrary, investigations by Yao et al, 2007 indicated that *S100A4* was underexpressed in bladder cancer. The expression analysis in the present study yielded no significant difference in the expression of *S100A4 and SNCG* in tumor samples in comparison to the normal tissues. In the case of the bladder carcinoma cell lines, the expression of the gene was heterogeneous. It might be interesting to investigate whether the expression of the gene in the cell lines was associated with the extent to which they exhibit characteristics of the EMT.

S100A9 was reportedly expressed in prostatic intraepithelial neoplasia and selectively in high-grade adenocarcinomas, whereas benign prostatic tissue was negative or showed weak expression of the protein. This was interpreted to mean that S100A9 is critically involved in both early events in prostate tumor development and progression of prostate carcinomas

[Hermani et al, 2005]. The protein was likewise reported to contribute to the progression of malignant phenotypes such as invasion, migration and proteinase expression in gastric cancer cells [Yong and Moon, 2007]. *S100A9* was also overexpressed in breast cancer cell lines in comparison to normal breast myoepithelial cells [Salama et al, 2008] and also in bladder cancer [Yao et al, 2007]. The present study confirmed the tendency of *S100A9* towards being overexpressed in bladder cancer tissues in comparison to the normal tissues, although the expression in bladder cancer lines was rather heterogeneous. Therefore, it might be worthwhile investigating the expression of the S100A9 protein in tissues and cell lines, considering especially differences among individual tumor cells, and to investigate its function in some detail.

LCN2 has been implicated in the progression of breast cancer, because high expression correlated with more invasive breast cancer. Also, overexpression of Lipocalin-2 in breast cancer cells increased the expression of mesenchymal markers, while suppressing the expression of epithelial markers. It was also found to increase cell motility and invasiveness through the EMT regulating transcription factor Slug, whereas *LCN2* knockdown led to reduced cell migration and loss of the mesenchymal phenotype [Yang et al, 2009]. Therefore, like S100A4, Lipocalin-2 appears to possess a function in EMT.

There were no previous studies on *LCN2* in bladder cancer. According to the expression analysis performed in this study, *LCN2* was significantly increased in the bladder tumor tissues in comparison to in the normal tissues. However, expression of these two genes in the bladder cancer cell lines was rather heterogeneous in nature and rarely exceeded that in normal urothelial cells. This difference could be explained by assuming that the overexpression of *LCN*2 occurring in urothelial carcinoma tissues could be due to inflammatory reactions often seen in these tumors. Lipocalin-2 is known to be upregulated in epithelia in response to infections to modulate inflammation (see section 1.6.3), but also in some cases during tissue regeneration. For instance, kidney regeneration induced by ischemia/reperfusion damage, is stimulated by Lipocalin-2 interacting with various inflammatory cytokines [Vinuesa et al. 2008]. This physiological situation resembles evidently the situation in a growing urothelial cancer with ongoing hypoxia/reoxygenation cycles and inflammation. Because of its role in tissue regeneration and its potential to regulate apoptosis, Lipocalin-2 is an interesting protein for closer analysis in bladder cancer.

4.1.2 Relationship between expression and methylation of *SNCG, S100A4, S100A9* and *LCN2* in bladder cancer

The main aim of this thesis was to identify genes overexpressed in bladder cancers as a consequence of DNA hypomethylation. The four genes, *SNCG, S100A4, S100A9* and *LCN2*, were all overexpressed in some bladder cancer cell lines and at least the latter two in tissues as well. Three of these genes, namely *SNCG, S100A4,* and *LCN2*, had previously been reported as activated by DNA hypomethylation in other cancer types (see section 1.6).

This study revealed that *SNCG* is partially methylated in fibroblast, blood leukocytes and ureteral connective tissue, but not methylated in either normal urothelial or prostate epithelial cells. In the same manner, the promoter of *SNCG* in most bladder cancer cell lines with moderate or high expression was unmethylated, but interestingly bladder cancer cell lines with low expression were heavily methylated. Both prostate cancer cell lines investigated lacked detectable expression and displayed dense promoter methylation of *SNCG*. Furthermore, the DNA methyltransferase inhibitor 5-aza-2-deoxycytidine (5-aza-dC) was capable of re-inducing the expression of *SNCG* to detectable levels in both urothelial and prostate cancer cell lines that otherwise had low expression, while exerting minimal or no effect on urothelial cancer cell lines that previously had high expression of the gene. Since the gene is non-methylated in normal epithelial cells of bladder or prostate tissues, overexpression in bladder or prostate carcinomas cannot be simply represent a consequence of hypomethylation. Therefore, the increased expression found in some bladder cancer cells compared to normal urothelial cells must be caused by other mechanisms independent of DNA methylation.

In fact, it seems plausible that *SNCG* is transcriptionally inactivated by DNA hypermethylation in some of the bladder cancer cell lines examined. Actually, similar variations in *SNCG* methylation between cell lines have been found in other cancers. A report by Gupta et al, 2003 demonstrated that expression of *SNCG* in breast cancer cells and ovarian cancer cells correlated strictly with different methylation pattern of the gene, as in the bladder cancer cell lines. The difference towards this thesis is that these authors regarded methylation rather than unmethylation as the default state of the normal epithelial cells. In fact, however, their data show minimal methylation at a few CpG sites in normal mammary epithelial cells. In other studies, e.g. by Yanagawa et al, 2004 on gastric cancer, normal epithelial cells from the respective tissues were not available, but the normal tissue appeared completely or partly methylated in most cases.

Differences in techniques, such as the use of nested-PCR for DNA methylation analysis, may contribute to these discrepancies. Nevertheless, the major reason may be biological. Fig. 4.1

illustrates the MeDIP data implemented in the Ensembl server [Rakyan et al, 2008] for the region around the *SNCG* transcription start site. It is clearly differentially methylated between different tissues with a moderate to strong methylation in the region investigated in this and the studies cited above. For instance, methylation is most intense in liver and CD8 T-cells and relatively low in prostate and uterus. Thus, gastrointestinal tissues may differ in *SNCG* methylation from those of the genitourinary tract. Moreover, analysis in tissues does not reveal differences in DNA methylation between various cell types within the tissues. In this thesis, partial methylation was observed in mesenchymal cells like fibroblasts and in leukocytes, which would be present in all tissues and in most tumor samples and lead to a degree of methylation in all samples. Measurements of changes in the methylation of the epithelial cells during carcinogenesis, be they hypermethylation or hypomethylation, would be confounded by DNA from these cells. This factor has not been considered in previous studies.

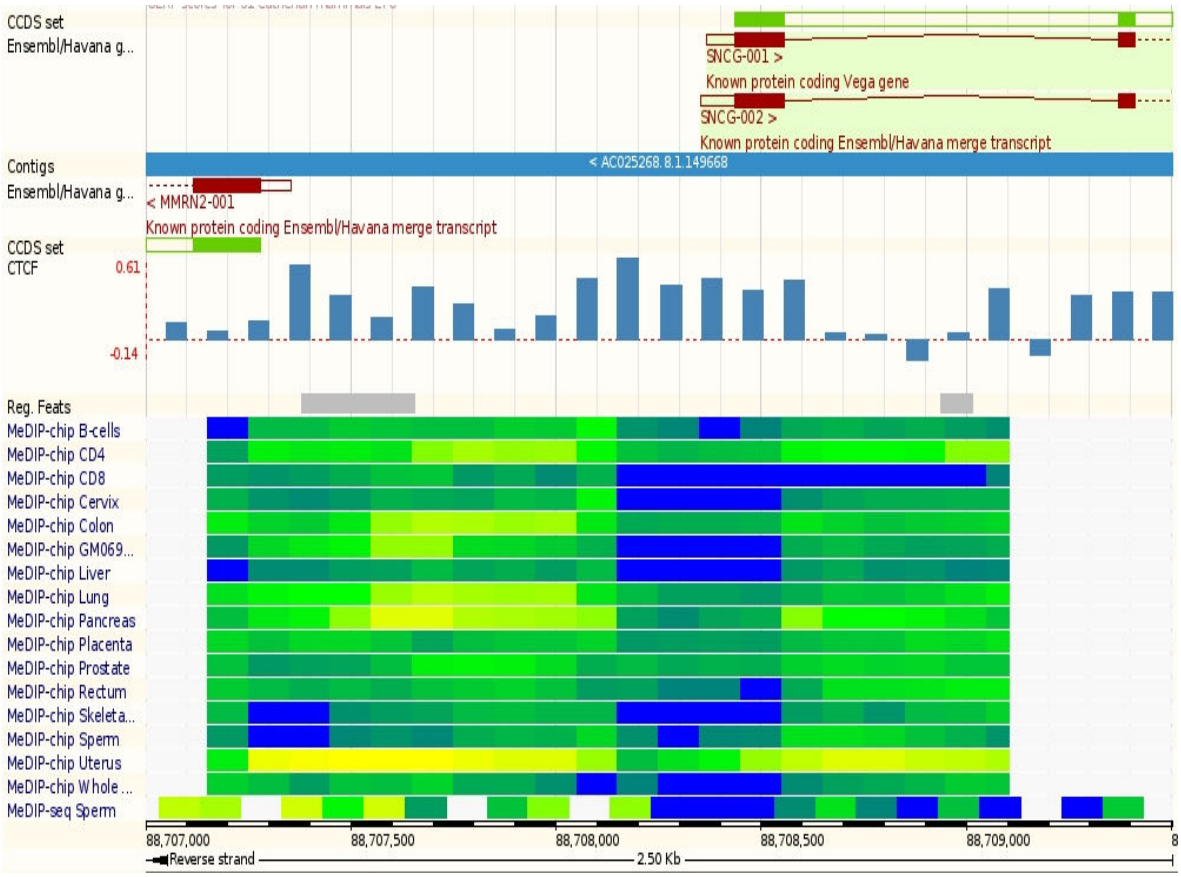

Fig. 4.1: DNA methylation pattern of SNCG in normal tissues using Ensembl genome-wide MeDIP data. Screenshot of MeDIP data integrated into the Ensembl genome browser (www.ensembl.org). The web display uses a color gradient to show the methylation score for each of the tissue samples. The color represents the value of the methylation score on a sliding scale from bright yellow (unmethylated) to dark blue (methylated).

A known example for the potential confusion caused by cell-type specific methylation is the case of Maspin (gene name: *SERPINB5*). The gene had been documented as overexpressed in some cancers such as pancreatic cancer but downregulated in others such as breast cancer. It has also been shown to exhibit a seemingly paradoxical expression in ovarian cancer [Sood et al, 2002]. These expression changes were ascribed in some reports to DNA hypermethylation, while others suggested that they were caused by DNA hypomethylation, until it became evident that *SERPINB5* was expressed and methylated in a cell-type specific pattern [Futscher et al, 2002].

DNA hypomethylation of the first intronic sequence of *S100A4* containing 4 CpG sites has been implicated as the mechanism initiating the increased expression of *S100A4* in many cancers [Rosty et al, 2002]. This result has been confirmed by many other studies in other cancer types (see section 1.6.1). For instance, a study on endometrial carcinoma revealed methylation of the *S100A4* gene in both benign endometrium and grade 1 tumors characterised by low *S100A4* expression, whereas grade 3 endometrial cancers with high *S100A4* expression showed no methylation of the gene [Xie et al, 2007].

In this study, the sites in the first intronic region of *S100A4* investigated were slightly methylated in normal urothelial cells, ureteral connective tissue and blood leukocytes. However, a higher level of methylation was observed in the bladder cancer cell lines. Notably, the methylation seemed rather variable and not homogeneous across the four sites. A recent study by Rehman et al, 2007 elucidating the function of DNA methylation in the regulation of *S100A4* in prostate cancer revealed methylation in all cancer samples, non-malignant epithelium, and in prostate cancer cell lines, but its absence from blood DNA. The methylation pattern they report for blood DNA is very similar to that for leukocytes in this study. In fact, close inspection of their data shows that the methylation in the prostate tissue samples is partial. Another concording point is the strong expression of *S100A4* in fibroblasts which is common between their data and the data from this study.

Surprisingly, previous studies have not reported on the methylation state of the *S100A4* promoter. The data from this study revealed also major differences in the methylation pattern of *S100A4* promoter between cell types like blood leukocytes and in the mesenchymal layers of ureteral tissue in comparison to cell types of urothelial (i.e. epithelial) origin like the normal urothelial cells and bladder cancer cell lines. Blood leukocytes and ureteral connective tissue were either not methylated or weakly methylated, whereas the normal urothelial cells and the bladder cancer cell lines were densely methylated. In this respect, *S100A4* methylation results are similar to those with *SNCG*, indicating that to some degree the *S100A4* is

methylated in a cell-type specific pattern. In addition, this is consistent with the MeDIP data in the Ensembl database (Fig 4.2), where differential methylation around the *S100A4* start site is shown for the investigated tissues or cell types.

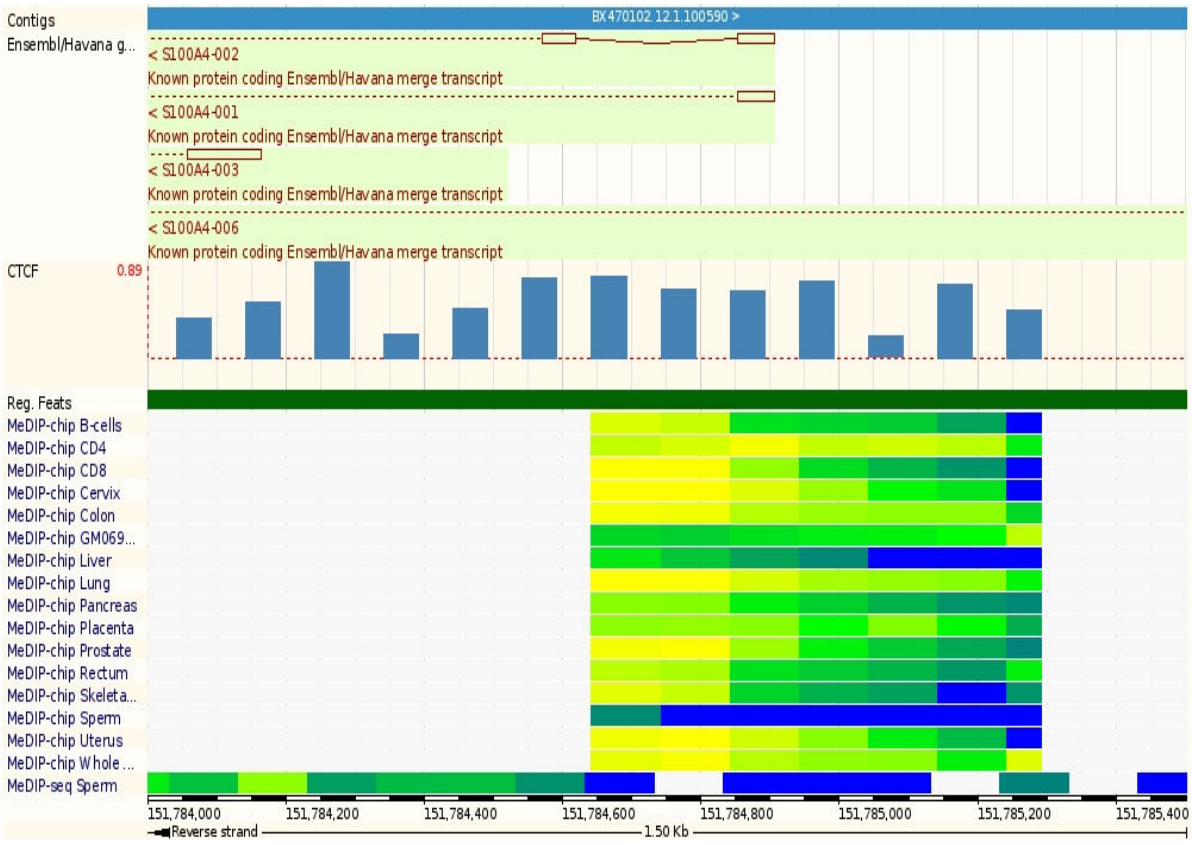

Fig. 4.2: DNA methylation pattern of S100A4 in normal tissues using Ensembl genome-wide MeDIP data. Screenshot of MeDIP data integrated into the Ensembl genome browser (www.ensembl.org). The web display uses a color gradient to show the methylation score for each of the tissue samples. The color represents the value of the methylation score on a sliding scale from bright yellow (unmethylated) to dark blue (methylated).

A difference towards *SNCG* is that the methylation of *S100A4* is not strictly related to its expression, especially methylation of the promoter. Nevertheless, this study confirmed that DNA methylation is likely involved in the regulation of *S100A4*. Notably, the treatment of the bladder cancer cell lines with the DNA methyltransferase inhibitor 5-aza-2-deoxycytidine (5-aza-dC) initiated the upregulation of *S100A4* in some of the previously low or non-expressing cells, both a normal urothelial cell culture and several bladder cancer cell lines.

These apparently contradictory results can be reconciled by the recent recognition that the relationship between DNA methylation and expression is less strict in genes with lower CpG content in their regulatory regions than in those with true CpG-islands [Weber et al. 2007]. The cases of *S100A4* (as well as *LCN2* and *S100A9* discussed below) on one hand and *SNCG* on the other hand underline this conclusion. Weber et al. also noted in their study that

methylation of genes with lower CpG-density tended to occur in a patchy pattern and to be heterogeneous. This is likewise exemplified by the genes investigated in the present thesis. On a critical note, this latter conclusion begs the question, to which extent the heterogeneity and variability of DNA methylation patterns in genes like S100A4 needs to be considered when studying changes of their methylation patterns in cancers. Certainly, the variation should be quantitated and a statistical significance for the changes be calculated. Categories like „methylated“ and „hypomethylated“ might be too coarse in such cases.

There are also a couple of reports on the expression and methylation pattern of *LCN2* in human cancers. Upregulation of *LCN2* in pancreatic cancer has been linked to DNA hypomethylation but paradoxically decreased expression of *LCN2* in breast cancer has also been associated with DNA hypermethylation [Sato et al, 2003; Roll et al, 2008]. Again, such differences in methylation pattern could be explained in part by the hypothesis discussed above [Weber et al, 2007] that promoters with lower CpG content tend to exhibit more diverse methylation patterns and the link between DNA methylation and gene expression is weaker in such cases. Interestingly, the MeDIP data in the Ensembl database for this gene do show strong methylation in all tissues, but this is located in the transcribed region, whereas methylation of the actual promoter region (at the level of resolution of this technique) appeared to be moderate to low in various tissues (Fig. 4.3).

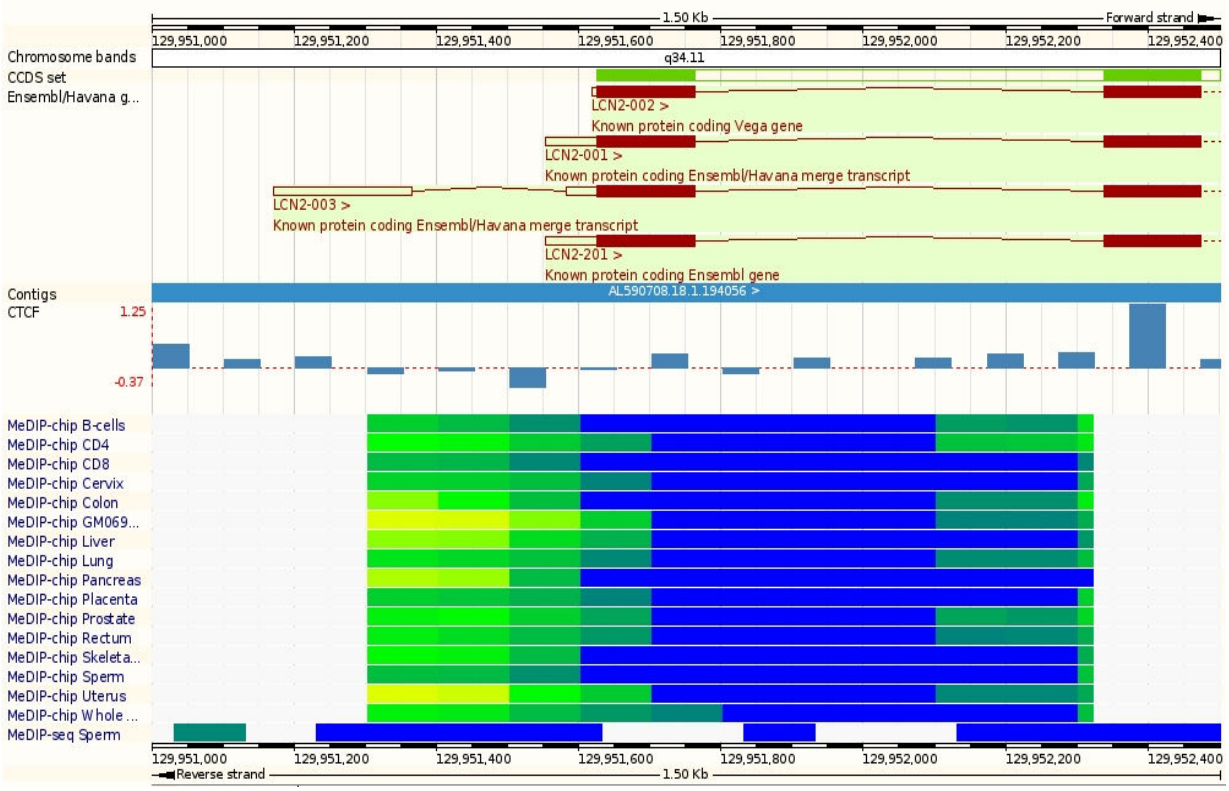

Fig. 4.3: DNA methylation pattern of LCN2 in normal tissues using Ensembl genome-wide MeDIP data. Screenshot of MeDIP data integrated into the Ensembl genome browser (www.ensembl.org). The web display uses a color gradient to show the methylation score for each of the tissue samples. The color represents the value of the methylation score on a sliding scale from bright yellow (unmethylated) to dark blue (methylated).

The results from this study fit with the MeDIP data. Heterogeneous methylation was observed in most cell lines examined. In general, cells with high expression of *LCN2* tended to display low DNA methylation, whereas cells with low expression tended towards heavier methylation. Also, 5-aza-dC induced the gene in some cases. Remarkably, the relationship between DNA methylation and gene expression in the context of *LCN2* is far from perfect. This is most dramatically illustrated in the case of fibroblasts which had low methylation but nevertheless failed to express *LCN2*. Nevertheless, the heavy methylation seen in the blood leukocytes suggests a degree of cell-type specific methylation.

Yao et al, 2007 demonstrated that *S100A9* is overexpressed in bladder cancer. Interestingly there was a close relationship between DNA methylation patterns and gene expression with respect to *S100A9*. Cells with high expression of *S100A9* exhibited no methylation and cells lacking expression of *S100A9* displayed heterogeneous methylation patterns. Notably, the DNA methyltransferase inhibitor 5-aza-2-deoxycytidine (5-aza-dC) had no effect on inducing the expression of *S100A9* in cells lacking its expression. Put together, these data suggest that there are possibly other mechanisms in addition to DNA methylation are most important in

the transcriptional inactivation of *S100A9* and that DNA methylation rather follows than determines the expression state of the gene.

In summary, the data originating from this study suggest a role for DNA methylation in the regulation of *SNCG, S100A4, S100A9* and *LCN2*. One of the key findings in this study is that overexpression of these genes in bladder cancer - in so far as it occurs at all - is not solely due to DNA hypomethylation. Most interestingly, the data generated from this study rather implicate DNA hypermethylation in the transcriptional inactivation of *SNCG* expression in a group of urothelial carcinomas. However, in other cases the naturally unmethylated gene is overexpressed. Significantly, this study highlighted the importance of considering cell type specific methylation pattern as seen most obviously in the case of *SNCG*. Also the investigation underlined the importance of the CpG content of the gene promoter region when considering the relationship between DNA methylation and gene expression. This is best illustrated by the case of *S100A4* characterised by moderate CpG content which may exhibit variable patterns of methylation in the urothelial carcinomas and in the normal bladder tissues. Such genes can show very variable and heterogeneous methylation patterns. It is anticipated that putting these two factors into consideration will facilitate a more accurate interpretation of DNA methylation analysis data.

4.2 Analysis of further hypomethylation candidate genes

4.2.1 Searching further hypomethylation candidate genes by microarray expression analysis of differential response to 5-aza-dC

The “hypomethylation candidate” genes investigated during the first part of the present thesis had been identified in a microarray analysis that was in no way specifically designed for identifying genes differentially expressed due to DNA hypomethylation. Rather, the only requirement was that they were upregulated in carcinoma cells over normal urothelial cells cultured from the same patient. An important advantage of this first microarray study was that cultured cells derived from one person could be investigated, which in the study of urothelial carcinoma represents a rare opportunity.

The second microarray was specifically designed to reveal genes overexpressed in carcinoma cells as a consequence of DNA hypomethylation. The disadvantage was that no paired cultures of normal and carcinoma cells were available. This resulted in a very large number of differentially expressed genes in the basal state between the normal urothelial cells and the carcinoma cell lines, between the two carcinoma cell lines and even between the two independent cultures of normal urothelial cells (compare Fig. 3.10). It seems very likely that

these variations substantially confuted the results from the main comparisons made to identify genes activated in the urothelial carcinoma cell lines by DNA hypomethylation, namely differential expression between normal and cancerous cells and differential response to the DNA methyltransferase inhibitor 5-aza-dC. The results from the subsequent analyses of the expression of selected genes by quantitative RT-PCR illustrate this variation by showing that many genes had a broad range of expression across the carcinoma cell lines. In many cases, some carcinoma lines had lower and some higher expression than the normal urothelial cells. Notably, this variation was also observed for genes investigated in the first part of the thesis. A similar variability in gene expression is apparent from the measurements in tissues. It has been speculated that the inconsistent results of microarray analyses of tumor tissues may be a consequence of the pronounced chromosomal instability in invasive bladder cancers leading to many incidental variations in gene dosage and subsequent variability in expression between different tissue samples [Schulz 2006]. This may also constitute one source of variation in the present study. To exclude this variation, a much larger number of cell cultures and ideally paired normal and carcinoma cultures should have been used, which was not feasible with the available ressources.

The list of candidate genes derived from the second microarray analysis as such must therefore be considered with caution, the more so as in silico analyses of the candidate genes using various bioinformatic tools such as a methylation prediction algorithm [Bock et al, 2006] (Fig. 3.15), and analysis of tissue-specific expression patterns (Fig 3.14) and of in vivo methylation status according to the MeDIP results implemented in the Ensembl database (Fig. 4.1-4.3) did not reveal many good hypomethylation candidates. Nevertheless, the “candidate II” list contains a number of genes that are relevant in the present context, namely a small number of genes known to be activated by hypomethylation in cancer, a number of genes that are known to respond to 5-aza-dC, and an apparently large number of genes differentially expressed between normal bladder and bladder cancers, independent of their methylation state. Most intriguingly, this last group includes many chromatin constituents and regulators that had not been known to play a role in urothelial tumors before (see details below).

The best characterised genes activated by DNA hypomethylation in cancer are the MAGE cancer-testis antigens [De Smet et al, 2004]. These are well represented in the candidate II list. Reactivation of MAGE-A1 and MAGE-A3 genes has been linked to promoter hypomethylation in many cancers beyond melanoma, such as colorectal cancer [Kim et al, 2006]. MAGE-A1 and MAGE-A3 were also differentially upregulated in an array studies elucidating the effect of 5-aza-dC on T24 bladder cancer cell line [Liang et al, 2002] and

several family members are known to be overexpressed in bladder cancer [Fradet et al, 2005; Sharma et al, 2006].

In addition to reactivating genes silenced by hypermethylation, 5-aza-dC has additional effects. The nucleoside is incorporated into the DNA of the replicating cells where it prevents the activities of DNA methyltransferases because of its ability to form covalent complexes with the enzymes. This mechanism has made 5-aza-dC a very effective agent in reactivating epigenetically silenced genes. However, like other nucleoside analogs used in chemotherapy it also leads to DNA damage, prominently by covalent DNA-protein crosslinks. This DNA damage leads to activation of checkpoints, involving the major checkpoint effector p53. In this fashion, 5-aza-dC treatment results in inhibition of cell proliferation due to p53-dependent activation of p21Waf1/Cip1. Notably, in almost all invasive bladder cancers, p53 is inactivated and most cell lines used in the present study, including VMCub1 and UMUC3 contain mutations in the DNA binding domain of p53 [Grimm et al. 1995; Grossman et al 1998]. 5-aza-dC also induces apoptosis, either in a p53-dependent or p53-independent manner. Aside from p53, the means by which the cellular DNA repair machinery recognizes and responds to this form of damage is not known [Palii etl al 2008]. Interestingly, some of the genes upregulated in our array study function in DNA repair pathways; this includes *POL1* and *POLM* genes encoding two DNA polymerases competent in bypassing "unreadable" nucleotides like 5-aza-dC and protein-DNA crosslinks.

In principle 5-aza-dC-induced DNA damage might lead to an irreversible cell proliferation arrest known as cellular senescence. The microarray data indicated an upregulation of a histone H2A variant known as MacroH2A (encoded by the *H2AFY* gene). This is one of the heterochromatin-forming proteins in the *s*enescence-*a*ssociated *h*eterochromatin *f*oci (SAHF), SAHF are believed to contribute to the irreversible cell cycle exit in many senescent cells by repressing the expression of proliferation-promoting genes. Senescence arrest is mediated by p16INK4A- and p21CIP1-dependent pathways both leading to retinoblastoma protein (pRB) activation. p53 plays a relay role between DNA damage sensing and p21 activation. pRB arrests the cell cycle by recruiting proliferation genes into facultative heterochromatin for permanent silencing [Ozturk et al, 2008; Zhang et al, 2007]. Other chromatin factors identified in the analysis and discussed below could also be involved in this phenomenon.

KEGG pathway analysis of the upregulated genes in this microarray revealed the presence of 8 genes linked to the Jak-STAT signaling pathway, namely *SPRY2*, *IL10RB*, *IL13RA2*, *LIF*, *PIK3R3*, *OSMR*, *SOCS6* and *SOCS5*. This finding is not unexpected as genes from this pathway are also represented in many other microarray studies employing 5-aza-dC (see Table 4.1 for examples and [Karpf 2007] for a review). For instance, a microarray study investigating differentially expressed genes in 5-aza-dC treated and untreated Hodgkin lymphoma cell lines [Ehlers et al, 2008] also revealed the expression of some of the same genes (Table 4.1).

Table 4.1: Selected genes upregulated in our microarray and other microarray studies on the effects of 5-aza-dC

Symbol	locus link id	map_location	gene_name	cancer cell line	treatment	reference
CITED2	10370	6q23.3	Cbp/p300-interacting transactivator, with Glu/Asp-rich carboxy-terminal domain, 2	prostate cancer	5-aza-dC + TSA	Lodygin et al, 2005
DAPK1	1612	9q34.1	death-associated protein kinase 1	Hodgkin's lymphoma	5-aza-dC	Ehlers et al, 2008
DUSP1	1843	5q34	dual specificity phosphatase 1	prostate cancer	5-aza-dC + TSA	Lodygin et al, 2005
F2RL1	2150	5q13	coagulation factor II (thrombin) receptor-like 1	cervical cancer	5-aza-dC + TSA	Sova et al, 2006
GADD45B	4616	19p13.3	growth arrest and DNA-damage-inducible, beta	Hodgkin's lymphoma	5-aza-dC	Ehlers et al, 2008
H2BFS	54145	21q22.3	H2B histone family, member S	Hodgkin's lymphoma	5-aza-dC	Ehlers et al, 2008
HIST1H1C	3006	6p21.3	histone cluster 1, H1c	Hodgkin's lymphoma	5-aza-dC	Ehlers et al, 2008
HIST1H2BC	8347	6p21.3	histone cluster 1, H2bc	Hodgkin's lymphoma	5-aza-dC	Ehlers et al, 2008
HIST1H2BD	3017	6p21.3	histone cluster 1, H2bd	Hodgkin's lymphoma	5-aza-dC	Ehlers et al, 2008
HIST1H2BE	8344	6p21.3	histone cluster 1, H2be	Hodgkin's lymphoma	5-aza-dC	Ehlers et al, 2008
HIST1H2BG	8339	6p21.3	histone cluster 1, H2bg	Hodgkin's lymphoma	5-aza-dC	Ehlers et al, 2008
HIST1H2BK	85236	6p21.33	histone cluster 1, H2bk	Hodgkin's lymphoma	5-aza-dC	Ehlers et al, 2008
ID3	3399	1p36.13-p36.12	inhibitor of DNA binding 3, dominant negative helix-loop-helix protein	prostate cancer	5-aza-dC + TSA	Lodygin et al, 2005
IFI44	10561	1p31.1	interferon-induced protein 44	Hodgkin's lymphoma	5-aza-dC	Ehlers et al, 2008
IFIT1	3434	10q25-q26	interferon-induced protein with tetratricopeptide repeats 1	bladder cancer	5-aza-dC	Liang et al, 2002
IFIT3	3437	10q24	interferon-induced protein with tetratricopeptide repeats 3	Hodgkin's lymphoma	5-aza-dC	Ehlers et al, 2008
IL13RA2	3598	Xq13.1-q28	interleukin 13 receptor, alpha 2	bladder cancer	5-aza-dC	Liang et al, 2002
MAGEA4	4103	Xq28	melanoma antigen family A, 4	bladder cancer	5-aza-dC	Liang et al, 2002
SGK	6446	6q23	serum/glucocorticoid regulated kinase	breast cancer	5-aza-dC	Ostrow et al, 2009
TIAM1	7074	21q22.1	T-cell lymphoma invasion and metastasis 1	Hodgkin's lymphoma	5-aza-dC	Ehlers et al, 2008
UCHL1	7345	4p14	ubiquitin carboxyl-terminal esterase L1 (ubiquitin thiolesterase)	bladder cancer	5-aza-dC	Liang et al, 2002

This pathway was in particular highlighted in a microarray study comparing the 5-aza-dC response in fibroblasts and the T24 bladder cancer cell line [Liang et al, 2002] revealing additionally upregulation of genes involved in the related interferon (IFN) pathways. Of such genes, *DDX58*, *IFIT1*, *IRF7*, *IL6* and *IL13RA2* were significant in my microarray study. The mechanisms by which 5-aza-dC activates the IFN signaling pathway are poorly understood, and a current topic of research in this lab. However, interferons are known to play a role in inhibition of cell growth, control of apoptosis and activation of the immune system (reviewed in [Samuel 2001]).

Liang et al 2002 demonstrated that many of the upregulated genes in their microarray data, including several which also appear in our microarray study, do not have CpG islands at their 5'-ends. Examples of such genes are *IFIT1*, *IRF7*, *IL6*, *IL13RA2*, *SOD2*, *STC1* and *MAGEA4*. This suggests that activation by 5-aza-dC is not restricted to genes with methylated CpG islands. Others have confirmed that silenced genes with unmethylated CpG islands or without CpG islands can be induced by 5-aza-dC [Soengas et al, 2001; Eggert et al, 2001]. The methylation of CpG-poor promoters may affect gene expression in ways that are not yet fully understood (see section 4.1). Such genes most likely correspond to the category of non-CpG island genes that may show extensive promoter methylation without affecting gene expression (Weber et al., 2007). A likely possibility is that induction of genes acting upstream of these genes may be responsible for the global changes in expression. However, the analysis of *S100A4* in the first part of this study shows that genes of this sort are still sensitive to the level of methylation, albeit not strictly.

Another group of genes upregulated in our microarray data are those encoding replication-dependent histones. All belong to the same large cluster of histone genes, *HIST1* which is located on human chromosome 6 (6p21–p22) and contains about 55 histone genes [Marzluff et al, 2002], from which 10 were upregulated in our microarray, namely, *HIST1H1*, *HIST1H2AC*, *HIST1H2BC*, *HIST1H2BD*, *HIST1H2BE*, *HIST1H2BG*, *HIST1H2BI*, *HIST1H2BK*, *HIST1H2AA* and *HIST1H2BE*. The reason for the appearence of these genes in the present study is not fully understood, however their chromosomal location is particularly interesting. This region contains approximately half of the genes on all of chromosome 6 and one third of the number of CpG islands on this chromosome [Santos et al, 2006] and may harbor one or more oncogenes directly involved in tumour progression, including bladder cancer [Oeggerli et al. 2006]. Alternatively, overexpression of *HIST1* genes may be simply a consequence of enhanced cell proliferation in urothelial cancer cells.

There were a considerable number of additional genes emerging from this microarray that encode proteins functioning in the regulation of chromatin structure, such as *JMJD1A*, *MYST4*, *PCAF*, *H2AFY* and *CBX7*, which were included among those investigated in more detail in the last part of this thesis.

4.2.2 Expression analysis of candidate genes from microarray II in urothelial carcinoma

From the strict list of candidate genes obtained from microarray II and from a preliminary analysis, a selection of genes was made for closer expression analysis in cell lines and tissue, following a similar approach as in the first part of the thesis. Given the dominance of chromatin factors revealed by the GO group analysis (Fig. 3.11-12) and the epigenetic focus of the group, the focus of the selection was on genes encoding chromatin proteins, encompassing *JMJD1A*, *MYST4*, *PCAF*, *H2AFY, CBX7*, and the Sirtuin genes *SIRT1* and *SIRT7*. *KLF4* and *LOXL2* could also be counted among that group with some right. In addition, *DEPDC1* was included having been reported to be epigenetically activated in bladder cancer and *DDX58* as a representative of the IFN/STAT pathway genes.

The Chromobox 7 (*CBX7)* gene located on chromosome 22q13.1 encodes a polycomb protein. The CBX family is characterized by a chromodomain, comprising the amino acids 10 to 46 in CBX7. CBX7 has more similarities to other family members such as CBX2, CBX4, CBX6 and CBX8 than to the subfamily of HP1 proteins such as CBX1, CBX3 and CBX5. CBX7 is a component of the polycomb repressive complex 1 (PRC1) that is known to alter the chromatin structure leading to transcriptional repression [Scott et al, 2007]. Its best-established function is the downregulation of the expression of the INK4A/ARF proteins from the *CDKN2A* locus, thereby prolonging the lifespan of mouse fibroblasts and extending the viability of many human cells as well. CBX7 can exert this function independently of BMI-1, the PRC1 component best known to repress this locus in stem cells [Gil et al, 2004]. In mouse models, CBX7 interacts with the facultative heterochromatin and the inactive X chromosome which suggest that it plays a role in the repression of gene transcription [Bernstein et al, 2006]. The expression of *CBX7* in human cancers has been studied and both oncogenic and tumor suppressor roles have been proposed for the gene

The data generated from the expression analysis of *CBX7* in this thesis showed that it was significantly downregulated in the bladder tumors in comparison to normal bladder tissues. This finding is in excellent accord with a previous report that *CBX7* mRNA levels gradually decrease with the progression of tumor stage and grade in bladder cancer [Hinz et al, 2008]. Nevertheless, the finding of an inverse correlation of *CBX7* expression with disease

progression seems to conflict with published papers suggesting an oncogenic function for *CBX7*. For instance, in follicular lymphoma *CBX7* is highly expressed and its expression correlated with high *c-MYC* expression and a more advanced tumor grade [Scott et al, 2007]. CBX7 facilitates T-cell lymphomagenesis and associates with c-MYC to favor the development and progression of B-cell lymphomas [Scott et al, 2007]. Similarly, the protein was reported to favor prostate cancer development through suppression of INK4A/ARF [Bernhard et al. 2005]. However, our data is in agreement with other studies proposing a tumor suppressor function of *CBX7* especially in solid tumors. *CBX7* is downregulated in thyroid carcinoma cell lines in comparison to the normal cells and decreases in cancers along with progression. Functional analyses confirmed that CBX7 contributes to the proliferation of transformed thyroid cells [Pallante et al, 2008]. Taken together these data along with ours suggest that CBX7 has both oncogenic and tumor suppressor function and it seems likely that it exhibits oncogenic function mostly in hematological cancers and tumor suppressor function in many solid tumors. One factor relevant in this context might be that the *CDKN2A* locus encoding the INK4A/ARF proteins is deleted in a large fraction of bladder cancers [Knowles 2006; Schulz 2006], making the repressive function of CBX7 at this gene irrelevant. A preliminary analysis of a region preceding the gene promoter conducted in relation to this thesis yielded evidence that the downregulation of the gene in bladder cancers could be mediated by DNA hypermethylation (Sorokina, Dokun & Schulz, unpublished data).

MYST4 is a member of the MYST family proteins that function in the regulation of many cellular processes including cell cycle, apoptosis and adult stem cell homeostasis. MYST proteins are histone acetyltransferases. Mutations affecting the *MYST* genes have been linked to many pathological diseases such as leukemia [Thomas and Voss 2007; Yang and Ullah 2007]. MYST4 is also known as MORF and its gene is located on chromosome 10q22.2. The *MYST4* gene – like the related *MYST3* gene - is rearranged in chromosome translocations associated with specific acute myeloid leukemias [Yang and Ullah 2007]. MYST4 is also involved in early mammalian gametogenesis [McGraw et al, 2007]

MYST4 acts most similarly to another member of the family known as MYST3 (also named MOZ). In normal cells, these proteins form tetrameric complexes with other proteins namely ING5, EAF6 and BRPF, to acetylate H3 and H4 histones for the maintenance of normal epigenetic programs [Ullah et al. 2008]. The MOZ/MORF acetyltransferases complex also regulate the function of RUNX transcription factors by displacing transcriptional corepressors such as HDACs and TLE proteins and subsequently initiating transcription [Yang and Ullah 2007]. RUNX factors are lineage determinants that are frequently altered in various cancers.

For instance, RUNX3 regulating epithelial differentiation is frequently inactivated by promoter hypermethylation in bladder cancer [Kim et al, 2005]. Similarly, *MYST4* has been proposed to have a role in normal and cancer stem cell development. For instance, chromosomal translocation lead to the formation of fusion proteins such as MORF-CBP, these abnormal complexes deregulate the normal epigenetic program, chromatin structure and gene expression patterns [Yang and Ullah 2007].

Expression data generated in this thesis indicated that MYST4 was significantly downregulated in bladder cancers compared to normal bladder tissues and its expression was higher in the normal urothelial cells than in 75% of the bladder carcinoma cell lines investigated. No significant effect of the DNA methyltransferase inhibitor 5-aza-dC on MYST4 expression was found suggesting that the downregulation was not mediated through DNA methylation. In the future, it should be determined which mechanisms underlie MYST4 downregulation and how it relates to RUNX3 inactivation and altered histone modifications in bladder cancer. As a prerequisite, the protein level of MYST4 should be investigated in normal and cancerous urothelial cells and tissues. Fig. 4.4 shows a pilot experiment supporting the idea that MYST4 protein expression is also affected in bladder cancer cell lines, like its mRNA.

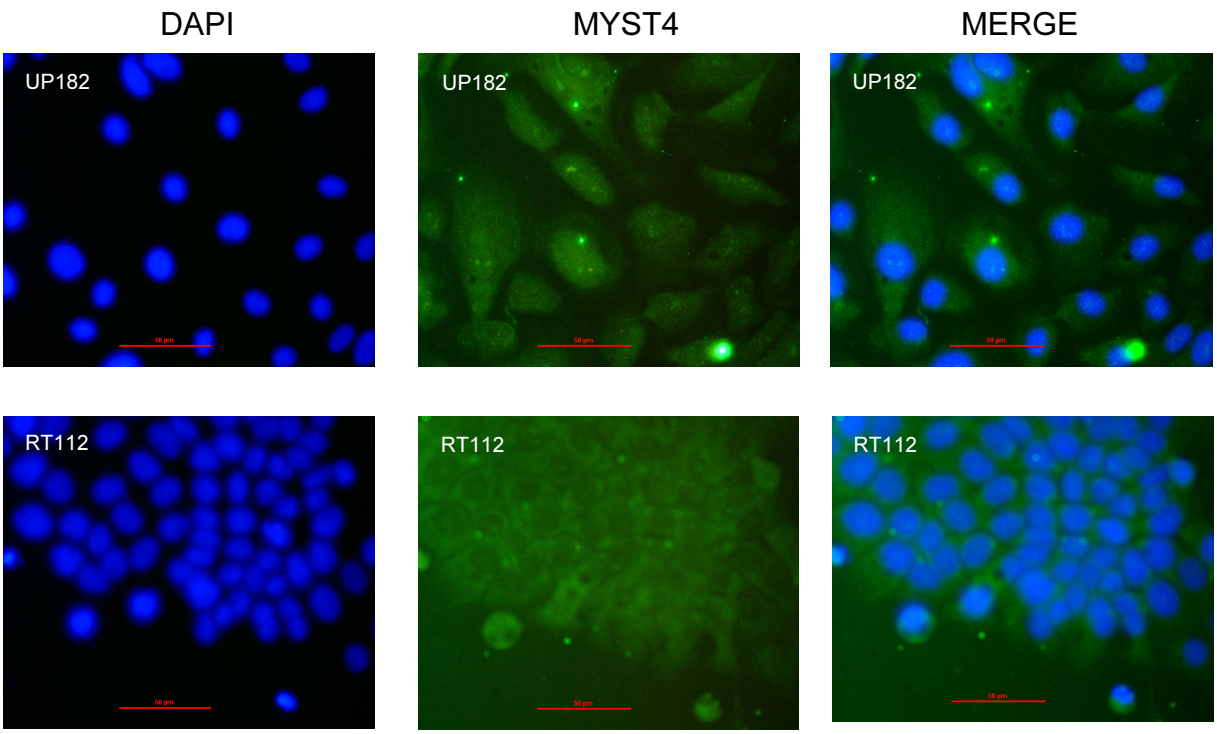

Fig. 4.4: Localization of MYST4 protein in normal urothelial cells and a bladder cancer cell line. UP182 and RT112 were immunocytochemically stained with anti-MORF (MYST4) antibody. Twenty four hours after seeding, cells were fixed with 100% ice-cold methanol, followed by blocking for 1 h at room temperature with 1 ml of blocking reagent (4% BSA; 0.05% Saponin, 1X PBS). Subsequently the cells were incubated overnight with anti-MORF antibody (Abcam, ab58823, Germany) diluted at 1:300 in blocking reagent. After three washings with 4% BSA in PBS of 10 min each, the cells were stained using Alexa 488 HRP-conjugated anti-rabbit immunoglobulin secondary antibody (Invitrogen, Eugene, Oregon, USA) at a 1:500 dilution in PBS (green fluorescence). Nuclei were counter-stained with 4',6'-diamidine-2'-phenylindole dihydrochloride (DAPI) at a 1: 1000 dilution in PBS (blue fluorescence). After additional washing steps, fluorescent images were obtained under a Nikon Eclipse E400 microscope after an exposure of 167 ms for DAPI and 5 s for the antibody stainings.

JMJD1A (jumonji domain containing 1A, also known as jumonji C domain containing histone demethylase 2A, JHDM2A) is one of the only recently discovered histone demethylases. Functionally, it demethylases mono- and dimethylated H3K9 and thereby aids in activating many target genes [Yamane et al, 2006; Okada et al, 2007]. The demethylation initiated by JMJD1A occurs through a hydroxylation reaction that requires α-ketogutarate and Fe(II) as cofactors [Tsukada et al, 2006]. JMJD1A protects the promoter regions of pluripotency-associated genes from H3K9 dimethylation, thereby playing a role in the regulation of pluripotency [Loh et al, 2007]. *JMJD1A* can be upregulated by hypoxia and this involves the binding of HIF-1 to a specific region in the *JMJD1A* promoter [Wellmann et al, 2008]. JMJD1A is also involved in spermatogenesis [Okada et al, 2007].

There was a slight, but not significant decrease in the expression of *JMJD1A* in the bladder tumor tissues in comparison to the normal tissues observed in this study. However, there was a heterogeneous pattern of expression of *JMJD1A* in the bladder cancer cell lines examined and most of the cell lines had an expression level below that of the normal urothelial cells. The functions of JMJD1A in the maintenance of stem cell properties and in the cellular response to hypoxia suggest that it might possess an important role in cancer cells. However, in the short period since the protein was discovered, no specific investigations have been reported on this issue. Bladder cancer cell lines may therefore present a good model to study the involvement of this gene in cancer.

H2AFY encodes the histone variant MacroH2A, which has 3 isoforms [Thambirajah et al, 2009]. Incorporation of MacroH2A into the inactive X is critical in maintaining silencing through subsequent cell divisions (Costanzi et al, 1998, Hernandez-Munoz et al, 2005). Incorporation of such variant histones into nucleosomes is one method used by the cells to control the function of specific chromatin regions and establish an epigenetic inheritance. MacroH2A is vital for constitutive silencing of some autosomal genes, such as the *IL8* gene in B cells, and is enriched in senescence-associated heterochromatic foci, domains of repressed transcription associated with cell aging [Agelopoulos et al, 2006; Zhang et al, 2005]. Many details of the mechanism by which MacroH2A contribute to gene silencing remain unknown. MacroH2A nucleosomes serves as substrates for chromatin remodeling enzymes such as ISWI and SWI/SNF suggesting that MacroH2A may be involved in regulating the balance between activating and repressive remodelling complexes [Chang et al, 2008]. In human cancers, changes in MacroH2A have not been studied yet.

Intriguingly, embryonic stem cells with engineered DNMT inactivation leading to genome-wide hypomethylation displayed a marked redistribution of the protein [Ma et al, 2005]. This finding could explain the appearance of *H2AFY* in the present analysis. In bladder cancer tissues and cell lines, the gene was upregulated. The causes and effects of this upregulation deserve to be investigated closely. An interesting speculation is that increases in MacroH2A may contribute to aberrant gene silencing in bladder cancer cells.

PCAF (p300/CBP-associated factor) is a histone acetylase involved in transcriptional activation by many transcription factors (reviewed by [Nagy and Tora 2007]) and is encoded by the *KAT2B* gene. Its function are partly overlapping with that of the related GCN5 protein It is actively involved in acetylation of various lysines of H3, enabling access to chromatin. Apart from histones PCAF can acetylate the tumor suppressor protein p53 at lysine residues within its carboxyl terminal domain. This acetylation leads to increased affinity of p53 for its

DNA-binding sites [Schiltz and Nakatani 2000] and enhances transcriptional activation of specific target genes [Kruse et al, 2009]. PCAF has also been reported to act as E3-ubiquitin ligase for the p53 inhibitor MDM2 [Linares et al. 2007]. Related proteins such as GCN5 are involved in chromosomal translocation in various hematological cancers and PCAF interacts with several fusion proteins of this kind [Nagy and Tora 2007]. Nevertheless, although PCAF is known to interact with and regulated many transcription factors and chromatin regulators relevant to cancer, there are to date essentially no specific indications on altered expression of the factor itself.

The analyses of expression of PCAF mRNA observed in this thesis reveal a stronger expression in the normal urothelial cells in comparison to some cancer cell lines, whereas other bladder cancer cell lines displayed an expression of this gene at a level similar to those of the normal urothelial cells. Likewise, the expression of PCAF was higher in the normal bladder tissues in comparison to the bladder tumor samples. As a first step to understand these changes, expression of the PCAF protein should be investigated. If the protein levels change accordingly, there might be several interesting issues to address, among them how the changed expression relates to the p53 alterations that are common in bladder cancer [Cote et al, 1998; Knowles 2006] and to which extent large-scale changes in histone acetylation in this cancer may relate to PCAF downregulation.

Lysyl oxidase-like 2 (LOXL2) belongs to the lysyl oxidase protein family that consists of five members. This family of proteins possesses amine oxidase activity that requires a lysyl-tyrosyl quinine cofactor and the four-histidine copper-binding domain [Fong et al, 2006]. The expression of LOXL2 has been extensively studies in many cancers. Paradoxically, *LOXL2* is upregulated in some cancers and associated with tumor progression and metastasis, but is downregulated in others. Accordingly, both tumor suppression and oncogenic functions have been described [Payne et al, 2007].

The expression analysis of *LOXL2* from this thesis showed that *LOXL2* was downregulated in the normal urothelial cells but upregulated in most of the bladder carcinoma cell lines, in some cases dramatically. Only few carcinoma cell lines had basal expression levels similar to that witnessed in the normal urothelial cells or even lower. Our data is consistent with previous observations of increased *LOXL2* mRNA expression in many cancers. e.g. in breast cancer where the increased expression correlated with breast cancer tumor grade [Akiri et al, 2003; Kirschmann et al, 2002]. *LOXL2* mRNA has been variously reported to be highly expressed in esophageal carcinoma [Ban et al, 2005], head and neck squamous cell carcinoma [Chung et al, 2006] and pancreatic cancer [Gronborg et al, 2006]. In particular, *LOXL2* has

been shown to be upregulated in the epithelial-mesenchymal transition (EMT) that occurs during tumor progression and which facilitates migration, invasiveness and metastasis [Kiemer et al, 2001]. LOXL2 was reported to contribute to this process by increasing the protein stability of SNAIL, a critical transcription factor mediating EMT [Peinado et al, 2005].

The majority of the published data on *LOXL2* and the data generated in this thesis argue in favor of an oncogenic role for *LOXL2*. However, there are also few published data suggesting that *LOXL2* has a tumor suppressor function. In another study on head and neck squamous cell carcinomas and in ovarian tumors, *LOXL2* mRNA was downregulated [Hough et al, 2000; Ono et al, 2000; Rost et al, 2003]. The downregulation was specific to the serous subtype of ovarian adenocarcinoma [Ono et al, 2000]. From the expression analysis on *LOXL2* in bladder cancer cell lines generated in this thesis we obtained evidence that *LOXL2* could be upregulated or downregulated in cancer cell lines of the same tissue origin. This is also in accord with the paradoxical reports on the upregulation and downregulation of *LOXL2* in the head and neck squamous cell carcinomas [Chung et al, 2006; Rost et al, 2003]. Overall, the upregulation and downregulation of *LOXL2* witnessed among different cancer types as well as within specific cancers suggests that *LOXL2* has a complex role in tumor progression and such differences could be due to the stage of tumor progression, invasion and EMT. Futhermore this complexity is not specific to *LOXL2* alone, another characterized member of the lysyl oxidase family known as *LOX* has been reported to be upregulated in some cancers such as breast cancer [Kirschmann et al, 2002] but down- regulated in others e.g. gastric cancer [Kaneda et al, 2004].

Most interestingly, two related genes, namely LOXL1 and LOXL4, have been reported to be downregulated in bladder cancer by promoter hypermethylation [Wu et al. 2007]. It is therefore tempting to speculate that changes in *LOXL2* expression might also be associated with DNA methylation changes. An according analysis should however consider the issues raised in the context of the first part of this thesis [Dokun et al. 2008].

Kruppel-like factor 4 (*KLF4)* is a transcription factor that is crucial to the normal functioning of diverse biological processes such as terminal cell differentiation and carcinogenesis [Behr et al, 2007]. KLF4 regulates histone H4 acetylation at the promoter of its target genes. The ability of KLF4 to change chromatin structure is probably relevant in its recently discovered function to contribute to the reprogramming of cells to a pluripotent state [Pei 2009].

The *KLF4* gene is located on chromosome 9q in a region frequently undergoing allelic loss in bladder cancer. Accordingly, the only previous study in bladder cancer reported that the

expression of KLF4 was predominantly downregulated [Ohnishi et al, 2003]. Our data rather suggest a heterogeneous pattern of expression in the bladder cancer cell lines, but an overall higher expression when compared with the normal urothelial cells. The differences towards the previous study can be explained based on two reasons. First, they may relate to the methodology used. The expression of *KLF4* in this thesis was quantified by real-time PCR, whereas the older study was performed using RNA blots and in situ hybridization. Second, from the panel of 8 and 13 bladder cancers cell lines studied, respectively, only 5 lines were common to the two panels. Interestingly, the data generated on the expression of *KLF4* in these cell lines were consistent. HT-1376 and UM-UC3 had the highest and lowest expression respectively while the other cell lines had a moderate expression of *KLF4*. In other cancers, *KLF4* has been variously reported as upregulated as in breast cancer [Foster et al, 2000] or downregulated as in colorectal cancer [Zhao et al, 2004]. Taken together, the data from the two studies suggest that this is also true of bladder cancer.

This paradoxical expression of *KLF4* in cancers could be explained based on its known molecular activities. It can act as activator or repressor of transcription depending on whether it associates with co-activators such as p300 and CREB-binding proteins or co-repressors such as HDAC3 [Evans et al, 2007]. Furthermore, KLF4 normally acts as a tumor suppressor through p21CIP1-dependent cell cycle arrest, but under the influence of oncogenic signals - elicited e.g. by mutant RAS - the p21CIP pathway is inactivated and the anti-apoptotic activity of KLF4 provides a survival advantage which facilitates cellular transformation [McConnell et al, 2007]. Therefore, the variations in the expression of KLF4 in bladder cancer cell lines should be considered in the context of other genetic alterations, such as RAS mutations.

SIRT1 and SIRT7 are members of the Sirtuin protein family. These are NAD+-dependent histone deacetylases (HDACs) that interact with many proteins in the nucleolus, cytoplasm and mitochondria for posttranslational modification by acetylation or ADP ribosylation. SIRT1 responds to changes in nutrient availability and in stress responses to promote cell survival by deacetylating histone and non-histone targets in the nucleus. SIRT7 is localized to the nucleolus and interacts with RNA Polymerase-I to promote transcription of rRNA genes [Saunders and Verdin, 2007]. Altered expression of both genes has been shown in cancers. Especially *SIRT1* has been intensely studied because it is considered as oncogenic in many cancers and a promising drug target. However, it behaves as a tumor suppressor in other cancers [Liu et al. 2009; Brooks & Gu 2009].

The analysis of *SIRT1* in this thesis revealed a slightly higher level of expression in the bladder carcinoma cell lines in comparison to normal urothelial cells. This is consistent with previous published data on the expression of *SIRT1* in e.g prostate cancer [Hoffmann et al, 2007; Huffman et al, 2007] and colon cancer [Stunkel et al, 2007]. However, *SIRT1* is downregulated in some cancers such as liver carcinoma [Wang et al, 2008]. These conflicting roles of *SIRT1* could be reconciled with its biological functions. As an oncogene SIRT1 deacetylases and inactivates p53 preventing p53-mediated growth arrest and apoptosis. In its role as a tumor suppressor, increased SIRT1 prevents the expression of many oncogenes leading to reduced cell proliferation and increases apoptosis [Deng et al, 2009]. The function of SIRT1 therefore depends on which oncogenes are relevant in a cancer and on the p53 status. The expression analysis of *SIRT7* showed a similar pattern to that of *SIRT1*. It has been reported to be upregulated in thyroid carcinoma [De Nigris et al, 2002; Frye 2002] and breast cancers [Ashraf et al, 2006]. It seems promising to investigate the expression of these two factors in more detail in bladder cancer.

DEP domain containing 1 (DEPDC1) is a gene located on chromosome 1p31.2 which was first discovered by Kanehira et al, 2007 by using cDNA microarrays to screen for genes significantly activated in bladder cancer cells. *DEPDC1* was not expressed in 24 normal human tissues examined except in the testis suggesting that it might encode a novel cancer testis antigen. The authors presented data according to which *DEPDC1* is not only upregulated in bladder cancer, but also plays a key role in the growth of bladder cancer cells. The function of the protein is still unknown, but Kanehira et al. reported it as nuclear. In light of their data, it is highly interesting that this gene was also identified by our microarray data. The data generated in this thesis showed that DEPDC1 is upregulated in many bladder cancer cell lines, thereby confirming the previous report [Kanehira et al, 2007]. A preliminary analysis conducted in the course of this thesis showed that the gene promoter was unmethylated in normal cells. Therefore, it seems unlikely that the upregulation in bladder cancer occurred as a result of DNA hypomethylation of the gene promoter. Evidently, the regulation of this quite recently discovered gene must be studied in more detail to understand the mechanisms leading to its apparently specific upregulation in bladder cancer.

DEAD (Asp-Glu-Ala-Asp) box polypeptide 58 (DDX58) is also known as RIG-I. The gene is interestingly located on chromosome 9p12. Its product is involved in recognition of viral double-stranded (ds) RNA and the regulation of immune responses. It is a well-known target of interferons and can be strongly induced by them. Since interferon target genes are often induced by DNA hypomethylation, induction of *DDX58* in urothelial cells by the methylation

inhibitor 5-aza-dC is not unexpected. However, it is unknown whether the gene might be in generally upregulated in bladder cancers, as had been reported in Kaposi's sarcoma [Livengood et al, 2007]. The expression data generated in this thesis showed that *DDX58* was expressed at a low level in most bladder cancer cell lines and normal urothelial cells except for three bladder cancer cell lines in which the gene was highly expressed. It is therefore possible that a subset of bladder cancers might overexpress this gene constitutively. However, it is very difficult to ascertain this assumption in tissues, as the expression of the gene might be strongly modulated by inflammatory reactions commonly found in bladder cancer tissues.

A clustering analysis of 11 genes vs the 12 bladder cancer cell lines illustrates the very heterogeneous expression patterns of the genes DDX58 and LOXL2, and SIRT1 and DEPDC1 show related patterns among the cell lines (Fig. 4.5). Only the 647v and J82 lines display closely related patterns. However the most obvious feature in this graph is the relatively coordinate change in the chromatin factors PCAF, MYST4 and JMJD1A between various cell lines.

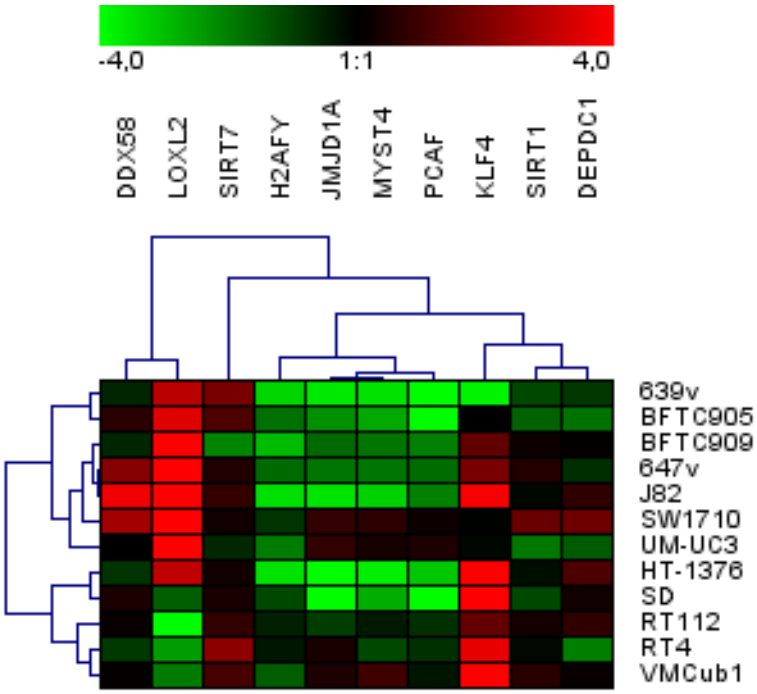

Fig. 4.5: The Hierarchical clustering analysis of gene expression in bladder cancer cell lines generated with Genesis 1.0 based on Pearson correlation. The graph depicts the degree of similarity that existing among the 11 selected genes (top) and among the 12 bladder cancer cell lines used (right) respectively. The color represents the relative expression of the genes in the cell lines on a sliding $\log_2$ scale from -4 (green) to 4 (red).

In summary, the expression analysis of individual candidate genes in bladder cancer cell lines and of some in tissues as well identified several that seem to exhibit relatively consistent changes in bladder cancer. Notably, however, as seen with many candidates from the first microarray, many candidate genes were characterized by highly variable expression patterns, with downregulation relative to normal cells in some and upregulation in other cell lines. A few of these genes, such as *CBX7* and *LOXL2*, may be directly regulated by DNA methylation, although the actual mechanisms might be as complicated as in the cases of *SNCG* and *S100A4*, given the presence of both up- and downregulation in various cancers. Therefore the most important finding in the second part of this thesis may be the evidence that the expression of a number of chromatin factors that had not previously been implicated in this cancer type may be changed in bladder cancer, perhaps even in a coordinate fashion. Since many of these factors play fundamental roles in cell differentiation and gene expression, it seems likely that these changes contribute significantly to the phenotype of bladder cancers

SUMMARY

Two different changes of DNA methylation are common in human cancers. On one hand, CpG-rich sequences surrounding the transcription start sites of individual genes, which are never methylated in normal tissues, become aberrantly hypermethylated. On the other hand, sequences that are densely methylated in normal somatic tissues, such as CpG-rich satellites and interspersed retrotransposon repeat sequences, become hypomethylated. With the exception of genes encoding cancer-testis antigens, the range of single copy genes affected by hypomethylation is still poorly defined. The aim of this thesis was to identify genes activated by DNA hypomethylation in invasive bladder cancers.

Four genes were selected as candidates from microarray gene expression profiles of cancerous and normal urothelial cells cultured from the same patient. Real-time RT-PCR was used to investigate expression and bisulfite sequencing to analyze methylation of *SNCG*, *S100A4*, *S100A9* and *LCN2* in urothelial cancer cell lines and tissues. *SNCG* and *S100A4* were overexpressed in some cancer tissues and cell lines compared to normal controls, but downregulated in others, whereas *LCN2* and *S100A9* were upregulated in few cancer cell lines, but regularly in tissues. Normal and cancerous urothelial cells expressing *SNCG* lacked promoter methylation. *SNCG* downregulation was associated with hypermethylation and could be reversed by the DNA methyltransferase inhibitor 5-aza-2′-deoxycytidine (5-aza-dC). Partial *SNCG* methylation associated with low expression was found in mesenchymal cells. *S100A4* methylation at regulatory intronic sites and in the promoter region was lowest in leukocytes and fibroblasts, denser in urothelial cells, and often heterogeneous. *LCN2* promoter methylation was variable and even less consistently related to expression. 5-aza-dC increased expression of these two genes in some lines. The *S100A9* promoter was partially methylated in nonexpressing cells.

The data suggest that DNA methylation is involved in the regulation of *SNCG*, *S100A4*, *S100A9* and *LCN2*. In particular, *SNCG* and *S100A4* show cell-type specific methylation. However, any overexpression of these genes in urothelial cancer does not seem to represent primarily a consequence of DNA hypomethylation. Rather, we have obtained strong evidence that hypermethylation is involved in the downregulation of *SNCG* in a subset of urothelial carcinomas. Our analysis indicates that cell type-specific DNA methylation patterns should be considered when interpreting DNA methylation analyses of human cancers. Moreover, genes with moderate CpG-content, exemplified by *S100A4*, may often be partially and variably methylated in normal tissues and accordingly in cancers.

In order to identify further candidate genes activated by DNA hypomethylation, a second microarray investigation was performed designed more specifically for this purpose. Gene expression profiles of two cultures of normal urothelial cells and two bladder cancer cell lines with or without 5-aza-dC treatment were compared using Affymetrix HG-U133A microarrays. Overall, 205 genes met the filtering criteria of being upregulated by 5-aza-dC in normal cells and overexpressed in the carcinoma cell lines. Interestingly, genes encoding chromatin proteins were overrepresented among these. Following bioinformatic analyses for tissue-specific expression and predicted methylation patterns, 11 genes were analysed for expression as above, namely *DEPDC1, SIRT1, SIRT7, DDX58, LOXL2, KLF4, H2AFY, PCAF, CBX7, JMJD1A* and *MYST4.*

Overall, many of these genes had heterogeneous pattern of expression, with upregulation or downregulation in individual bladder cell lines. In general, *DEPDC1, SIRT1, SIRT7, LOXL2* and *H2AFY* tended to be upregulated, whereas *PCAF, CBX7,* and *MYST4* tended to be downregulated. For the latter four genes, this tendency was also confirmed in cancer compared to normal bladder tissues. None of these genes seemed to be straightforwardly activated by hypomethylation.

Taken together, the second part of the thesis identified a number of genes that deserve to be investigated for their expression, especially additionally at the protein level, in bladder cancers and some also for their regulation by DNA methylation. Most importantly, the analysis identified novel expression changes in several genes encoding chromatin factors, which could be crucial for chromatin reorganisation events during the progression of bladder cancer.

In menschlichen Tumoren kommen zwei verschiedene Arten von Veränderungen der DNA-Methylierung vor. Einerseits werden CpG-reiche Sequenzen um den Transkriptionsstart einzelner Gene, die sonst niemals methyliert sind, aberrant hypermethyliert. Andererseits werden ansonsten in normalen Geweben dicht methylierte Sequenzen wie CpG-reiche Satelliten und Retrotransposone, hypomethyliert. Mit Ausnahme der Cancer-Testis-Antigen-Gene ist bisher recht wenig bekannt, welche Einzelkopie-Gene von Hypomethylierung betroffen werden. Ziel der vorgelegten Arbeit war es Gene zu identifizieren, die in invasiven Harnblasenkarzinomen durch DNA-Hypomethylierung aktiviert werden.

Zu Beginn wurden aus mittels competitiver Hybridisierung von Microarrays erstellten Genexpressionsprofilen von kultivierten Tumor- und Normal-Urothelzellen eines Patienten vier Gene als Kandidaten ausgewählt. Von diesen, SNCG, S100A4,, S100A9 und LCN2, wurde mittels quantitativer RT-PCR die Expression und mittels Bisulfit-Sequenzierung die DNA-Methylierung in urothelialen Tumor-Zelllinien und -Geweben bestimmt. SNCG und S100A4 waren in einigen Tumorgeweben und –Zelllinien gegenüber normalen Kontrollen überexprimiert, aber in anderen vermindert. Dagegen waren LCN2 und S100A9 in nur wenigen Tumorzelllinien verstärkt exprimiert, jedoch in den Tumorgeweben im Durchschnitt signifikant erhöht. Der SNCG Promotor war unmethyliert in normalen und Tumor-Urothelzellen mit Expression. Fehlende Expression ging mit Hypermethylierung einher und wurde durch den DNA-Methyltransferaseinhibitor 5-Aza-2-Desoxycytidin (5aza-dC) induziert. In mesenchymalen Zellen fand sich niedrige Expression mit partieller Methylierung. Die Methylierung von regulatorischen Abschnitten im Intron und Promoter von S100A4 war in Leukozyten und Fibroblasten schwach, in urothelialen Zellen dichter und oft heterogen. Die Methylierung des LCN2 Promotors war variabel und noch weniger eng mit der Expression verbunden. Beide Gene wurden in einigen Zelllinien durch 5aza-dC induziert. Der S100A9 Promotor war in Zellen ohne Expression teilmethyliert.

Zusammengenommen scheint DNA-Methylierung für die Regulation von SNCG, S100A4,, S100A9 und LCN2 bedeutsam zu sein. Speziell zeigen SNCG und S100A4 zelltyp-spezifische Methylierung. Jedoch resultieren Überexpressionen dieser Gene im Urothelkarzinom offenbar nicht primär aus DNA Hypomethylierung. Vielmehr ergaben sich starke Hinweise darauf, dass SNCG in einigen Urothelkarzinomen durch Hypermethylierung inaktiviert wird. Daher sollte bei der Interpretation von DNA-Methylierungsanalysen in menschlichen Tumoren auch an die Möglichkeit zelltypspezifischer Methylierung gedacht werden. Außerdem können Gene mit mäßigem CpG-Gehalt wie S100A4 partiell und variabel methyliert in normalen wie Tumor-Geweben vorliegen.

Um weitere durch DNA-Hypomethylierung aktivierte Gene zu entdecken, wurde eine weitere, zielgerichtetere Microarray-Analyse durchgeführt. Dazu wurden mittels Affymetrix HG-U133A Microarrays Genexpressionsprofile von zwei Kulturen normaler Urothelzellen und zwei Harnblasenkarzinom-Zelllinien mit und ohne 5aza-dC verglichen. Die Filterkriterien „Induktion durch 5aza-dC“ und „verstärkte Expression in Tumorzellen“ ergaben 205 definierte Gene. Unter diesen waren solche für Chromatinfaktoren überrepräsentiert. Nach bioinformatischen Analysen auf gewebespezifische Expression und vorgesagter DNA-Methylierung, wurden 11 Gene wie oben auf Expression analysiert, nämlich DEPDC1, SIRT1, SIRT7, DDX58, LOXL2, KLF4, H2AFY, PCAF, CBX7, JMJD1A und MYST4.
Die Expression vieler davon war heterogen und in einzelnen Harnblasenkarzinom-Zelllinien vermindert oder erhöht. Insgesamt waren DEPDC1, SIRT1, SIRT7, LOXL2 und H2AFY eher überexprimiert, dagegen nahm die Expression von PCAF, CBX7 und MYST4 eher ab. Bei den letzten 4 Genen zeigte sich diese Veränderung auch in Tumorgeweben. Keines der Gene scheint in einfacher Weise durch Hypomethylierung aktiviert zu werden.
Zusammengefasst wurden im zweiten Teil der Dissertation eine Reihe von Genen identifizert die in Harnblasenkarzinomen eine genauere Untersuchung lohnen, besonders ihrer Proteinprodukte und in Einzelfällen auch ihrer DNA-Methylierung. Den wichtigste Befund dürfte die Identifizierung veränderter Expression mehrerer Chromatinfaktoren darstellen, die für entscheidende Chromatin-Reorganisationsschritte während der Progression von Urotheltumoren verantwortlich sein könnten.

REFERENCES

Agelopoulos, M. and Thanos, D. (2006) Epigenetic determination of a cell-specific gene expression program by ATF-2 and the histone variant macroH2A. *Embo J,* **25:** 4843-53.

Agerbaek, M., Alsner, J., Marcussen, N., Lundbeck, F. and Von der Maase, H. (2006) Focal S100A4 protein expression is an independent predictor of development of metastatic disease in cystectomized bladder cancer patients. *Eur Urol,* **50:** 777-85.

Ahmad, M., Attoub, S., Singh, M. N., Martin, F. L. and El-Agnaf, O. M. (2007) Gamma-synuclein and the progression of cancer. *Faseb J,* **21:** 3419-30.

Akiri, G., Sabo, E., Dafni, H., Vadasz, Z., Kartvelishvily, Y., Gan, N., Kessler, O., Cohen, T., Resnick, M., Neeman, M. and Neufeld, G. (2003) Lysyl oxidase-related protein-1 promotes tumor fibrosis and tumor progression in vivo. *Cancer Res,* **63:** 1657-66.

Alexe, G., Dalgin, G. S., Scanfeld, D., Tamayo, P., Mesirov, J. P., Ganesan, S., Delisi, C. and Bhanot, G. (2007) Breast cancer stratification from analysis of micro-array data of micro-dissected specimens. *Genome Inform,* **18:** 130-40.

Armas-Pineda, C., Arenas-Huertero, F., Perezpenia-Diazconti, M., Chico-Ponce de Leon, F., Sosa-Sainz, G., Lezama, P. and Recillas-Targa, F. (2007) Expression of PCAF, p300 and Gcn5 and more highly acetylated histone H4 in pediatric tumors. *J Exp Clin Cancer Res,* **26:** 269-76.

Ashraf, N., Zino, S., Macintyre, A., Kingsmore, D., Payne, A. P., George, W. D. and Shiels, P. G. (2006) Altered sirtuin expression is associated with node-positive breast cancer. *Br J Cancer,* **95:** 1056-61.

Bakkar, A. A., Wallerand, H., Radvanyi, F., Lahaye, J. B., Pissard, S., Lecerf, L., Kouyoumdjian, J. C., Abbou, C. C., Pairon, J. C., Jaurand, M. C., Thiery, J. P., Chopin, D. K. and de Medina, S. G. (2003) FGFR3 and TP53 gene mutations define two distinct pathways in urothelial cell carcinoma of the bladder. *Cancer Res,* **63:** 8108-12.

Ban, S., Ishikawa, K., Kawai, S., Koyama-Saegusa, K., Ishikawa, A., Shimada, Y., Inazawa, J. and Imai, T. (2005) Potential in a single cancer cell to produce heterogeneous morphology, radiosensitivity and gene expression. *J Radiat Res (Tokyo),* **46:** 43-50.

Barreto, G., Schafer, A., Marhold, J., Stach, D., Swaminathan, S. K., Handa, V., Doderlein, G., Maltry, N., Wu, W., Lyko, F. and Niehrs, C. (2007) Gadd45a promotes epigenetic gene activation by repair-mediated DNA demethylation. *Nature,* **445:** 671-5.

Baylin, S. B., Makos, M., Wu, J. J., Yen, R. W., de Bustros, A., Vertino, P. and Nelkin, B. D. (1991) Abnormal patterns of DNA methylation in human neoplasia: potential consequences for tumor progression. *Cancer Cells,* **3:** 383-90.

Behr, R., Deller, C., Godmann, M., Muller, T., Bergmann, M., Ivell, R. and Steger, K. (2007) Kruppel-like factor 4 expression in normal and pathological human testes. *Mol Hum Reprod,* **13:** 815-20.

Bera, T. K., Tsukamoto, T., Panda, D. K., Huang, T., Guzman, R. C., Hwang, S. I. and Nandi, S. (1998) Defective retrovirus insertion activates c-Ha-ras protooncogene in an MNU-induced rat mammary carcinoma. *Biochem Biophys Res Commun,* **248:** 835-40.

Bernard, D., Martinez-Leal, J. F., Rizzo, S., Martinez, D., Hudson, D., Visakorpi, T., Peters, G., Carnero, A., Beach, D. and Gil, J. (2005) CBX7 controls the growth of normal and tumor-derived prostate cells by repressing the Ink4a/Arf locus. *Oncogene,* **24:** 5543-51.

Bernstein, E., Duncan, E. M., Masui, O., Gil, J., Heard, E. and Allis, C. D. (2006) Mouse polycomb proteins bind differentially to methylated histone H3 and RNA and are enriched in facultative heterochromatin. *Mol Cell Biol,* **26:** 2560-9.

Beyer, S., Kristensen, M. M., Jensen, K. S., Johansen, J. V. and Staller, P. (2008) The histone demethylases JMJD1A and JMJD2B are transcriptional targets of hypoxia-inducible factor HIF. *J Biol Chem,* **283:** 36542-52.

Bock, C., Paulsen, M., Tierling, S., Mikeska, T., Lengauer, T. and Walter, J. (2006) CpG island methylation in human lymphocytes is highly correlated with DNA sequence, repeats, and predicted DNA structure. *PLoS Genet,* **2:** e26.

Brooks, C. L. and Gu, W. (2009) How does SIRT1 affect metabolism, senescence and cancer? *Nat Rev Cancer,* **9:** 123-8.

Cabezon, T., Celis, J. E., Skibshoj, I., Klingelhofer, J., Grigorian, M., Gromov, P., Rank, F., Myklebust, J. H., Maelandsmo, G. M., Lukanidin, E. and Ambartsumian, N. (2007) Expression of S100A4 by a variety of cell types present in the tumor microenvironment of human breast cancer. *Int J Cancer,* **121:** 1433-44.

Chan, T. L., Yuen, S. T., Kong, C. K., Chan, Y. W., Chan, A. S., Ng, W. F., Tsui, W. Y., Lo, M. W., Tam, W. Y., Li, V. S. and Leung, S. Y. (2006) Heritable germline epimutation of MSH2 in a family with hereditary nonpolyposis colorectal cancer. *Nat Genet,* **38:** 1178-83.

Chang, E. Y., Ferreira, H., Somers, J., Nusinow, D. A., Owen-Hughes, T. and Narlikar, G. J. (2008) MacroH2A allows ATP-dependent chromatin remodeling by SWI/SNF and ACF complexes but specifically reduces recruitment of SWI/SNF. *Biochemistry,* **47:** 13726-32.

Chang, S. C., Tucker, T., Thorogood, N. P. and Brown, C. J. (2006) Mechanisms of X-chromosome inactivation. *Front Biosci,* **11:** 852-66.

Cheng, X. and Blumenthal, R. M. (2008) Mammalian DNA methyltransferases: a structural perspective. *Structure,* **16:** 341-50.

Cho, B., Lee, H., Jeong, S., Bang, Y. J., Lee, H. J., Hwang, K. S., Kim, H. Y., Lee, Y. S., Kang, G. H. and Jeoung, D. I. (2003) Promoter hypomethylation of a novel cancer/testis antigen gene CAGE is correlated with its aberrant expression and is seen in premalignant stage of gastric carcinoma. *Biochem Biophys Res Commun,* **307:** 52-63.

Chow, J. C. and Brown, C. J. (2003) Forming facultative heterochromatin: silencing of an X chromosome in mammalian females. *Cell Mol Life Sci,* **60:** 2586-603.

Chow, J. C., Yen, Z., Ziesche, S. M. and Brown, C. J. (2005) Silencing of the mammalian X chromosome. *Annu Rev Genomics Hum Genet,* **6:** 69-92.

Chuang, L. S., Ian, H. I., Koh, T. W., Ng, H. H., Xu, G. and Li, B. F. (1997) Human DNA-(cytosine-5) methyltransferase-PCNA complex as a target for p21WAF1. *Science,* **277:** 1996-2000.

Chung, C. H., Parker, J. S., Ely, K., Carter, J., Yi, Y., Murphy, B. A., Ang, K. K., El-Naggar, A. K., Zanation, A. M., Cmelak, A. J., Levy, S., Slebos, R. J. and Yarbrough, W. G. (2006) Gene expression profiles identify epithelial-to-mesenchymal transition and activation of nuclear factor-kappaB signaling as characteristics of a high-risk head and neck squamous cell carcinoma. *Cancer Res,* **66:** 8210-8.

Costanzi, C. and Pehrson, J. R. (1998) Histone macroH2A1 is concentrated in the inactive X chromosome of female mammals. *Nature,* **393:** 599-601.

Cote, R. J., Dunn, M. D., Chatterjee, S. J., Stein, J. P., Shi, S. R., Tran, Q. C., Hu, S. X., Xu, H. J., Groshen, S., Taylor, C. R., Skinner, D. G. and Benedict, W. F. (1998) Elevated and absent pRb expression is associated with bladder cancer progression and has cooperative effects with p53. *Cancer Res,* **58:** 1090-4.

Cui, H., Cruz-Correa, M., Giardiello, F. M., Hutcheon, D. F., Kafonek, D. R., Brandenburg, S., Wu, Y., He, X., Powe, N. R. and Feinberg, A. P. (2003) Loss of IGF2 imprinting: a potential marker of colorectal cancer risk. *Science,* **299:** 1753-5.

Cui, H., Onyango, P., Brandenburg, S., Wu, Y., Hsieh, C. L. and Feinberg, A. P. (2002) Loss of imprinting in colorectal cancer linked to hypomethylation of H19 and IGF2. *Cancer Res,* **62:** 6442-6.

Cunningham, J. M., Christensen, E. R., Tester, D. J., Kim, C. Y., Roche, P. C., Burgart, L. J. and Thibodeau, S. N. (1998) Hypermethylation of the hMLH1 promoter in colon cancer with microsatellite instability. *Cancer Res,* **58:** 3455-60.

Das, P. M. and Singal, R. (2004) DNA methylation and cancer. *J Clin Oncol,* **22:** 4632-42.

Davies, B. R., O'Donnell, M., Durkan, G. C., Rudland, P. S., Barraclough, R., Neal, D. E. and Mellon, J. K. (2002) Expression of S100A4 protein is associated with metastasis and reduced survival in human bladder cancer. *J Pathol,* **196:** 292-9.

de Nigris, F., Cerutti, J., Morelli, C., Califano, D., Chiariotti, L., Viglietto, G., Santelli, G. and Fusco, A. (2002) Isolation of a SIR-like gene, SIR-T8, that is overexpressed in thyroid carcinoma cell lines and tissues. *Br J Cancer,* **86:** 917-23.

De Smet, C., De Backer, O., Faraoni, I., Lurquin, C., Brasseur, F. and Boon, T. (1996) The activation of human gene MAGE-1 in tumor cells is correlated with genome-wide demethylation. *Proc Natl Acad Sci U S A,* **93:** 7149-53.

De Smet, C., Loriot, A. and Boon, T. (2004) Promoter-dependent mechanism leading to selective hypomethylation within the 5' region of gene MAGE-A1 in tumor cells. *Mol Cell Biol,* **24:** 4781-90.

de Vere White, R. (2008) Re: defining optimal therapy for muscle-invasive bladder cancer. *Eur Urol,* **53:** 1295-6.

Deng, C. X. (2009) SIRT1, is it a tumor promoter or tumor suppressor? *Int J Biol Sci,* **5:** 147-52.

Dobosy, J. R. and Selker, E. U. (2001) Emerging connections between DNA methylation and histone acetylation. *Cell Mol Life Sci,* **58:** 721-7.

Dokun, O. Y., Florl, A. R., Seifert, H. H., Wolff, I. and Schulz, W. A. (2008) Relationship of SNCG, S100A4, S100A9 and LCN2 gene expression and DNA methylation in bladder cancer. *Int J Cancer,* **123:** 2798-807.

Duffy, M. J. (2007) Role of tumor markers in patients with solid cancers: A critical review. *Eur J Intern Med,* **18:** 175-184.

Duffy, M. J., Napieralski, R., Martens, J. W., Span, P. N., Spyratos, F., Sweep, F. C., Brunner, N., Foekens, J. A. and Schmitt, M. (2009) Methylated genes as new cancer biomarkers. *Eur J Cancer,* **45:** 335-46.

Dyrskjot, L. (2003) Classification of bladder cancer by microarray expression profiling: towards a general clinical use of microarrays in cancer diagnostics. *Expert Rev Mol Diagn,* **3:** 635-47.

Dyrskjot, L., Thykjaer, T., Kruhoffer, M., Jensen, J. L., Marcussen, N., Hamilton-Dutoit, S., Wolf, H. and Orntoft, T. F. (2003) Identifying distinct classes of bladder carcinoma using microarrays. *Nat Genet,* **33:** 90-6.

Eden, A., Gaudet, F., Waghmare, A. and Jaenisch, R. (2003) Chromosomal instability and tumors promoted by DNA hypomethylation. *Science,* **300:** 455.

Eggert, A., Grotzer, M. A., Zuzak, T. J., Wiewrodt, B. R., Ho, R., Ikegaki, N. and Brodeur, G. M. (2001) Resistance to tumor necrosis factor-related apoptosis-inducing ligand (TRAIL)-induced apoptosis in neuroblastoma cells correlates with a loss of caspase-8 expression. *Cancer Res,* **61:** 1314-9.

Ehlers, A., Oker, E., Bentink, S., Lenze, D., Stein, H. and Hummel, M. (2008) Histone acetylation and DNA demethylation of B cells result in a Hodgkin-like phenotype. *Leukemia,* **22:** 835-41.

Ehrlich, M. (2002) DNA methylation in cancer: too much, but also too little. *Oncogene,* **21:** 5400-13.

Esteller, M. (2007) Epigenetic gene silencing in cancer: the DNA hypermethylome. *Hum Mol Genet,* **16 Spec No 1:** R50-9.

Esteller, M. (2008) Epigenetics in cancer. *N Engl J Med,* **358:** 1148-59.

Esteller, M., Gaidano, G., Goodman, S. N., Zagonel, V., Capello, D., Botto, B., Rossi, D., Gloghini, A., Vitolo, U., Carbone, A., Baylin, S. B. and Herman, J. G. (2002) Hypermethylation of the DNA repair gene O(6)-methylguanine DNA methyltransferase and survival of patients with diffuse large B-cell lymphoma. *J Natl Cancer Inst,* **94:** 26-32.

Evans, P. M., Zhang, W., Chen, X., Yang, J., Bhakat, K. K. and Liu, C. (2007) Kruppel-like factor 4 is acetylated by p300 and regulates gene transcription via modulation of histone acetylation. *J Biol Chem,* **282:** 33994-4002.

Firestein, R., Blander, G., Michan, S., Oberdoerffer, P., Ogino, S., Campbell, J., Bhimavarapu, A., Luikenhuis, S., de Cabo, R., Fuchs, C., Hahn, W. C., Guarente, L. P. and Sinclair, D. A. (2008) The SIRT1 deacetylase suppresses intestinal tumorigenesis and colon cancer growth. *PLoS ONE,* **3:** e2020.

Florl, A. R., Lower, R., Schmitz-Drager, B. J. and Schulz, W. A. (1999) DNA methylation and expression of LINE-1 and HERV-K provirus sequences in urothelial and renal cell carcinomas. *Br J Cancer,* **80:** 1312-21.

Florl, A. R., Steinhoff, C., Muller, M., Seifert, H. H., Hader, C., Engers, R., Ackermann, R. and Schulz, W. A. (2004) Coordinate hypermethylation at specific genes in prostate carcinoma precedes LINE-1 hypomethylation. *Br J Cancer,* **91:** 985-94.

Fong, S. F., Dietzsch, E., Fong, K. S., Hollosi, P., Asuncion, L., He, Q., Parker, M. I. and Csiszar, K. (2007) Lysyl oxidase-like 2 expression is increased in colon and esophageal tumors and associated with less differentiated colon tumors. *Genes Chromosomes Cancer,* **46:** 644-55.

Foster, K. W., Frost, A. R., McKie-Bell, P., Lin, C. Y., Engler, J. A., Grizzle, W. E. and Ruppert, J. M. (2000) Increase of GKLF messenger RNA and protein expression during progression of breast cancer. *Cancer Res,* **60:** 6488-95.

Fradet, Y., Picard, V., Bergeron, A. and LaRue, H. (2005) Cancer-testis antigen expression in bladder cancer. *Prog Urol,* **15:** 1303-13.

Fraga, M. F., Ballestar, E., Villar-Garea, A., Boix-Chornet, M., Espada, J., Schotta, G., Bonaldi, T., Haydon, C., Ropero, S., Petrie, K., Iyer, N. G., Perez-Rosado, A., Calvo, E., Lopez, J. A., Cano, A., Calasanz, M. J., Colomer, D., Piris, M. A., Ahn, N., Imhof, A., Caldas, C., Jenuwein, T. and Esteller, M. (2005) Loss of acetylation at Lys16 and trimethylation at Lys20 of histone H4 is a common hallmark of human cancer. *Nat Genet,* **37:** 391-400.

Frye, R. (2002) "SIRT8" expressed in thyroid cancer is actually SIRT7. *Br J Cancer,* **87:** 1479.

Futscher, B. W., Oshiro, M. M., Wozniak, R. J., Holtan, N., Hanigan, C. L., Duan, H. and Domann, F. E. (2002) Role for DNA methylation in the control of cell type specific maspin expression. *Nat Genet,* **31:** 175-9.

Gallucci, M., Guadagni, F., Marzano, R., Leonardo, C., Merola, R., Sentinelli, S., Ruggeri, E. M., Cantiani, R., Sperduti, I., Lopez Fde, L. and Cianciulli, A. M. (2005) Status of the p53, p16, RB1, and HER-2 genes and chromosomes 3, 7, 9, and 17 in advanced bladder cancer: correlation with adjacent mucosa and pathological parameters. *J Clin Pathol,* **58:** 367-71.

Garrett, S. C., Varney, K. M., Weber, D. J. and Bresnick, A. R. (2006) S100A4, a mediator of metastasis. *J Biol Chem,* **281:** 677-80.

Gaudet, F., Hodgson, J. G., Eden, A., Jackson-Grusby, L., Dausman, J., Gray, J. W., Leonhardt, H. and Jaenisch, R. (2003) Induction of tumors in mice by genomic hypomethylation. *Science,* **300:** 489-92.

Gibbons, R. J., McDowell, T. L., Raman, S., O'Rourke, D. M., Garrick, D., Ayyub, H. and Higgs, D. R. (2000) Mutations in ATRX, encoding a SWI/SNF-like protein, cause diverse changes in the pattern of DNA methylation. *Nat Genet,* **24:** 368-71.

Gil, J., Bernard, D., Martinez, D. and Beach, D. (2004) Polycomb CBX7 has a unifying role in cellular lifespan. *Nat Cell Biol,* **6:** 67-72.

Goll, M. G. and Bestor, T. H. (2005) Eukaryotic cytosine methyltransferases. *Annu Rev Biochem,* **74:** 481-514.

Grimm, M. O., Jurgens, B., Schulz, W. A., Decken, K., Makri, D. and Schmitz-Drager, B. J. (1995) Inactivation of tumor suppressor genes and deregulation of the c-myc gene in urothelial cancer cell lines. *Urol Res,* **23:** 293-300.

Gronbaek, K., Hother, C. and Jones, P. A. (2007) Epigenetic changes in cancer. *Apmis,* **115:** 1039-59.

Gronborg, M., Kristiansen, T. Z., Iwahori, A., Chang, R., Reddy, R., Sato, N., Molina, H., Jensen, O. N., Hruban, R. H., Goggins, M. G., Maitra, A. and Pandey, A. (2006) Biomarker discovery from pancreatic cancer secretome using a differential proteomic approach. *Mol Cell Proteomics,* **5:** 157-71.

Grossman, H. B., Liebert, M., Antelo, M., Dinney, C. P., Hu, S. X., Palmer, J. L. and Benedict, W. F. (1998) p53 and RB expression predict progression in T1 bladder cancer. *Clin Cancer Res,* **4:** 829-34.

Guo, J., Shou, C., Meng, L., Jiang, B., Dong, B., Yao, L., Xie, Y., Zhang, J., Chen, Y., Budman, D. R. and Shi, Y. E. (2007) Neuronal protein synuclein gamma predicts poor clinical outcome in breast cancer. *Int J Cancer,* **121:** 1296-305.

Gupta, A., Godwin, A. K., Vanderveer, L., Lu, A. and Liu, J. (2003) Hypomethylation of the synuclein gamma gene CpG island promotes its aberrant expression in breast carcinoma and ovarian carcinoma. *Cancer Res,* **63:** 664-73.

Hainaut, P. and Hollstein, M. (2000) p53 and human cancer: the first ten thousand mutations. *Adv Cancer Res,* **77:** 81-137.

Hayes, V. M., Severi, G., Padilla, E. J., Eggleton, S. A., Southey, M. C., Sutherland, R. L., Hopper, J. L. and Giles, G. G. (2005) Genetic variants in the vitamin D receptor gene and prostate cancer risk. *Cancer Epidemiol Biomarkers Prev,* **14:** 997-9.

Heard, E. and Disteche, C. M. (2006) Dosage compensation in mammals: fine-tuning the expression of the X chromosome. *Genes Dev,* **20:** 1848-67.

Helfman, D. M., Kim, E. J., Lukanidin, E. and Grigorian, M. (2005) The metastasis associated protein S100A4: role in tumour progression and metastasis. *Br J Cancer,* **92:** 1955-8.

Hermani, A., Hess, J., De Servi, B., Medunjanin, S., Grobholz, R., Trojan, L., Angel, P. and Mayer, D. (2005) Calcium-binding proteins S100A8 and S100A9 as novel diagnostic markers in human prostate cancer. *Clin Cancer Res,* **11:** 5146-52.

Hernandez, S., Lopez-Knowles, E., Lloreta, J., Kogevinas, M., Amoros, A., Tardon, A., Carrato, A., Serra, C., Malats, N. and Real, F. X. (2006) Prospective study of FGFR3 mutations as a prognostic factor in nonmuscle invasive urothelial bladder carcinomas. *J Clin Oncol,* **24:** 3664-71.

Hernandez-Munoz, I., Lund, A. H., van der Stoop, P., Boutsma, E., Muijrers, I., Verhoeven, E., Nusinow, D. A., Panning, B., Marahrens, Y. and van Lohuizen, M. (2005) Stable X chromosome inactivation involves the PRC1 Polycomb complex and requires histone MACROH2A1 and the CULLIN3/SPOP ubiquitin E3 ligase. *Proc Natl Acad Sci U S A,* **102:** 7635-40.

Hinz, S., Kempkensteffen, C., Christoph, F., Krause, H., Schrader, M., Schostak, M., Miller, K. and Weikert, S. (2008) Expression parameters of the polycomb group proteins BMI1, SUZ12, RING1 and CBX7 in urothelial carcinoma of the bladder and their prognostic relevance. *Tumour Biol,* **29:** 323-9.

Hoffmann, M. J., Engers, R., Florl, A. R., Otte, A. P., Muller, M. and Schulz, W. A. (2007) Expression changes in EZH2, but not in BMI-1, SIRT1, DNMT1 or DNMT3B are associated with DNA methylation changes in prostate cancer. *Cancer Biol Ther,* **6:** 1403-12.

Hoffmann, M. J., Florl, A. R., Seifert, H. H. and Schulz, W. A. (2005) Multiple mechanisms downregulate CDKN1C in human bladder cancer. *Int J Cancer,* **114:** 406-13.

Hoffmann, M. J. and Schulz, W. A. (2005) Causes and consequences of DNA hypomethylation in human cancer. *Biochem Cell Biol,* **83:** 296-321.

Hough, C. D., Sherman-Baust, C. A., Pizer, E. S., Montz, F. J., Im, D. D., Rosenshein, N. B., Cho, K. R., Riggins, G. J. and Morin, P. J. (2000) Large-scale serial analysis of gene expression reveals genes differentially expressed in ovarian cancer. *Cancer Res,* **60:** 6281-7.

Huffman, D. M., Grizzle, W. E., Bamman, M. M., Kim, J. S., Eltoum, I. A., Elgavish, A. and Nagy, T. R. (2007) SIRT1 is significantly elevated in mouse and human prostate cancer. *Cancer Res,* **67:** 6612-8.

Hurst, C. D., Tomlinson, D. C., Williams, S. V., Platt, F. M. and Knowles, M. A. (2008) Inactivation of the Rb pathway and overexpression of both isoforms of E2F3 are obligate events in bladder tumours with 6p22 amplification. *Oncogene,* **27:** 2716-27.

Ismail, N. I., Kaur, G., Hashim, H. and Hassan, M. S. (2008) S100A4 overexpression proves to be independent marker for breast cancer progression. *Cancer Cell Int,* **8:** 12.

Jelinic, P. and Shaw, P. (2007) Loss of imprinting and cancer. *J Pathol,* **211:** 261-8.

Jicai, Z., Zongtao, Y., Jun, L., Haiping, L., Jianmin, W. and Lihua, H. (2006) Persistent infection of hepatitis B virus is involved in high rate of p16 methylation in hepatocellular carcinoma. *Mol Carcinog,* **45:** 530-6.

Jones, P. A. and Baylin, S. B. (2007) The epigenomics of cancer. *Cell,* **128:** 683-92.

Kanai, Y., Saito, Y., Ushijima, S. and Hirohashi, S. (2004) Alterations in gene expression associated with the overexpression of a splice variant of DNA methyltransferase 3b, DNMT3b4, during human hepatocarcinogenesis. *J Cancer Res Clin Oncol,* **130:** 636-44.

Kanai, Y., Ushijima, S., Kondo, Y., Nakanishi, Y. and Hirohashi, S. (2001) DNA methyltransferase expression and DNA methylation of CPG islands and peri-centromeric satellite regions in human colorectal and stomach cancers. *Int J Cancer,* **91:** 205-12.

Kaneda, M., Okano, M., Hata, K., Sado, T., Tsujimoto, N., Li, E. and Sasaki, H. (2004) Essential role for de novo DNA methyltransferase Dnmt3a in paternal and maternal imprinting. *Nature,* **429:** 900-3.

Kanehira, M., Harada, Y., Takata, R., Shuin, T., Miki, T., Fujioka, T., Nakamura, Y. and Katagiri, T. (2007) Involvement of upregulation of DEPDC1 (DEP domain containing 1) in bladder carcinogenesis. *Oncogene,* **26:** 6448-55.

Kangaspeska, S., Stride, B., Metivier, R., Polycarpou-Schwarz, M., Ibberson, D., Carmouche, R. P., Benes, V., Gannon, F. and Reid, G. (2008) Transient cyclical methylation of promoter DNA. *Nature,* **452:** 112-5.

Karpf, A. R. (2007) Epigenomic reactivation screening to identify genes silenced by DNA hypermethylation in human cancer. *Curr Opin Mol Ther,* **9:** 231-41.

Kiemer, A. K., Takeuchi, K. and Quinlan, M. P. (2001) Identification of genes involved in epithelial-mesenchymal transition and tumor progression. *Oncogene,* **20:** 6679-88.

Kim, G. D., Ni, J., Kelesoglu, N., Roberts, R. J. and Pradhan, S. (2002) Co-operation and communication between the human maintenance and de novo DNA (cytosine-5) methyltransferases. *Embo J,* **21:** 4183-95.

Kim, K. H., Choi, J. S., Kim, I. J., Ku, J. L. and Park, J. G. (2006) Promoter hypomethylation and reactivation of MAGE-A1 and MAGE-A3 genes in colorectal cancer cell lines and cancer tissues. *World J Gastroenterol,* **12:** 5651-7.

Kim, W. J., Kim, E. J., Jeong, P., Quan, C., Kim, J., Li, Q. L., Yang, J. O., Ito, Y. and Bae, S. C. (2005) RUNX3 inactivation by point mutations and aberrant DNA methylation in bladder tumors. *Cancer Res,* **65:** 9347-54.

Kimura, F., Florl, A. R., Steinhoff, C., Golka, K., Willers, R., Seifert, H. H. and Schulz, W. A. (2001) Polymorphic methyl group metabolism genes in patients with transitional cell carcinoma of the urinary bladder. *Mutat Res,* **458:** 49-54.

Kirschmann, D. A., Seftor, E. A., Fong, S. F., Nieva, D. R., Sullivan, C. M., Edwards, E. M., Sommer, P., Csiszar, K. and Hendrix, M. J. (2002) A molecular role for lysyl oxidase in breast cancer invasion. *Cancer Res,* **62:** 4478-83.

Kisseljova, N. P. and Kisseljov, F. L. (2005) DNA demethylation and carcinogenesis. *Biochemistry (Mosc),* **70:** 743-52.

Knowles, M. A. (2006) Molecular subtypes of bladder cancer: Jekyll and Hyde or chalk and cheese? *Carcinogenesis,* **27:** 361-73.

Knowles, M. A. (2008) Molecular pathogenesis of bladder cancer. *Int J Clin Oncol,* **13:** 287-97.

Kondo, Y. and Issa, J. P. (2004) Epigenetic changes in colorectal cancer. *Cancer Metastasis Rev,* **23:** 29-39.

Koturbash, I., Pogribny, I. and Kovalchuk, O. (2005) Stable loss of global DNA methylation in the radiation-target tissue--a possible mechanism contributing to radiation carcinogenesis? *Biochem Biophys Res Commun,* **337:** 526-33.

Kruse, J. P. and Gu, W. (2009) Modes of p53 regulation. *Cell,* **137:** 609-22.

Lafon-Hughes, L., Di Tomaso, M. V., Mendez-Acuna, L. and Martinez-Lopez, W. (2008) Chromatin-remodelling mechanisms in cancer. *Mutat Res,* **658:** 191-214.

Laird, P. W. (1997) Oncogenic mechanisms mediated by DNA methylation. *Mol Med Today,* **3:** 223-9.

Laird, P. W. (2003) The power and the promise of DNA methylation markers. *Nat Rev Cancer,* **3:** 253-66.

Lan, F., Nottke, A. C. and Shi, Y. (2008) Mechanisms involved in the regulation of histone lysine demethylases. *Curr Opin Cell Biol,* **20:** 316-25.

Liang, G., Gonzales, F. A., Jones, P. A., Orntoft, T. F. and Thykjaer, T. (2002) Analysis of gene induction in human fibroblasts and bladder cancer cells exposed to the methylation inhibitor 5-aza-2'-deoxycytidine. *Cancer Res,* **62:** 961-6.

Lin, C. H., Hsieh, S. Y., Sheen, I. S., Lee, W. C., Chen, T. C., Shyu, W. C. and Liaw, Y. F. (2001) Genome-wide hypomethylation in hepatocellular carcinogenesis. *Cancer Res,* **61:** 4238-43.

Linares, L. K., Kiernan, R., Triboulet, R., Chable-Bessia, C., Latreille, D., Cuvier, O., Lacroix, M., Le Cam, L., Coux, O. and Benkirane, M. (2007) Intrinsic ubiquitination activity of PCAF controls the stability of the oncoprotein Hdm2. *Nat Cell Biol,* **9:** 331-8.

Liu, H., Liu, W., Wu, Y., Zhou, Y., Xue, R., Luo, C., Wang, L., Zhao, W., Jiang, J. D. and Liu, J. (2005) Loss of epigenetic control of synuclein-gamma gene as a molecular indicator of metastasis in a wide range of human cancers. *Cancer Res,* **65:** 7635-43.

Liu, T., Liu, P. Y. and Marshall, G. M. (2009) The critical role of the class III histone deacetylase SIRT1 in cancer. *Cancer Res,* **69:** 1702-5.

Livengood, A. J., Wu, C. C. and Carson, D. A. (2007) Opposing roles of RNA receptors TLR3 and RIG-I in the inflammatory response to double-stranded RNA in a Kaposi's sarcoma cell line. *Cell Immunol,* **249:** 55-62.

Loh, Y. H., Zhang, W., Chen, X., George, J. and Ng, H. H. (2007) Jmjd1a and Jmjd2c histone H3 Lys 9 demethylases regulate self-renewal in embryonic stem cells. *Genes Dev,* **21:** 2545-57.

Loppin, B., Bonnefoy, E., Anselme, C., Laurencon, A., Karr, T. L. and Couble, P. (2005) The histone H3.3 chaperone HIRA is essential for chromatin assembly in the male pronucleus. *Nature,* **437:** 1386-90.

Ma, Y., Jacobs, S. B., Jackson-Grusby, L., Mastrangelo, M. A., Torres-Betancourt, J. A., Jaenisch, R. and Rasmussen, T. P. (2005) DNA CpG hypomethylation induces heterochromatin reorganization involving the histone variant macroH2A. *J Cell Sci,* **118:** 1607-16.

Marzluff, W. F., Gongidi, P., Woods, K. R., Jin, J. and Maltais, L. J. (2002) The human and mouse replication-dependent histone genes. *Genomics,* **80:** 487-98.

Matsumoto, K., Irie, A., Satoh, T., Ishii, J., Iwabuchi, K., Iwamura, M., Egawa, S. and Baba, S. (2007) Expression of S100A2 and S100A4 predicts for disease progression and patient survival in bladder cancer. *Urology,* **70:** 602-7.

McConnell, B. B., Ghaleb, A. M., Nandan, M. O. and Yang, V. W. (2007) The diverse functions of Kruppel-like factors 4 and 5 in epithelial biology and pathobiology. *Bioessays,* **29:** 549-57.

McGraw, S., Morin, G., Vigneault, C., Leclerc, P. and Sirard, M. A. (2007) Investigation of MYST4 histone acetyltransferase and its involvement in mammalian gametogenesis. *BMC Dev Biol,* **7:** 123.

Miranda, T. B. and Jones, P. A. (2007) DNA methylation: the nuts and bolts of repression. *J Cell Physiol,* **213:** 384-90.

Mitra, A. P. and Cote, R. J. (2009) Molecular pathogenesis and diagnostics of bladder cancer. *Annu Rev Pathol,* **4:** 251-85.

Modlich, O., Prisack, H. B., Pitschke, G., Ramp, U., Ackermann, R., Bojar, H., Vogeli, T. A. and Grimm, M. O. (2004) Identifying superficial, muscle-invasive, and metastasizing transitional cell carcinoma of the bladder: use of cDNA array analysis of gene expression profiles. *Clin Cancer Res,* **10:** 3410-21.

Muegge, K. (2005) Lsh, a guardian of heterochromatin at repeat elements. *Biochem Cell Biol,* **83:** 548-54.

Nagy, Z. and Tora, L. (2007) Distinct GCN5/PCAF-containing complexes function as co-activators and are involved in transcription factor and global histone acetylation. *Oncogene,* **26:** 5341-57.

Nan, X., Hou, J., Maclean, A., Nasir, J., Lafuente, M. J., Shu, X., Kriaucionis, S. and Bird, A. (2007) Interaction between chromatin proteins MECP2 and ATRX is disrupted by mutations that cause inherited mental retardation. *Proc Natl Acad Sci U S A,* **104:** 2709-14.

Nardone, G., Compare, D., De Colibus, P., de Nucci, G. and Rocco, A. (2007) Helicobacter pylori and epigenetic mechanisms underlying gastric carcinogenesis. *Dig Dis,* **25:** 225-9.

Neuhausen, A., Florl, A. R., Grimm, M. O. and Schulz, W. A. (2006) DNA methylation alterations in urothelial carcinoma. *Cancer Biol Ther,* **5:** 993-1001.

Neveling, K., Kalb, R., Florl, A. R., Herterich, S., Friedl, R., Hoehn, H., Hader, C., Hartmann, F. H., Nanda, I., Steinlein, C., Schmid, M., Tonnies, H., Hurst, C. D., Knowles, M. A., Hanenberg, H., Schulz, W. A. and Schindler, D. (2007) Disruption of the FA/BRCA pathway in bladder cancer. *Cytogenet Genome Res,* **118:** 166-76.

Nusinow, D. A., Hernandez-Munoz, I., Fazzio, T. G., Shah, G. M., Kraus, W. L. and Panning, B. (2007) Poly(ADP-ribose) polymerase 1 is inhibited by a histone H2A variant, MacroH2A, and contributes to silencing of the inactive X chromosome. *J Biol Chem,* **282:** 12851-9.

Oeggerli, M., Tomovska, S., Schraml, P., Calvano-Forte, D., Schafroth, S., Simon, R., Gasser, T., Mihatsch, M. J. and Sauter, G. (2004) E2F3 amplification and overexpression is associated with invasive tumor growth and rapid tumor cell proliferation in urinary bladder cancer. *Oncogene,* **23:** 5616-23.

Ogawa, Y., Sun, B. K. and Lee, J. T. (2008) Intersection of the RNA interference and X-inactivation pathways. *Science,* **320:** 1336-41.

Ohm, J. E., McGarvey, K. M., Yu, X., Cheng, L., Schuebel, K. E., Cope, L., Mohammad, H. P., Chen, W., Daniel, V. C., Yu, W., Berman, D. M., Jenuwein, T., Pruitt, K., Sharkis, S. J., Watkins, D. N., Herman, J. G. and Baylin, S. B. (2007) A stem cell-like chromatin pattern may predispose tumor suppressor genes to DNA hypermethylation and heritable silencing. *Nat Genet,* **39:** 237-42.

Ohnishi, S., Ohnami, S., Laub, F., Aoki, K., Suzuki, K., Kanai, Y., Haga, K., Asaka, M., Ramirez, F. and Yoshida, T. (2003) Downregulation and growth inhibitory effect of epithelial-type Kruppel-like transcription factor KLF4, but not KLF5, in bladder cancer. *Biochem Biophys Res Commun,* **308:** 251-6.

Okada, Y., Scott, G., Ray, M. K., Mishina, Y. and Zhang, Y. (2007) Histone demethylase JHDM2A is critical for Tnp1 and Prm1 transcription and spermatogenesis. *Nature,* **450:** 119-23.

Okumura, K., Mendoza, M., Bachoo, R. M., DePinho, R. A., Cavenee, W. K. and Furnari, F. B. (2006) PCAF modulates PTEN activity. *J Biol Chem,* **281:** 26562-8.

Ono, K., Tanaka, T., Tsunoda, T., Kitahara, O., Kihara, C., Okamoto, A., Ochiai, K., Takagi, T. and Nakamura, Y. (2000) Identification by cDNA microarray of genes involved in ovarian carcinogenesis. *Cancer Res,* **60:** 5007-11.

Ozturk, M., Arslan-Ergul, A., Bagislar, S., Senturk, S. and Yuzugullu, H. (2008) Senescence and immortality in hepatocellular carcinoma. *Cancer Lett*.

Pakneshan, P., Szyf, M., Farias-Eisner, R. and Rabbani, S. A. (2004) Reversal of the hypomethylation status of urokinase (uPA) promoter blocks breast cancer growth and metastasis. *J Biol Chem,* **279:** 31735-44.

Pakneshan, P., Szyf, M. and Rabbani, S. A. (2005) Methylation and inhibition of expression of uPA by the RAS oncogene: divergence of growth control and invasion in breast cancer cells. *Carcinogenesis,* **26:** 557-64.

Palii, S. S., Van Emburgh, B. O., Sankpal, U. T., Brown, K. D. and Robertson, K. D. (2008) DNA methylation inhibitor 5-Aza-2'-deoxycytidine induces reversible genome-wide DNA damage that is distinctly influenced by DNA methyltransferases 1 and 3B. *Mol Cell Biol,* **28:** 752-71.

Pallante, P., Federico, A., Berlingieri, M. T., Bianco, M., Ferraro, A., Forzati, F., Iaccarino, A., Russo, M., Pierantoni, G. M., Leone, V., Sacchetti, S., Troncone, G., Santoro, M. and Fusco, A. (2008) Loss of the CBX7 gene expression correlates with a highly malignant phenotype in thyroid cancer. *Cancer Res,* **68:** 6770-8.

Park, I. K., Qian, D., Kiel, M., Becker, M. W., Pihalja, M., Weissman, I. L., Morrison, S. J. and Clarke, M. F. (2003) Bmi-1 is required for maintenance of adult self-renewing haematopoietic stem cells. *Nature,* **423:** 302-5.

Patel, J. H., Du, Y., Ard, P. G., Phillips, C., Carella, B., Chen, C. J., Rakowski, C., Chatterjee, C., Lieberman, P. M., Lane, W. S., Blobel, G. A. and McMahon, S. B. (2004) The c-MYC oncoprotein is a substrate of the acetyltransferases hGCN5/PCAF and TIP60. *Mol Cell Biol,* **24:** 10826-34.

Payne, S. L., Hendrix, M. J. and Kirschmann, D. A. (2007) Paradoxical roles for lysyl oxidases in cancer--a prospect. *J Cell Biochem,* **101:** 1338-54.

Pei, D. (2009) Regulation of pluripotency and reprogramming by transcription factors. *J Biol Chem,* **284:** 3365-9.

Peinado, H., Portillo, F. and Cano, A. (2005) Switching on-off Snail: LOXL2 versus GSK3beta. *Cell Cycle,* **4:** 1749-52.

Pietersen, A. M., Horlings, H. M., Hauptmann, M., Langerod, A., Ajouaou, A., Cornelissen-Steijger, P., Wessels, L. F., Jonkers, J., van de Vijver, M. J. and van Lohuizen, M. (2008) EZH2 and BMI1 inversely correlate with prognosis and TP53 mutation in breast cancer. *Breast Cancer Res,* **10:** R109.

Pradhan, S. and Kim, G. D. (2002) The retinoblastoma gene product interacts with maintenance human DNA (cytosine-5) methyltransferase and modulates its activity. *Embo J,* **21:** 779-88.

Rakyan, V. K., Down, T. A., Thorne, N. P., Flicek, P., Kulesha, E., Graf, S., Tomazou, E. M., Backdahl, L., Johnson, N., Herberth, M., Howe, K. L., Jackson, D. K., Miretti, M. M., Fiegler, H., Marioni, J. C., Birney, E., Hubbard, T. J., Carter, N. P., Tavare, S. and Beck, S. (2008) An integrated resource for genome-wide identification and analysis of human tissue-specific differentially methylated regions (tDMRs). *Genome Res,* **18:** 1518-29.

Rehman, I., Goodarzi, A., Cross, S. S., Leiblich, A., Catto, J. W., Phillips, J. T. and Hamdy, F. C. (2007) DNA methylation and immunohistochemical analysis of the S100A4 calcium binding protein in human prostate cancer. *Prostate,* **67:** 341-7.

Reik, W. (2007) Stability and flexibility of epigenetic gene regulation in mammalian development. *Nature,* **447:** 425-32.

Rhee, I., Bachman, K. E., Park, B. H., Jair, K. W., Yen, R. W., Schuebel, K. E., Cui, H., Feinberg, A. P., Lengauer, C., Kinzler, K. W., Baylin, S. B. and Vogelstein, B. (2002) DNMT1 and DNMT3b cooperate to silence genes in human cancer cells. *Nature,* **416:** 552-6.

Robertson, K. D. and Wolffe, A. P. (2000) DNA methylation in health and disease. *Nat Rev Genet,* **1:** 11-9.

Roll, J. D., Rivenbark, A. G., Jones, W. D. and Coleman, W. B. (2008) DNMT3b overexpression contributes to a hypermethylator phenotype in human breast cancer cell lines. *Mol Cancer,* **7:** 15.

Rost, T., Pyritz, V., Rathcke, I. O., Gorogh, T., Dunne, A. A. and Werner, J. A. (2003) Reduction of LOX- and LOXL2-mRNA expression in head and neck squamous cell carcinomas. *Anticancer Res,* **23:** 1565-73.

Rosty, C., Ueki, T., Argani, P., Jansen, M., Yeo, C. J., Cameron, J. L., Hruban, R. H. and Goggins, M. (2002) Overexpression of S100A4 in pancreatic ductal adenocarcinomas is associated with poor differentiation and DNA hypomethylation. *Am J Pathol,* **160:** 45-50.

Rubinstein, T., Pitashny, M. and Putterman, C. (2008) The novel role of neutrophil gelatinase-B associated lipocalin (NGAL)/Lipocalin-2 as a biomarker for lupus nephritis. *Autoimmun Rev,* **7:** 229-34.

Saito, Y., Kanai, Y., Sakamoto, M., Saito, H., Ishii, H. and Hirohashi, S. (2002) Overexpression of a splice variant of DNA methyltransferase 3b, DNMT3b4, associated with DNA hypomethylation on pericentromeric satellite regions during human hepatocarcinogenesis. *Proc Natl Acad Sci U S A,* **99:** 10060-5.

Salama, I., Malone, P. S., Mihaimeed, F. and Jones, J. L. (2008) A review of the S100 proteins in cancer. *Eur J Surg Oncol,* **34:** 357-64.

Samuel, C. E. (2001) Antiviral actions of interferons. *Clin Microbiol Rev,* **14:** 778-809, table of contents.

Sanchez-Carbayo, M. (2003) Use of high-throughput DNA microarrays to identify biomarkers for bladder cancer. *Clin Chem,* **49:** 23-31.

Sanchez-Carbayo, M. and Cordon-Cardo, C. (2007) Molecular alterations associated with bladder cancer progression. *Semin Oncol,* **34:** 75-84.

Santos, G. C., Zielenska, M., Prasad, M. and Squire, J. A. (2007) Chromosome 6p amplification and cancer progression. *J Clin Pathol,* **60:** 1-7.

Sathyanarayana, U. G., Maruyama, R., Padar, A., Suzuki, M., Bondaruk, J., Sagalowsky, A., Minna, J. D., Frenkel, E. P., Grossman, H. B., Czerniak, B. and Gazdar, A. F. (2004) Molecular detection of noninvasive and invasive bladder tumor tissues and exfoliated cells by aberrant promoter methylation of laminin-5 encoding genes. *Cancer Res,* **64:** 1425-30.

Sato, N., Maitra, A., Fukushima, N., van Heek, N. T., Matsubayashi, H., Iacobuzio-Donahue, C. A., Rosty, C. and Goggins, M. (2003) Frequent hypomethylation of multiple genes overexpressed in pancreatic ductal adenocarcinoma. *Cancer Res,* **63:** 4158-66.

Saunders, L. R. and Verdin, E. (2007) Sirtuins: critical regulators at the crossroads between cancer and aging. *Oncogene,* **26:** 5489-504.

Schiltz, R. L., Mizzen, C. A., Vassilev, A., Cook, R. G., Allis, C. D. and Nakatani, Y. (1999) Overlapping but distinct patterns of histone acetylation by the human coactivators p300 and PCAF within nucleosomal substrates. *J Biol Chem,* **274:** 1189-92.

Schiltz, R. L. and Nakatani, Y. (2000) The PCAF acetylase complex as a potential tumor suppressor. *Biochim Biophys Acta,* **1470:** M37-53.

Schlesinger, Y., Straussman, R., Keshet, I., Farkash, S., Hecht, M., Zimmerman, J., Eden, E., Yakhini, Z., Ben-Shushan, E., Reubinoff, B. E., Bergman, Y., Simon, I. and Cedar, H. (2007) Polycomb-mediated methylation on Lys27 of histone H3 pre-marks genes for de novo methylation in cancer. *Nat Genet,* **39:** 232-6.

Schulz, W. A. (2006) Understanding urothelial carcinoma through cancer pathways. *Int J Cancer,* **119:** 1513-8.

Schulz, W. A. and Dokun, O.Y. (2009) DNA methylation and human diseases: an overview. In DNA and RNA Modification Enzymes: Comparative Structure, Mechanism, Functions, Cellular Interactions and Evolution (Grosjean H, ed) Landes Biosciences, pp86-99.

Schulz, W. A. and Hoffmann, M. J. (2009) Epigenetic mechanisms in the biology of prostate cancer. *Semin Cancer Biol,* **19:** 172-80.

Schulz, W. A., Steinhoff, C. and Florl, A. R. (2006) Methylation of endogenous human retroelements in health and disease. *Curr Top Microbiol Immunol,* **310:** 211-50.

Scott, C. L., Gil, J., Hernando, E., Teruya-Feldstein, J., Narita, M., Martinez, D., Visakorpi, T., Mu, D., Cordon-Cardo, C., Peters, G., Beach, D. and Lowe, S. W. (2007) Role of the chromobox protein CBX7 in lymphomagenesis. *Proc Natl Acad Sci U S A,* **104:** 5389-94.

Sharma, P., Shen, Y., Wen, S., Bajorin, D. F., Reuter, V. E., Old, L. J. and Jungbluth, A. A. (2006) Cancer-testis antigens: expression and correlation with survival in human urothelial carcinoma. *Clin Cancer Res,* **12:** 5442-7.

Sherbet, G. V. (2009) Metastasis promoter S100A4 is a potentially valuable molecular target for cancer therapy. *Cancer Lett,* **280:** 15-30.

Soengas, M. S., Capodieci, P., Polsky, D., Mora, J., Esteller, M., Opitz-Araya, X., McCombie, R., Herman, J. G., Gerald, W. L., Lazebnik, Y. A., Cordon-Cardo, C. and Lowe, S. W. (2001) Inactivation of the apoptosis effector Apaf-1 in malignant melanoma. *Nature,* **409:** 207-11.

Sood, A. K., Fletcher, M. S., Gruman, L. M., Coffin, J. E., Jabbari, S., Khalkhali-Ellis, Z., Arbour, N., Seftor, E. A. and Hendrix, M. J. (2002) The paradoxical expression of maspin in ovarian carcinoma. *Clin Cancer Res,* **8:** 2924-32.

Steinhoff, C. and Schulz, W. A. (2003) Transcriptional regulation of the human LINE-1 retrotransposon L1.2B. *Mol Genet Genomics,* **270:** 394-402.

Strathdee, G. and Brown, R. (2002) Aberrant DNA methylation in cancer: potential clinical interventions. *Expert Rev Mol Med,* **4:** 1-17.

Stunkel, W., Peh, B. K., Tan, Y. C., Nayagam, V. M., Wang, X., Salto-Tellez, M., Ni, B., Entzeroth, M. and Wood, J. (2007) Function of the SIRT1 protein deacetylase in cancer. *Biotechnol J,* **2:** 1360-8.

Suter, C. M., Martin, D. I. and Ward, R. L. (2004) Germline epimutation of MLH1 in individuals with multiple cancers. *Nat Genet,* **36:** 497-501.

Suzuki, K., Suzuki, I., Leodolter, A., Alonso, S., Horiuchi, S., Yamashita, K. and Perucho, M. (2006) Global DNA demethylation in gastrointestinal cancer is age dependent and precedes genomic damage. *Cancer Cell,* **9:** 199-207.

Tagami, H., Ray-Gallet, D., Almouzni, G. and Nakatani, Y. (2004) Histone H3.1 and H3.3 complexes mediate nucleosome assembly pathways dependent or independent of DNA synthesis. *Cell,* **116:** 51-61.

Thambirajah, A. A., Li, A., Ishibashi, T. and Ausio, J. (2009) New developments in post-translational modifications and functions of histone H2A variants. *Biochem Cell Biol,* **87:** 7-17.

Thomas, T. and Voss, A. K. (2007) The diverse biological roles of MYST histone acetyltransferase family proteins. *Cell Cycle,* **6:** 696-704.

Tsukada, Y., Fang, J., Erdjument-Bromage, H., Warren, M. E., Borchers, C. H., Tempst, P. and Zhang, Y. (2006) Histone demethylation by a family of JmjC domain-containing proteins. *Nature,* **439:** 811-6.

Ullah, M., Pelletier, N., Xiao, L., Zhao, S. P., Wang, K., Degerny, C., Tahmasebi, S., Cayrou, C., Doyon, Y., Goh, S. L., Champagne, N., Cote, J. and Yang, X. J. (2008) Molecular architecture of quartet MOZ/MORF histone acetyltransferase complexes. *Mol Cell Biol,* **28:** 6828-43.

Vaissiere, T., Sawan, C. and Herceg, Z. (2008) Epigenetic interplay between histone modifications and DNA methylation in gene silencing. *Mutat Res,* **659:** 40-8.

van Rhijn, B. W., van der Kwast, T. H., Vis, A. N., Kirkels, W. J., Boeve, E. R., Jobsis, A. C. and Zwarthoff, E. C. (2004) FGFR3 and P53 characterize alternative genetic pathways in the pathogenesis of urothelial cell carcinoma. *Cancer Res,* **64:** 1911-4.

Villa, R., Pasini, D., Gutierrez, A., Morey, L., Occhionorelli, M., Vire, E., Nomdedeu, J. F., Jenuwein, T., Pelicci, P. G., Minucci, S., Fuks, F., Helin, K. and Di Croce, L. (2007) Role of the polycomb repressive complex 2 in acute promyelocytic leukemia. *Cancer Cell,* **11:** 513-25.

Vinuesa, E., Sola, A., Jung, M., Alfaro, V. and Hotter, G. (2008) Lipocalin-2-induced renal regeneration depends on cytokines. *Am J Physiol Renal Physiol,* **295:** F1554-62.

Vire, E., Brenner, C., Deplus, R., Blanchon, L., Fraga, M., Didelot, C., Morey, L., Van Eynde, A., Bernard, D., Vanderwinden, J. M., Bollen, M., Esteller, M., Di Croce, L., de Launoit, Y. and Fuks, F. (2006) The Polycomb group protein EZH2 directly controls DNA methylation. *Nature,* **439:** 871-4.

Wang, G., Rudland, P. S., White, M. R. and Barraclough, R. (2000) Interaction in vivo and in vitro of the metastasis-inducing S100 protein, S100A4 (p9Ka) with S100A1. *J Biol Chem,* **275:** 11141-6.

Wang, R. H., Zheng, Y., Kim, H. S., Xu, X., Cao, L., Luhasen, T., Lee, M. H., Xiao, C., Vassilopoulos, A., Chen, W., Gardner, K., Man, Y. G., Hung, M. C., Finkel, T. and Deng, C. X. (2008) Interplay among BRCA1, SIRT1, and Survivin during BRCA1-associated tumorigenesis. *Mol Cell,* **32:** 11-20.

Watt, P. M., Kumar, R. and Kees, U. R. (2000) Promoter demethylation accompanies reactivation of the HOX11 proto-oncogene in leukemia. *Genes Chromosomes Cancer,* **29:** 371-7.

Weber, M., Hellmann, I., Stadler, M. B., Ramos, L., Paabo, S., Rebhan, M. and Schubeler, D. (2007) Distribution, silencing potential and evolutionary impact of promoter DNA methylation in the human genome. *Nat Genet,* **39:** 457-66.

Wei, H., Gan, B., Wu, X. and Guan, J. L. (2009) Inactivation of FIP200 leads to inflammatory skin disorder, but not tumorigenesis, in conditional knock-out mouse models. *J Biol Chem,* **284:** 6004-13.

Wellmann, S., Bettkober, M., Zelmer, A., Seeger, K., Faigle, M., Eltzschig, H. K. and Buhrer, C. (2008) Hypoxia upregulates the histone demethylase JMJD1A via HIF-1. *Biochem Biophys Res Commun,* **372:** 892-7.

Widschwendter, M. and Jones, P. A. (2002a) DNA methylation and breast carcinogenesis. *Oncogene,* **21:** 5462-82.

Widschwendter, M. and Jones, P. A. (2002b) The potential prognostic, predictive, and therapeutic values of DNA methylation in cancer. Commentary re: J. Kwong et al., Promoter hypermethylation of multiple genes in nasopharyngeal carcinoma. Clin. Cancer Res., 8: 131-137, 2002, and H-Z. Zou et al., Detection of aberrant p16 methylation in the serum of colorectal cancer patients. Clin. Cancer Res., 8: 188-191, 2002. *Clin Cancer Res,* **8:** 17-21.

Wilson, A. S., Power, B. E. and Molloy, P. L. (2007) DNA hypomethylation and human diseases. *Biochim Biophys Acta,* **1775:** 138-62.

Wu, G., Guo, Z., Chang, X., Kim, M. S., Nagpal, J. K., Liu, J., Maki, J. M., Kivirikko, K. I., Ethier, S. P., Trink, B. and Sidransky, D. (2007) LOXL1 and LOXL4 are epigenetically silenced and can inhibit ras/extracellular signal-regulated kinase signaling pathway in human bladder cancer. *Cancer Res,* **67:** 4123-9.

Wu, Q., Hoffmann, M. J., Hartmann, F. H. and Schulz, W. A. (2005) Amplification and overexpression of the ID4 gene at 6p22.3 in bladder cancer. *Mol Cancer,* **4:** 16.

Xie, R., Loose, D. S., Shipley, G. L., Xie, S., Bassett, R. L., Jr. and Broaddus, R. R. (2007) Hypomethylation-induced expression of S100A4 in endometrial carcinoma. *Mod Pathol,* **20:** 1045-54.

Yamane, K., Toumazou, C., Tsukada, Y., Erdjument-Bromage, H., Tempst, P., Wong, J. and Zhang, Y. (2006) JHDM2A, a JmjC-containing H3K9 demethylase, facilitates transcription activation by androgen receptor. *Cell,* **125:** 483-95.

Yanagawa, N., Tamura, G., Honda, T., Endoh, M., Nishizuka, S. and Motoyama, T. (2004) Demethylation of the synuclein gamma gene CpG island in primary gastric cancers and gastric cancer cell lines. *Clin Cancer Res,* **10:** 2447-51.

Yang, J., Bielenberg, D. R., Rodig, S. J., Doiron, R., Clifton, M. C., Kung, A. L., Strong, R. K., Zurakowski, D. and Moses, M. A. (2009) Lipocalin 2 promotes breast cancer progression. *Proc Natl Acad Sci U S A,* **106:** 3913-8.

Yang, X., Yan, L. and Davidson, N. E. (2001) DNA methylation in breast cancer. *Endocr Relat Cancer,* **8:** 115-27.

Yang, X. J. and Ullah, M. (2007) MOZ and MORF, two large MYSTic HATs in normal and cancer stem cells. *Oncogene,* **26:** 5408-19.

Yao, R., Lopez-Beltran, A., Maclennan, G. T., Montironi, R., Eble, J. N. and Cheng, L. (2007) Expression of S100 protein family members in the pathogenesis of bladder tumors. *Anticancer Res,* **27:** 3051-8.

Yates, D. R., Rehman, I., Abbod, M. F., Meuth, M., Cross, S. S., Linkens, D. A., Hamdy, F. C. and Catto, J. W. (2007) Promoter hypermethylation identifies progression risk in bladder cancer. *Clin Cancer Res,* **13:** 2046-53.

Yegnasubramanian, S., Haffner, M. C., Zhang, Y., Gurel, B., Cornish, T. C., Wu, Z., Irizarry, R. A., Morgan, J., Hicks, J., DeWeese, T. L., Isaacs, W. B., Bova, G. S., De Marzo, A. M. and Nelson, W. G. (2008) DNA hypomethylation arises later in prostate cancer progression than CpG island hypermethylation and contributes to metastatic tumor heterogeneity. *Cancer Res,* **68:** 8954-67.

Yong, H. Y. and Moon, A. (2007) Roles of calcium-binding proteins, S100A8 and S100A9, in invasive phenotype of human gastric cancer cells. *Arch Pharm Res,* **30:** 75-81.

Zhang, H. (2007) Molecular signaling and genetic pathways of senescence: Its role in tumorigenesis and aging. *J Cell Physiol,* **210:** 567-74.

Zhang, R., Poustovoitov, M. V., Ye, X., Santos, H. A., Chen, W., Daganzo, S. M., Erzberger, J. P., Serebriiskii, I. G., Canutescu, A. A., Dunbrack, R. L., Pehrson, J. R., Berger, J. M., Kaufman, P. D. and Adams, P. D. (2005) Formation of MacroH2A-containing senescence-associated heterochromatin foci and senescence driven by ASF1a and HIRA. *Dev Cell,* **8:** 19-30.

Zhao, W., Hisamuddin, I. M., Nandan, M. O., Babbin, B. A., Lamb, N. E. and Yang, V. W. (2004) Identification of Kruppel-like factor 4 as a potential tumor suppressor gene in colorectal cancer. *Oncogene,* **23:** 395-402.

Zou, M., Al-Baradie, R. S., Al-Hindi, H., Farid, N. R. and Shi, Y. (2005) S100A4 (Mts1) gene overexpression is associated with invasion and metastasis of papillary thyroid carcinoma. *Br J Cancer,* **93:** 1277-84.

APPENDIX

APPENDIX 1

Differential gene expression between urothelial carcinoma and normal cells
A: Genes overexpressed in BC19 cultures compared to UP91; B: Genes overexpressed in UP91 compared to BC19 cultures
Abbreviations: ECM extracellular matrix; IFN interferon

up regulated genes

HGNC Symbol	RefSeq DNA ID	Ensembl Gene ID	Chromosome	Band	Function	Expression
SPINK1	NM_003122_1	ENSG00000164266	5	q32	protease inhibitor	**149.73**
IQSEC1	NM_014869_1	ENSG00000144711	3	p25.2	cell adhesion	**114.60**
KRT13	NM_002274_1	ENSG00000171401	17	q21.2	cytokeratin	**75.23**
UPK1A	NM_007000_1	ENSG00000105668	19	q13.12	uroplakin, plasma membrane	**74.67**
LSP1	NM_002339_1	ENSG00000130592	11	p15.5	plasma membrane/cytoskeleton	**40.70**
PSMB10	NM_002801_1	ENSG00000205220	16	q22.1	proteasom; IFN-inducible	**28.47**
TJP3	NM_014428_1	ENSG00000105289	19	p13.3	tight junction	**28.40**
RARRES3	NM_004585_1	ENSG00000133321	11	q12.3	antiviral response; IFN-inducible	**28.00**
KRT15	NM_002275_1	ENSG00000171346	17	q21.2	cytokeratin	**27.83**
IVL	NM_005547_1	ENSG00000163207	1	q21.3	cytoskeleton, epidermal	**27.60**
SERPING1	NM_000062_1	ENSG00000149131	11	q12.1	protease inhibitor	**24.30**
TSPAN6	NM_003270_1	ENSG00000000003	X	q22.1	plasma membrane	**23.90**
E2F1	NM_005225_1	ENSG00000101412	20	q11.22	transcription factor	**23.67**
ELF3	NM_004433_1	ENSG00000163435	1	q32.1	transcription factor	**23.17**
GBP2	NM_004120_1	ENSG00000162645	1	p22.2	G-Protein	**22.70**
PPYR1	NM_005972_1	ENSG00000204174	10	q11.22	receptor	**18.53**
CYP4B1	NM_000779_1	ENSG00000142973	1	p33	xenobiotic metabolism	**18.13**
CDH11	NM_001797_1	ENSG00000140937	16	q21	cell adhesion	**17.70**
SLC15A3	NM_016582_1	ENSG00000110446	11	q12.2	amino acid transport	**16.73**
EPS8L1	NM_017729_1	ENSG00000131037	19	q13.42	*unknown*	**15.87**
CFB	NM_001710_1	ENSG00000204359	6	p21.32	complement	**15.53**

LCN2	NM_005564_1	ENSG00000148346	9	q34.11	stress response	**13.30**
GDPD3	NM_024307_1	ENSG00000102886	16	p11.2	phospholipid metabolism	**13.23**
MX2	NM_002463_1	ENSG00000183486	21	q22.3	antiviral response; IFN-inducible	**13.20**
CLIC3	NM_004669_1	ENSG00000169583	9	q34.3	ion channel	**12.73**
HLA-DMA	NM_006120_1	ENSG00000204257	6	p21.32	antigen presentation	**12.13**
VSIG2	NM_014312_1	ENSG00000019102	11	q24.2	antiviral response; IFN-inducible	**11.27**
C2	NM_000063_1	ENSG00000204364	6	p21.32	complement	**11.13**
UPK1B	NM_006952_1	ENSG00000114638	3	q13.32	uroplakin, plasma membrane	**10.83**
WNK2	NM_006648_1	ENSG00000165238	9	q22.32	protein kinase	**9.83**
ASS1	NM_054012_1	ENSG00000130707	9	q34.12	amino acid and NO metabolism	**9.63**
ACSL5	NM_016234_1	ENSG00000197142	10	q25.2	lipid metabolism	**9.23**
RIPK3	NM_006871_1	ENSG00000129465	14	q11.2	protein kinase, apoptosis regulation	**9.20**
LIMK1	NM_002314_1	ENSG00000106683	7	q11.23	protein kinase, cytoskeleton	**8.23**
KRT16	NM_005557_1	ENSG00000186832	17	q21.2	cytokeratin, epidermal suprabasal	**8.20**
RBP4	NM_006744_1	ENSG00000138207	10	q23.33	retinol-binding	**8.17**
C1orf116	NM_023938_1	ENSG00000182795	1	q32.2	*unknown*	**8.10**
PRSS22	NM_022119_1	ENSG00000005001	16	p13.3	protease	**7.83**
ARHGDIB	NM_001175_1	ENSG00000111348	12	p12.3	cytoskeleton	**7.70**
TMPRSS4	NM_019894_1	ENSG00000137648	11	q23.3	protease	**7.57**
GBA	M16328_1	ENSG00000177628	1	q21	epidermal differentiation?	**7.30**
DHRS2	NM_005794_1	ENSG00000100867	14	q11.2	xenobiotic metabolism	**6.93**
GADD45B	XM_030485	ENSG00000099860	19	p13.3	damage response	**6.83**
SIRT4	NM_012240_1	ENSG00000089163	12	q24.31	amino acid metabolism regulation	**6.50**
SLC44A2	NM_020428_1	ENSG00000129353	19	p13.2	transporter	**6.23**
GABRE	NM_004961_1	ENSG00000102287	X	q28	receptor	**6.13**
ANXA10	NM_007193_1	ENSG00000109511	4	q32.3	signaling regulation	**6.07**
GSDML	NM_018530_1	ENSG00000073605	17	q21.1	*unknown*	**5.93**
S100B	NM_006272_1	ENSG00000160307	21	q22.3	damage response?, apoptosis	**5.93**
FXYD3	XM_015780_1	ENSG00000089356	19	q13.12	ion channel	**5.77**
AGTR1	NM_031850_1	ENSG00000144891	3	q24	receptor	**5.47**
CRCT1	NM_019060_1	ENSG00000169509	1	q21.3	epidermal differentiation	**5.37**
GDF15	NM_004864_1	ENSG00000130513	19	p13.11	growth factor	**5.27**

NCOA1	NM_003743_1	ENSG00000084676	2	p23.3	transcription factor	**5.07**
S100A9	NM_002965_1	ENSG00000163220	1	q21.3	damage response?	**5.00**
RHOG	NM_001665_1	ENSG00000177105	11	p15.4	cytoskeleton, G-Protein	**4.93**
SNCG	NM_003087_1	ENSG00000173267	10	q23.2	damage response?	**4.87**
HSPB1	NM_001540_1	ENSG00000106211	7	q11.23	damage response?	**4.77**
MAP4K1	NM_007181_1	ENSG00000104814	19	q13.2	protein kinase, apoptosis regulation	**4.70**
FAM14A	NM_032036_1	ENSG00000119632	14	q32.13	IFN-inducible	**4.47**
NR0B2	NM_021969_1	ENSG00000131910	1	p36.11	transcription factor	**4.40**
KRT8	NM_002273_1	ENSG00000170421	12	q13.13	cytokeratin	**4.40**
IFI6	NM_022872_1	ENSG00000126709	1	p36.11	mitochondrial, IFN-inducible	**4.27**
IFIT3	NM_001549_1	ENSG00000119917	10	q23.31	IFN-inducible	**4.27**
LEFTY2	NM_003240_1	ENSG00000143768	1	q42.12	growth factor	**4.23**
EDN1	NM_001955_1	ENSG00000078401	6	p24.1	growth factor	**4.17**
IFI30	NM_006332_1	ENSG00000105648	19	p13.11	IFN-inducible	**4.10**
NRSN2	NM_024958_1	ENSG00000125841	20	p13	*unknown*	**4.00**
TAGLN	NM_003186_1	ENSG00000149591	11	q23.3	cytoskeleton	**3.63**
UBE2L6	NM_004223_1	ENSG00000156587	11	q12.1	IFN-inducible	**3.37**
TNFRSF25	NM_003790_1	ENSG00000171680	1	p36.31	receptor, growth and apoptosis	**3.33**
ANXA11	NM_001157_1	ENSG00000122359	10	q22.3	signaling regulation	**3.33**
CSTB	NM_000100_1	ENSG00000160213	21	q22.3	protease inhibitor	**3.23**
B2M	NM_004048_1	ENSG00000166710	15	q21.1	antigen presentation	**3.17**
GALNT1	NM_020474_1	ENSG00000141429	18	q12.2	glycoprotein metabolism	**3.17**
STIM1	NM_003156_1	ENSG00000167323	11	p15.4	ER/plasma membrane	**3.03**
APOBEC3B	NM_004900_1	ENSG00000179750	22	q13.1	antiviral response	**2.90**
MARCH6	NM_005885_1	ENSG00000145495	5	p15.2	ER ubiquitination	**2.80**
SYNGR1	NM_004711_1	ENSG00000100321	22	q13.1	vesicle transport	**2.80**
KLF5	NM_001730_1	ENSG00000102554	13	q22.1	transcription factor	**2.77**
CLDN7	NM_001307_1	ENSG00000181885	17	p13.1	tight junction	**2.73**
ZSCAN18	NM_023926_1	ENSG00000121413	19	q13.43	*unknown*	**2.47**

down regulated genes

HGNC Symbol	RefSeq DNA ID	Ensembl Gene ID	Chromosome	Band	Function	Expression
VIM	NM_003380_1	ENSG00000026025	10	p12.33	cytokeratin	**-146.30**
SRGN	NM_002727_1	ENSG00000122862	10	q22.1	apopotosis	**-65.30**
AREG	NM_001657_1	ENSG00000109321	4	q13.3	growth factor	**-49.40**
TFPI2	NM_006528_1	ENSG00000105825	7	q21.3	protease inhibitor	**-26.40**
EFEMP1	NM_018894_1	ENSG00000115380	2	p16	ECM	**-25.97**
TNC	NM_002160_1	ENSG00000041982	9	q33.1	ECM	**-23.70**
LAMA3	NM_000227_1	ENSG00000053747	18	q11.2	ECM	**-21.80**
STAT4	NM_003151_1	ENSG00000138378	2	q32.3	transcription factor	**-17.77**
STK17A	NM_004760_1	ENSG00000164543	7	p13	protein kinase; apoptosis	**-16.20**
VEGFC	NM_005429_1	ENSG00000150630	4	q34.3	growth factor	**-15.30**
INHBA	NM_002192_1	ENSG00000122641	7	p14.1	growth factor	**-14.73**
FGFBP1	NM_005130_1	ENSG00000137440	4	p15.32	growth factor binding protein	**-14.60**
KRT5	NM_000424_1	ENSG00000186081	12	q13.13	cytokeratin	**-12.60**
IL1B	NM_000576_1	ENSG00000125538	2	q13	cytokine	**-12.33**
PTHLH	NM_002820_1	ENSG00000087494	12	p11.22	growth factor	**-11.70**
TPBG	NM_006670_1	ENSG00000146242	6	q14.1	plasma membrane	**-10.90**
OAT	NM_000274_1	ENSG00000065154	10	q26.13	amino acid metabolism	**-10.70**
IGFBP7	NM_001553_1	ENSG00000163453	4	q12	growth factor binding protein	**-9.90**
LAMB1	NM_002291_1	ENSG00000091136	7	q31.1	ECM	**-9.77**
CTSL1	NM_001912_1	ENSG00000135047	9	q22.1	protease	**-9.50**
SMURF2	NM_022739_1	ENSG00000108854	17	q24.1	signaling regulation	**-9.17**
CTNNAL1	NM_003798_1	ENSG00000119326	9	q31.3	cell adhesion	**-8.23**
TGFBI	NM_000358_1	ENSG00000120708	5	q31.1	growth factor	**-8.10**
BCAR3	NM_003567_1	ENSG00000137936	1	p22.1	signaling regulation	**-8.03**

MGLL	NM_007283_1	ENSG00000074416	3	q21.3	lipid metabolism	**-7.77**
FEZ1	NM_005103_1	ENSG00000149557	11	q24.2	cytoskeleton	**-7.70**
STAG2	NM_006603_1	ENSG00000101972	X	q25	mitosis	**-7.63**
ME1	NM_002395_1	ENSG00000065833	6	q14.2	lipid metabolism	**-7.50**
CD44	NM_000610_1	ENSG00000026508	11	p13	cell adhesion	**-7.43**
PLEK2	NM_016445_1	ENSG00000100558	14	q23.3	plasma membrane/cytoskeleton	**-7.23**
GCSH	NM_004483_1	ENSG00000140905	16	q23.2	amino acid metabolism	**-7.13**
SMOC1	NM_022137_1	ENSG00000198732	14	q24.2	ECM	**-6.93**
TMEPAI	NM_020182_1	ENSG00000124225	20	q13.32	signaling regulation	**-6.60**
C16orf3	NM_001214_1	ENSG00000183591	16	q24.3	*unknown*	**-6.50**
TXN	NM_003329_1	ENSG00000136810	9	q31.3	redox regulation	**-6.43**
DIO3	NM_001362_1	ENSG00000197406	14	q32.31	hormone metabolism	**-6.23**
TYMS	NM_001071_1	ENSG00000176890	18	p11.32	nucleotide metabolism	**-6.10**
LAMC2	NM_005562_1	ENSG00000058085	1	q25.3	ECM	**-5.93**
LAMB3	NM_000228_1	ENSG00000196878	1	q32.2	ECM	**-5.83**
MMP10	NM_002425_1	ENSG00000166670	11	q22.2	protease/ECM	**-5.63**
CAPRIN2	NM_023925_1	ENSG00000110888	12	p11.21	growth regulation	**-5.13**
HOXA1	NM_005522_1	ENSG00000105991	7	p15.2	transcription factor	**-4.97**
RGS10	NM_002925_1	ENSG00000148908	10	q26.11	signaling regulation	**-4.97**
ANXA3	NM_005139_1	ENSG00000138772	4	q21.21	signaling regulation	**-4.67**
DIMT1L	NM_014473_1	ENSG00000086189	5	q12.1	RNA synthesis	**-4.63**
C9orf95	NM_017881_1	ENSG00000106733	9	q21.13	*unknown*	**-4.63**
G0S2	NM_015714_1	ENSG00000123689	1	q32.2	lipid metabolism	**-4.50**
SSR3	NM_007107_1	ENSG00000114850	3	q25.31	protein transport	**-4.43**
DERA	NM_015954_1	ENSG00000023697	12	p12.3	nucleotide metabolism	**-4.40**
ERO1L	NM_014584_1	ENSG00000197930	14	q22.1	ER function	**-4.37**
EEF1B2	NM_021121_1	ENSG00000114942	2	q33.3	protein synthesis	**-4.27**
GNAS	NM_000516_1	ENSG00000087460	20	q13.32	signaling regulation	**-4.27**
GGH	NM_003878_1	ENSG00000137563	8	q12.3	nucleotide metabolism	**-3.97**
INTS10	NM_018142_1	ENSG00000104613	8	p21.3	*unknown*	**-3.90**
PTX3	NM_002852_1	ENSG00000163661	3	q25.32	immunity	**-3.83**
SMS	NM_004595_1	ENSG00000102172	X	p22.11	protein synthesis; RNA synthesis	**-3.77**

TMSB4Y	NM_004202_1	ENSG00000154620	Y	q11.221	immunity	**-3.73**
ANXA6	NM_001155_1	ENSG00000197043	5	q33.1	signaling regulation	**-3.70**
KCNJ15	NM_002243_1	ENSG00000157551	21	q22.13	ion channel	**-3.70**
SAT1	NM_002970_1	ENSG00000130066	X	p22.11	protein synthesis; RNA synthesis	**-3.63**
BTG3	NM_006806_1	ENSG00000154640	21	q21.1	protein secretion	**-3.63**
CDA	NM_001785_1	ENSG00000158825	1	p36.12	nucleotide metabolism	**-3.60**
MSH6	NM_000179_1	ENSG00000116062	2	p16.3	DNA repair	**-3.60**
UCK2	NM_012474_1	ENSG00000143179	1	q24.1	nucleotide metabolism	**-3.50**
TSPAN1	NM_005727_1	ENSG00000117472	1	p34.1	plasma membrane	**-3.47**
GTPBP9	NM_013341_1	ENSG00000138430	2	q31.1	signaling	**-3.40**
KYNU	NM_003937_1	ENSG00000115919	2	q22.2	amino acid metabolism	**-3.37**
RAP1GDS1	NM_021159_1	ENSG00000138698	4	q23	signaling regulation	**-3.33**
EGFR	NM_005228_1	ENSG00000146648	7	p11.2	growth factor receptor	**-3.33**
ATP5C1	NM_005174_1	ENSG00000165629	10	p14	energy metabolism	**-3.33**
CADM1	NM_014333_1	ENSG00000182985	11	q23.3	Adhesion	**-3.30**
TIMM9	NM_012460_1	ENSG00000100575	14	q23.1	energy metabolism	**-3.30**
CCDC90A	NM_022102_1	ENSG00000050393	6	p24.3	*unknown*	**-3.27**
CCND2	NM_001759_1	ENSG00000118971	12	p13.32	cell cycle regulation	**-3.27**
ATP5H	NM_006356_1	ENSG00000167863	17	q25.1	energy metabolism	**-3.27**
RBBP8	NM_002894_1	ENSG00000101773	18	q11.2	checkpoint regulation	**-3.27**
RAC2	NM_014029_1	ENSG00000128340	22	q12.3	cytoskeleton	**-3.23**
EBNA1BP2	NM_006824_1	ENSG00000117395	1	p34.2	RNA synthesis	**-3.17**
DSE	NM_013352_1	ENSG00000111817	6	q22.1	ECM	**-3.17**
PDCD5	NM_004708_1	ENSG00000105185	19	q13.11	apoptosis	**-3.17**
AVPI1	NM_021732_1	ENSG00000119986	10	q24.2	signaling regulation	**-3.13**
ALDH7A1	NM_001182_1	ENSG00000164904	5	q23.2	amino acid metabolism	**-3.10**
GTF2F2	NM_004128_1	ENSG00000188342	13	q14.12	transcription factor	**-3.10**
MPHOSPH6	NM_005792_1	ENSG00000135698	16	q23.3	RNA synthesis	**-3.10**
CA12	NM_017689_1	ENSG00000074410	15	q22	pH regulation	**-3.03**
RAB32	NM_006834_1	ENSG00000118508	6	q24.3	organelle transport	**-2.97**
PSMA1	NM_002786_1	ENSG00000129084	11	p15.2	protein degradation	**-2.97**
UGCG	NM_003358_1	ENSG00000148154	9	q32	plasma membrane biosynthesis	**-2.97**

UBE2R2	NM_017811_1	ENSG00000107341	9	p13.3	protein metabolism	**-2.93**
TBC1D2	NM_018421_1	ENSG00000095383	9	q22.33	cytoskeleton	**-2.93**
TCEB1	NM_005648_1	ENSG00000154582	8	q21.11	protein synthesis	**-2.90**
DNAPTP6	NM_015535_1	ENSG00000196141	2	q33.1	?	**-2.87**
CDK7	NM_001799_1	ENSG00000134058	5	q13.2	cell cycle regulation	**-2.87**
IKBKAP	NM_003640_1	ENSG00000070061	9	q31.3	signaling regulation	**-2.87**
H2AFZ	NM_002106_1	ENSG00000164032	4	q23	transcription factor	**-2.83**
USP9Y	NM_004654_1	ENSG00000114374	Y	q11.21	protein degradation	**-2.80**
MAD2L1	XM_003560	ENSG00000164109	4	q27	mitosis	**-2.77**
HERPUD1	NM_014685_1	ENSG00000051108	16	q13	ER function	**-2.77**
ACAT2	NM_005891_1	ENSG00000120437	6	q25.3	lipid metabolism	**-2.77**
OSTF1	NM_012383_1	ENSG00000134996	9	q21.13	signaling regulation	**-2.73**
RPL35	NM_007209_1	ENSG00000136942	9	q33.3	protein synthesis	**-2.73**
ATP5F1	NM_001688_1	ENSG00000116459	1	p13.3	energy metabolism	**-2.70**
RHEB	NM_005614_1	ENSG00000106615	7	q36.1	Metabolic/protein synthesis regulation	**-2.70**
ANXA1	NM_000700_1	ENSG00000135046	9	q21.13	signaling regulation	**-2.70**
PPCS	BC012383_1	ENSG00000127125	1	p13.1	lipid metabolism	**-2.67**
DNAJC15	NM_013238_1	ENSG00000120675	13	q14.11	DNA repair	**-2.67**
EIF1AP1	NM_001412_1	ENSG00000173674	X	p22.12	protein synthesis	**-2.67**
PSMD14	NM_005805_1	ENSG00000115233	2	q24.2	protein degradation	**-2.63**
GABARAPL2	NM_007285_1	ENSG00000034713	16	q23.1	protein transport	**-2.60**
NP	NM_000270_1	ENSG00000198805	14	q11.2	nucleotide metabolism	**-2.57**
AP2B1	NM_001282_1	ENSG00000006125	17	q12	unknown	**-2.57**
EEF1E1	NM_004280_1	ENSG00000124802	6	p24.3	protein synthesis	**-2.57**
CCT4	NM_006430_1	ENSG00000115484	2	p15	RNA synthesis	**-2.53**
MUS81	NM_025128_1	ENSG00000172732	11	q13.1	DNA repair	**-2.53**
REXO2	NM_015523_1	ENSG00000076043	11	q23.2	RNA synthesis	**-2.53**
STRAP	NM_007178_1	ENSG00000023734	12	p12.3	signaling regulation	**-2.53**
PSMA2	NM_002787_1	ENSG00000106588	7	p14.1	protein degradation	**-2.50**
PTS	NM_000317_1	ENSG00000150787	11	q23.1	nucleotide metabolism	**-2.50**
BBS10	XM_071391_1	ENSG00000179941	12	q21.2	protein synthesis	**-2.47**
ALDH2	NM_000690_1	ENSG00000111275	12	q24.13	alcohol metabolism, mitochondrial	**-2.47**

UBE2E3	NM_006357_1	ENSG00000170035	2	q31.3	protein degradation	**-2.47**
PYGL	NM_002863_1	ENSG00000100504	14	q22.1	glucose metabolism	**-2.47**
SIX3	NM_005413_1	ENSG00000138083	2	p21	transcription factor	**-2.40**
COPS3	NM_003653_1	ENSG00000141030	17	p11.2	protein degradation	**-2.40**
CLIC1	NM_001288_1	ENSG00000204418	6	p21.33	ion channel	**-2.37**
DSCR2	NM_003720_1	ENSG00000183527	21	q22.2	unknown	**-2.30**
CHRNB4	NM_000750_1	ENSG00000117971	15	q25.1	receptor	**-2.27**
EIF1B	NM_005875_1	ENSG00000114784	3	p22.1	protein synthesis	**-2.20**
RNF7	NM_014245_1	ENSG00000114125	3	q23	protein degradation	**-2.20**
ARPC3B	AL133174_5	ENSG00000111229	20	q13.13	cytoskeleton	**-2.13**

APPENDIX 2

Genes induced in normal urothelial cells (UP159 & UP160) after treatment with 5-aza-dC (by 1.5-fold to 8-fold) AND differentially expressed in the bladder cancer cell lines (VMCub1 & UM-UC3) in comparison to the normal urothelial cells (by 1.5-fold to 25-fold) AND at most weakly induced by 5-aza-dC in bladder cancer cell lines (<1.5-fold).

Symbol	locus link id	map_location	gene_name
ABHD14A	25864	3p21.1	abhydrolase domain containing 14A
ACAA2	10449	18q21.1	acetyl-Coenzyme A acyltransferase 2 (mitochondrial 3-oxoacyl-Coenzyme A thiolase)
ACOX1	51	17q24-q25	acyl-Coenzyme A oxidase 1, palmitoyl
AKAP13	11214	15q24-q25	A kinase (PRKA) anchor protein 13
AKAP9	10142	7q21-q22	A kinase (PRKA) anchor protein (yotiao) 9
ALDH5A1	7915	6p22.2-p22.3	aldehyde dehydrogenase 5 family, member A1 (succinate-semialdehyde dehydrogenase)
AMACR	23600	5p13.2-q11.1	alpha-methylacyl-CoA racemase
AP1S2	8905	Xp22.2	adaptor-related protein complex 1, sigma 2 subunit
APOBEC3B	9582	22q13.1-q13.2	apolipoprotein B mRNA editing enzyme, catalytic polypeptide-like 3B
ARG2	384	14q24.1-q24.3	arginase, type II
ARHGEF7	8874	13q34	Rho guanine nucleotide exchange factor (GEF) 7
ASCC1	51008	10pter-q25.3	activating signal cointegrator 1 complex subunit 1
ATF3	467	1q32.3	activating transcription factor 3
ATF7IP	55729	12p13.1	activating transcription factor 7 interacting protein
ATP6V1C1	528	8q22.3	ATPase, H+ transporting, lysosomal 42kDa, V1 subunit C1
ATP9A	10079	20q13.2	ATPase, Class II, type 9A
BAG2	9532	6p12.3-p11.2	BCL2-associated athanogene 2
BCAT1	586	12pter-q12	branched chain aminotransferase 1, cytosolic
BST2	684	19p13.2	bone marrow stromal cell antigen 2
BTAF1	9044	10q22-q23	BTAF1 RNA polymerase II, B-TFIID transcription factor-associated, 170kDa (Mot1 homolog, S. cerevisiae)
C14orf101	54916	14q23.1	chromosome 14 open reading frame 101
C14orf103	55102	14q32.2	chromosome 14 open reading frame 103
C14orf11	55837	14q13.1	chromosome 14 open reading frame 11
C9orf82	79886	9p21.2	chromosome 9 open reading frame 82

CALB2	794	16q22.2	calbindin 2, 29kDa (calretinin)
CALM1	801	14q24-q31	calmodulin 1 (phosphorylase kinase, delta)
CAMSAP1	157922	9q34.3	calmodulin regulated spectrin-associated protein 1
CBX7	23492	22q13.1	chromobox homolog 7
CD58	965	1p13	CD58 molecule
CDC2L6	23097	6q21	cell division cycle 2-like 6 (CDK8-like)
CDK5	1020	7q36	cyclin-dependent kinase 5
CDS2	8760	20p13	CDP-diacylglycerol synthase (phosphatidate cytidylyltransferase) 2
CHST11	50515	12q	carbohydrate (chondroitin 4) sulfotransferase 11
CITED2	10370	6q23.3	Cbp/p300-interacting transactivator, with Glu/Asp-rich carboxy-terminal domain, 2
CLGN	1047	4q28.3-q31.1	calmegin
CLIC4	25932	1p36.11	chloride intracellular channel 4
CLPTM1	1209	19q13.2-q13.3	cleft lip and palate associated transmembrane protein 1
CLU	1191	8p21-p12	clusterin
COL6A2	1292	21q22.3	collagen, type VI, alpha 2
CPVL	54504	7p15-p14	carboxypeptidase, vitellogenic-like
CTSB	1508	8p22	cathepsin B
CUL4B	8450	Xq23	cullin 4B
CXCL1	2919	4q21	chemokine (C-X-C motif) ligand 1 (melanoma growth stimulating activity, alpha)
CXCL2	2920	4q21	chemokine (C-X-C motif) ligand 2
CXCL3	2921	4q21	chemokine (C-X-C motif) ligand 3
DAPK1	1612	9q34.1	death-associated protein kinase 1
DDX58	23586	9p12	DEAD (Asp-Glu-Ala-Asp) box polypeptide 58
DMXL1	1657	5q22	Dmx-like 1
DNAJB4	11080	1p31.1	DnaJ (Hsp40) homolog, subfamily B, member 4
DNAJB6	10049	7q36.3	DnaJ (Hsp40) homolog, subfamily B, member 6
DNAJC6	9829	1pter-q31.3	DnaJ (Hsp40) homolog, subfamily C, member 6
DPYSL2	1808	8p22-p21	dihydropyrimidinase-like 2
DSCR1	1827	21q22.1-q22.2	Down syndrome critical region gene 1
DST	667	6p12-p11	dystonin
DUSP1	1843	5q34	dual specificity phosphatase 1
DUSP3	1845	17q21	dual specificity phosphatase 3 (vaccinia virus phosphatase VH1-related)
EBAG9	9166	8q23	estrogen receptor binding site associated, antigen, 9
EGLN1	54583	1q42.1	egl nine homolog 1 (C. elegans)

ENO2	2026	12p13	enolase 2 (gamma, neuronal)
EPS8	2059	12q13	epidermal growth factor receptor pathway substrate 8
F2R	2149	5q13	coagulation factor II (thrombin) receptor
F2RL1	2150	5q13	coagulation factor II (thrombin) receptor-like 1
FAIM	55179	3q22.3	Fas apoptotic inhibitory molecule
FAM11B	79134	2q14.2	family with sequence similarity 11, member B
FBN1	2200	15q21.1	fibrillin 1
FBXL15	79176	10q24.32	F-box and leucine-rich repeat protein 15
FCHSD2	9873	11q13.4	FCH and double SH3 domains 2
FZD7	8324	2q33	frizzled homolog 7 (Drosophila)
G6PD	2539	Xq28	glucose-6-phosphate dehydrogenase
GADD45B	4616	19p13.3	growth arrest and DNA-damage-inducible, beta
GBA	2629	1q21	glucosidase, beta; acid (includes glucosylceramidase)
GCC2	9648	2q12.3	GRIP and coiled-coil domain containing 2
GLIPR1	11010	12q21.2	GLI pathogenesis-related 1 (glioma)
GLS	2744	2q32-q34	glutaminase
GLT28D1	55849	Xq23	glycosyltransferase 28 domain containing 1
GPD1L	23171	3p22.3	glycerol-3-phosphate dehydrogenase 1-like
GULP1	51454	2q32.3-q33	GULP, engulfment adaptor PTB domain containing 1
H2AFY	9555	5q31.3-q32	H2A histone family, member Y
H2BFS	54145	21q22.3	H2B histone family, member S
HAS2	3037	8q24.12	hyaluronan synthase 2
HEG1	57493	3q21.2	HEG homolog 1 (zebrafish)
HIST1H1C	3006	6p21.3	histone cluster 1, H1c
HIST1H2AC	8334	6p21.3	histone cluster 1, H2ac
HIST1H2BC	8347	6p21.3	histone cluster 1, H2bc
HIST1H2BD	3017	6p21.3	histone cluster 1, H2bd
HIST1H2BE	8344	6p21.3	histone cluster 1, H2be
HIST1H2BG	8339	6p21.3	histone cluster 1, H2bg
HIST1H2BI	8346	6p21.3	histone cluster 1, H2bi
HIST1H2BK	85236	6p21.33	histone cluster 1, H2bk
HMOX1	3162	22q12	heme oxygenase (decycling) 1
HPCAL1	3241	2p25.1	hippocalcin-like 1
HPS5	11234	11p14	Hermansky-Pudlak syndrome 5

HRASLS	57110	3q29	HRAS-like suppressor
HRASLS3	11145	11q12.3-q13.1	HRAS-like suppressor 3
HTATIP2	10553	11p15.1	HIV-1 Tat interactive protein 2, 30kDa
HTRA2	27429	2p12	HtrA serine peptidase 2
ID2	3398	2p25	inhibitor of DNA binding 2, dominant negative helix-loop-helix protein
ID3	3399	1p36.13-p36.12	inhibitor of DNA binding 3, dominant negative helix-loop-helix protein
IDS	3423	Xq28	iduronate 2-sulfatase (Hunter syndrome)
IFI44	10561	1p31.1	interferon-induced protein 44
IFIT1	3434	10q25-q26	interferon-induced protein with tetratricopeptide repeats 1
IFIT3	3437	10q24	interferon-induced protein with tetratricopeptide repeats 3
IFIT5	24138	10q23.31	interferon-induced protein with tetratricopeptide repeats 5
IGFBP6	3489	12q13	insulin-like growth factor binding protein 6
IL10RB	3588	21q22.1-q22.2	interleukin 10 receptor, beta
IL13RA2	3598	Xq13.1-q28	interleukin 13 receptor, alpha 2
IL8	3576	4q13-q21	interleukin 8
JMJD1A	55818	2p11.2	jumonji domain containing 1A
JUND	3727	19p13.2	jun D proto-oncogene
KBTBD4	55709	11p11.2	kelch repeat and BTB (POZ) domain containing 4
KCNMA1	3778	10q22.3	potassium large conductance calcium-activated channel, subfamily M, alpha member 1
KLF4	9314	9q31	Kruppel-like factor 4 (gut)
LEPREL1	55214	3q28	leprecan-like 1
LIF	3976	22q12.2	leukemia inhibitory factor (cholinergic differentiation factor)
LOXL2	4017	8p21.3-p21.2	lysyl oxidase-like 2
LRDD	55367	11p15.5	leucine-rich repeats and death domain containing
MACF1	23499	1p32-p31	microtubule-actin crosslinking factor 1
MAGEA4	4103	Xq28	melanoma antigen family A, 4
MAGEA5	4104	Xq28	melanoma antigen family A, 5
MME	4311	3q25.1-q25.2	membrane metallo-endopeptidase (neutral endopeptidase, enkephalinase)
MMP19	4327	12q14	matrix metallopeptidase 19
MYLK	4638	3q21	myosin, light chain kinase
MYST4	23522	10q22.2	MYST histone acetyltransferase (monocytic leukemia) 4
NEDD4	4734	15q	neural precursor cell expressed, developmentally down-regulated 4
NFYC	4802	1p32	nuclear transcription factor Y, gamma
NNMT	4837	11q23.1	nicotinamide N-methyltransferase

NOSIP	51070	19q13.33	nitric oxide synthase interacting protein
OCLN	4950	5q13.1	occludin
OSMR	9180	5p13.1	oncostatin M receptor
P4HA1	5033	10q21.3-q23.1	procollagen-proline, 2-oxoglutarate 4-dioxygenase (proline 4-hydroxylase), alpha polypeptide I
PARVA	55742	11p15.3	parvin, alpha
PCAF	8850	3p24	p300/CBP-associated factor
PIK3R3	8503	1p34.1	phosphoinositide-3-kinase, regulatory subunit 3 (p55, gamma)
PJA2	9867	5q21.3	praja 2, RING-H2 motif containing
PLEKHC1	10979	14q22.2	pleckstrin homology domain containing, family C (with FERM domain) member 1
PLOD1	5351	1p36.3-p36.2	procollagen-lysine 1, 2-oxoglutarate 5-dioxygenase 1
PLOD2	5352	3q23-q24	procollagen-lysine, 2-oxoglutarate 5-dioxygenase 2
PMAIP1	5366	18q21.32	phorbol-12-myristate-13-acetate-induced protein 1
PNMA1	9240	14q24.3	paraneoplastic antigen MA1
PODXL	5420	7q32-q33	podocalyxin-like
POLI	11201	18q21.1	polymerase (DNA directed) iota
POLM	27434	7p13	polymerase (DNA directed), mu
POPDC3	64208	6q21	popeye domain containing 3
PPGB	5476	20q13.1	protective protein for beta-galactosidase (galactosialidosis)
PPM1D	8493	17q23.2	protein phosphatase 1D magnesium-dependent, delta isoform
PRKAB1	5564	12q24.1	protein kinase, AMP-activated, beta 1 non-catalytic subunit
PRKCDBP	112464	11p15.4	protein kinase C, delta binding protein
PSEN1	5663	14q24.3	presenilin 1 (Alzheimer disease 3)
QKI	9444	6q26-q27	quaking homolog, KH domain RNA binding (mouse)
RAB3B	5865	1p32-p31	RAB3B, member RAS oncogene family
RABGEF1	27342	7q11.21	RAB guanine nucleotide exchange factor (GEF) 1
RB1CC1	9821	8p22-q21.13	RB1-inducible coiled-coil 1
RFXDC2	64864	15q21.3	regulatory factor X domain containing 2
RGS2	5997	1q31	regulator of G-protein signalling 2, 24kDa
RHOF	54509	12q24.31	ras homolog gene family, member F (in filopodia)
RIMS3	9783	1pter-p22.2	regulating synaptic membrane exocytosis 3
RNF24	11237	20p13-p12.1	ring finger protein 24
RSN	6249	12q24.3	restin (Reed-Steinberg cell-expressed intermediate filament-associated protein)
RTN3	10313	11q13	reticulon 3
SAMD9	54809	7q21.2	sterile alpha motif domain containing 9

SAMHD1	25939	20pter-q12	SAM domain and HD domain 1
SCHIP1	29970	3q25.33	schwannomin interacting protein 1
SEC14L1	6397	17q25.1-17q25.2	SEC14-like 1 (S. cerevisiae)
SGK	6446	6q23	serum/glucocorticoid regulated kinase
SLC39A8	64116	4q22-q24	solute carrier family 39 (zinc transporter), member 8
SLCO4A1	28231	20q13.33	solute carrier organic anion transporter family, member 4A1
SOCS5	9655	2p21	suppressor of cytokine signaling 5
SOCS6	9306	18q22.2	suppressor of cytokine signaling 6
SORT1	6272	1p21.3-p13.1	sortilin 1
SPAG1	6674	8q22.2	sperm associated antigen 1
SPAG4	6676	20q11.21	sperm associated antigen 4
SPRY2	10253	13q31.1	sprouty homolog 2 (Drosophila)
SS18L1	26039	20q13.3	synovial sarcoma translocation gene on chromosome 18-like 1
STXBP3	6814	1p13.3	syntaxin binding protein 3
SUV420H1	51111	11q13.2	suppressor of variegation 4-20 homolog 1 (Drosophila)
SYNGR1	9145	22q13.1	synaptogyrin 1
SYNJ1	8867	21q22.2	synaptojanin 1
SYNJ2BP	55333	14q24.2	synaptojanin 2 binding protein
TDRD7	23424	9q22.33	tudor domain containing 7
TFAP2C	7022	20q13.2	transcription factor AP-2 gamma (activating enhancer binding protein 2 gamma)
TFPI	7035	2q32	tissue factor pathway inhibitor (lipoprotein-associated coagulation inhibitor)
TIA1	7072	2p13	TIA1 cytotoxic granule-associated RNA binding protein
TIAM1	7074	21q22.1	T-cell lymphoma invasion and metastasis 1
TINF2	26277	14q12	TERF1 (TRF1)-interacting nuclear factor 2
TLE1	7088	9q21.32	transducin-like enhancer of split 1 (E(sp1) homolog, Drosophila)
TLR4	7099	9q32-q33	toll-like receptor 4
TM9SF1	10548	14q11.2	transmembrane 9 superfamily member 1
TMEM22	80723	3q22.3	transmembrane protein 22
TNS3	64759	7p12.3	tensin 3
TPM2	7169	9p13.2-p13.1	tropomyosin 2 (beta)
TRIM2	23321	4q31.3	tripartite motif-containing 2
TRIM24	8805	7q32-q34	tripartite motif-containing 24
TRIM26	7726	6p21.3	tripartite motif-containing 26
TRIM38	10475	6p21.3	tripartite motif-containing 38

TRIO	7204	5p15.1-p14	triple functional domain (PTPRF interacting)
UBXD6	7993	8p12-p11.2	UBX domain containing 6
UCHL1	7345	4p14	ubiquitin carboxyl-terminal esterase L1 (ubiquitin thiolesterase)
UPF3A	65110	13q34	UPF3 regulator of nonsense transcripts homolog A (yeast)
USP11	8237	Xp11.23	ubiquitin specific peptidase 11
VPS13B	157680	8q22.2	vacuolar protein sorting 13B (yeast)
WSB1	26118	17q11.1	WD repeat and SOCS box-containing 1
YIPF6	286451	Xq12	Yip1 domain family, member 6
ZBTB1	22890	14q23.3	zinc finger and BTB domain containing 1
ZFP95	23660	7q22	zinc finger protein 95 homolog (mouse)
ZNF91	7644	19p13.1-p12	zinc finger protein 91

LIST OF ABBREVIATIONS

DMEM	Dulbecco's Modified Eagle's Medium
DMSO	Dimethyl sulfoxide
HEPES	4-(2-hydroxyethyl)-1-piperazineethanesulfonic acid
PBS	Phosphate buffered saline
P/S	Penicillin/streptomycin
HBSS	Hanks Balanced Salt Solution
MEM	Minimum essential medium
KSFM	Keratinocyte Serum Free Medium
FCS	Fetal Calf Serum
DTT	Dithiothreitol
5-aza-dC	5-aza-2′-deoxycytidine
HG-U133A	Human Genome U133A 2.0 Array
DAG	Direct Acyclic Graph
MeDIP	Methylated DNA immunoprecipitation
DNMT	DNA methyltransferase enzyme
GO	Gene Ontology
SAPE	Streptavidin Phycoerythrin
DAPI	4', 6'-diamidine-2'-phenylindole dihydrochloride
HRP	Horseradish Peroxidase
GCOS	GeneChip Operating Software
IVT	In vitro transcription
UC	Urothelial Carcinoma

Acknowledgment

In the first place, I owe special gratitude to my parents and other members of the family for their endless love, encouragement and unconditional support of all my undertakings, scholastic and otherwise.

I would like to express my deepest gratitude to my supervisor Prof. Dr. Wolfgang Schulz, without his extremely valuable experiences, stimulating suggestions, insights and guidance this thesis would never have started let alone completed. He has provided for an optimum working environment and his uncompromising quest for excellence significantly shaped everyone in the lab. I consider myself very lucky to have such a friendly and approachable supervisor.

I am very thankful to Prof. Dr. Lutz Schmitt, Institute of Biochemistry for his support, helpful ideas throughout my PhD period and for reviewing my thesis on a very short notice. You have contributed very positively to my success.

I am highly indebted to Dr. Andrea Linnemann-Florl and Mrs Christiane Hader for their assistance and sharing of scientific expertise in the field of molecular biology during the three years of this thesis's work. I am grateful to Dr Wolfgang Göring for his careful reading and constructive comments on this thesis, my cordial appreciation toTeodora Ribarska for sacrificing her precious times and skills with the EndNote software, and I would like to recognize many valuable contributions that I received from other colleagues in the lab Stefan Bleckmann, Annemarie Koch and Michael Kloth.

I would like to thank all my co-authors including Dr. Hans-Helge Seifert, University Hospital Zürich and Dr Ingmar Wolff, University Hospital Dresden, for contributing significantly to my research article. I am very grateful to Dr. Christine Steinhoff, Max Planck Institute for Molecular Genetics, Berlin for assisting me with the microarray analysis.

Special thanks are due to Prof. Dr. P. Albers and members of the Department of Urology, for providing us with human tissue specimens, clinical and administrative support. Furthermore, the financial support of the Deutsche Forschungsgemeinschaft (German Research Foundation) is gratefully acknowledged.

DECLARATION

I hereby declare that this thesis is my own work and effort and that it has not been submitted anywhere for any award. Where other sources of information have been used, they have been acknowledged

Olusola Yakub Dokun

Duesseldorf, 13.06.09

aus dem Forschungslabor der Urologischen Klinik
der Heinrich-Heine Universität Düsseldorf

Gedruckt mit der Genehmigung der
Mathematisch-Naturwissenschaftlichen Fakultät der
Heinrich-Heine-Universität Düsseldorf

Referent: Prof. Dr. Wolfgang Schulz
Koreferent: Prof. Dr. Lutz Schmitt
Tag der mündlichen Prüfung: 10.07.09